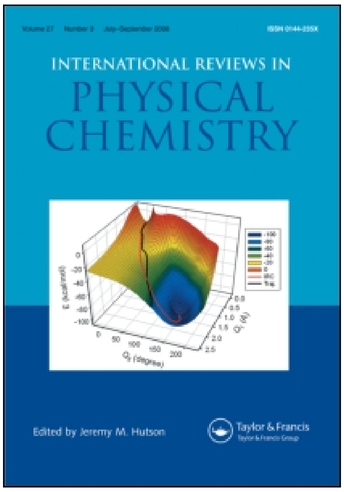

International Reviews in Physical Chemistry
Publication details, including instructions for authors and subscription information:
http://www.informaworld.com/smpp/title~content=t713724383

Density-functional studies of electronic properties of polymers

Michael Springborg[a]
[a] Fakultät für Chemie, Universität Konstanz, Konstanz, Germany

To cite this Article Springborg, Michael(1993) 'Density-functional studies of electronic properties of polymers', International Reviews in Physical Chemistry, 12: 2, 241 — 303
To link to this Article: DOI: 10.1080/01442359309353283
URL: http://dx.doi.org/10.1080/01442359309353283

INTERNATIONAL REVIEWS IN PHYSICAL CHEMISTRY, 1993, VOL. 12, NO. 2, 241–303

Density-functional studies of electronic properties of polymers

by MICHAEL SPRINGBORG
Fakultät für Chemie, Universität Konstanz,
W-7750 Konstanz, Germany

Results of parameter-free electronic-structure calculations on polymers are discussed. The calculations have been performed using various first-principles density-functional methods. Most first-principles studies have been devoted to finite molecules or infinite, periodic chains. Properties of structural defects which break the translational or helical symmetry can therefore most conveniently be studied by mapping the first-principles results on an adequate model Hamiltonian, which subsequently is used in studying the defects. As examples of applications we examine structural properties of sulphur and selenium helices and compare polyethylene and polytetrafluoroethylene. We then study in detail trans polyacetylene as the prototype of the conjugated polymers and discuss briefly a number of other conjugated polymers. Hydrogen fluoride is investigated as an example of a hydrogen-bonded polymer and some other hydrogen-bonded chains are briefly discussed. We finally mention other systems that have been or can be treated with the current density-functional methods and conclude by discussing their limitations and possible improvements.

1. Introduction

This century has experienced an enormous increase in the studies of atomic properties of materials and processes that take place at the atomic scale. It has become evident that many biological processes can only be understood from detailed knowledge of electronic properties of the participating atoms and molecules. As a single example we mention that it is believed that the description of proton transport in various biological and non-biological media requires quantum-mechanical descriptions of the media and/or of the protons (see, e.g., Bountis (1992).) Furthermore, technological developments like molecular-beam epitaxy have made it possible to control crystal growths at almost the atomic level and thus to synthesize materials with pre-defined properties controlled at the atomic or molecular level. Of more relevance to the present work is the possibility of modifying the structure of the so-called conjugated polymers, thereby to some extent tailoring their properties (see, e.g., Roth *et al.* (1991).)

Materials research has accordingly to deal with descriptions of the materials incorporating quantum-theoretical studies of the electrons and atoms of the materials. Often one is forced to apply simplifying quantum-theoretical models, therefore facing the problem of not knowing the range of validity of the model.

Detailed experimental studies of the properties of one specific material as well as experimental comparative studies of a larger class of related materials are two ways of exploring specific properties as well as the validity of models developed for describing these properties. One may thereby confirm predictions, discover new properties, arrive at improved models, reject models, etc. The advantage of the experimental studies is that one studies directly the capability of the models to describe the properties of the materials for which they have been developed. A disadvantage is, however, that

0144–235X/93 $10·00 © 1993 Taylor & Francis Ltd.

impurities, imperfections, surface effects, etc., may obscure any unique interpretation of the results of the experiments.

One way of avoiding these complications is to replace the experiments by detailed parameter-free computer calculations. The advantage is that one may, in principle, investigate any real or imaginary material thereby being able to explore any feature at will. The disadvantage is, however, that the required computational efforts may be so large that one has to study simpler, idealized compounds. But carefully chosen, the computational studies of such model compounds can be an important supplement to the experiments.

A number of theoretical parameter-free studies of the electronic properties of polymers take their starting point in the Hartree–Fock approximation as applied to extended systems (André *et al.* 1967, Del Re *et al.* 1967). These methods have the advantage that one may, in principle, improve the quality of the calculation by systematically increasing the size of the basis set and—if required—by going beyond the Hartree–Fock approximation by including correlation effects. For larger systems this approach becomes, however, prohibitively costly, and one has to compromise between computational costs and desired accuracy.

An alternative is to make use of the Hohenberg–Kohn density-functional theory (Hohenberg and Kohn 1964). This is the approach we shall discuss in detail here. We will put special emphasis on our own method (Springborg and Andersen 1987, Springborg 1989 *a*, Springborg *et al.* 1991 *b*) but shall at relevant places refer to other methods.

The first-principles density-functional methods for studying polymers are briefly described in Section 2. Most of these methods assume the polymers to be infinite and periodic. However, for some systems and/or properties, deviations from this idealization are crucial. This includes, e.g., defect-induced modifications which break the periodicity. Such systems are very difficult to treat with the first-principles methods, but first-principles calculations may form the basis for model studies. The principle behind this procedure is outlined in Section 3. Sections 4–9 contain various applications. In Section 4 we discuss differences between polymers having translational symmetry and those having a more general helical symmetry. We focus especially on chains consisting of either sulphur or selenium atoms as well as on polyethylene and polytetrafluoroethylene. Also the occurrence of a bond-length alternation in some simple, linear chains is discussed in Section 4. Section 5 contains a detailed discussion of the prototype of the conjugated polymers, trans polyacetylene, and in Section 6 a number of other conjugated polymers is discussed. Section 7 is devoted a simple hydrogen-bonded chain, hydrogen fluoride, whereas Section 8 treats other hydrogen-bonded systems. We discuss in Section 9 other helical polymers and in Section 10 possible improvements of the computational schemes. We conclude in Section 11.

It should finally be added that the list of references is not claimed to be complete but represents merely a subjective choice of the author. For more complete references the reader is referred to the various papers cited throughout this review.

2. The density-functional methods

In the present review we will focus on theoretical studies on quasi-one-dimensional compounds based on first-principles calculations on their electronic ground-state properties. Many materials consist of very long, more or less parallel chains that only interact weakly, e.g. through van-der-Waals forces. Each chain can be idealized as being finite and having a screw-axis symmetry. Assuming the screw-axis to be straight and the interchain interactions to be negligible, a single chain can hence be assumed as being (i) periodic, (ii) infinite, (iii) helical, (iv) with straight polymer-axis, and (v) isolated. In the study of their electronic ground-state properties it is furthermore practice to assume (vi) $T=0$ and only consider (vii) static properties. We shall here refer to systems obeying (i)–(v) as helical polymers.

Theoretical studies of compounds which possess the properties (i)–(vii) require dealing simultaneously with the finiteness of the system in two dimensions and the infiniteness in the third. Therefore, methods usually applied to three-dimensional, infinite crystals may not be suitable, and also methods usually applied for finite molecules can only be used with difficulty.

We assume that the Born–Oppenheimer approximation is valid, such that our problem is that of calculating the static distribution of N electrons moving in the field of the nuclei, whose positions are kept fixed. Instead of attempting to solve the N-electron Schrödinger equation we make use of the exact Hohenberg–Kohn theorem (Hohenberg and Kohn 1964) which states that the ground-state properties of the system of our interest are unique functionals of the electron density $\rho(\mathbf{r})$. Thus, the total energy E_{tot} is a functional of $\rho(\mathbf{r})$, whose precise form, however, is unknown.

It has turned out to be convenient to transform the problem of calculating the total energy of the system into that of solving the single-particle Kohn–Sham equations (Kohn and Sham 1965), which, using Ry atomic units, are

$$[-\nabla^2+V_{\mathrm{N}}(\mathbf{r})+V_{\mathrm{C}}(\mathbf{r})+V_{\mathrm{xc}}(\mathbf{r})]\psi_i(\mathbf{r})=\epsilon_i\psi_i(\mathbf{r}). \qquad (1)$$

Here, V_{N} and V_{C} are the Coulomb potential of the nuclei and electrons, respectively, and V_{xc} is the so-called exchange-correlation potential. The fact that the precise functional which yields the total energy as a functional of the electron density is unknown, manifests itself therein that the exchange-correlation potential is unknown. But experience has shown that for many systems and properties a local approximation is a good approximation. Thereby V_{xc} is written as a function of the density of the point of interest, and this function is often taken from calculations on homogeneous electron gases with the same density:

$$V_{\mathrm{xc}}(\mathbf{r})=V_{\mathrm{xc}}[\rho(\mathbf{r})]. \qquad (2)$$

In our own studies we will use the form given by von Barth and Hedin (1972) but replacing that with one of the others that throughout the years have been proposed leads only to minor modifications in the results. The so-called non-local approximations correspond to replacing V_{xc} of equation (2) with a function of both $\rho(\mathbf{r})$ and $|\nabla\rho(\mathbf{r})|$.

We now notice that both V_{C} and V_{xc} become well-defined functionals of the total electron density

$$\rho(\mathbf{r})=\sum_i^{\mathrm{occ}}|\psi_i(\mathbf{r})|^2. \qquad (3)$$

The advantage of solving the density-functional equations (1)–(3) instead of the Schrödinger equation is that one has to deal with N single-particle equations instead of one N-particle equation, meaning that the density-functional equations for medium-sized N can be solved more accurately than the Schrödinger equation can. On the other hand, one has to realize that the starting point is an approximated equation, and that, in principle, the single-particle eigenfunctions ψ_i and eigenvalues ϵ_i do not have anything to do with electronic orbitals and excitation energies, respectively. However, it has turned out that for a very large class of materials and properties it is a good approximation to neglect these formal inconsistencies (see, e.g. Jones and Gunnarsson 1989). The calculated structural properties, vibrational frequencies, relative stabilities of compounds with similar chemical bonds, electron densities, and single-particle energies of occupied orbitals are most often in good agreement with experimental findings, whereas the single-particle energies of the unoccupied orbitals appear at too low energies (Jones and Gunnarsson 1989). But there are cases where the density-functional methods fail. Although correlation effects are included in the density-functional, formalism (but most often according to a local approximation), these include many highly-correlated systems as well as absolute values of strengths of chemical bonds.

A further advantage of the density-functional approach is that it does only make minor differences whether one treats systems consisting of heavier atoms or systems with lighter atoms. For the heavier atoms it is convenient to use a frozen-core approximation in which the density of all but the valence electrons is kept as for the isolated atoms. These frozen-core electrons contribute solely with an extra density which is easily added to that of equation (3). Finally, density-functional methods treat metals and semiconductors/insulators on the same footing.

In solving the Kohn–Sham equations the eigenfunctions ψ_i are expanded in a set of basis functions. Here, many different choices are possible. For the polymers obeying (i)–(v) it is most convenient to work with a set of atom-centred functions, as also is the case when considering the polymer to be one single, large but finite molecule.

For the periodic, infinite polymers Mintmire and coworkers have used a basis set consisting of Gaussians (Mintmire and White 1983*a, b, c, d*, Mintmire *et al.* 1987, Mintmire 1992), as also has been used by von Boehm *et al.* 1987). Some of the oldest density-functional studies on single chains of polymers used linearized muffin-tin orbitals (LMTOs) as basis functions (Falk and Fleming 1973, 1975). LMTOs are also the basis function we shall use, but our approach should be more accurate than the older one by Falk and Fleming.

Ye *et al.* (1989 *a, b*) approximated the polymer as a single molecule and expanded the eigenfunctions in a basis of numerical functions. Their study seems to be the only density-functional study which considers a finite macromolecule as an approximation to an infinite polymer.

Since density-functional methods are used most often in solid-state physics for the study of electronic properties of three-dimensional infinite solids, some other approaches have studied the polymers by considering them forming a periodic array of parallel chains where the interchain distances are kept reasonably large. Both Kasowski *et al.* (1980 *a, b*), Zemach *et al.* (1989 *a, b*), and Albers (1989) have used LMTOs as basis functions for such studies. Closely related basis functions, the augmented spherical waves, have been used by Kübler *et al.* (1987), whereas Ashkenazi *et al.* (1989) used augmented plane waves. Finally, pseudopotential methods, in which the true Kohn–Sham potential is replaced by pseudopotentials giving the correct eigenfunctions outside the core region, with a plane-wave basis set have been used by Vogl and Campbell (1989, 1990) and by Jansen *et al.* (1987), whereas Takeda and Shiraishi (1989) used Gaussians.

Since we in the present review will put most emphasis on our own work, and since our basis functions, the LMTOs, are less familiar we start out with presenting those.

In figure 1 we show a hypothetical molecule consisting of four atoms A, B, C, and D. We define atom-centred, non-overlapping (muffin-tin) spheres such that the nuclei

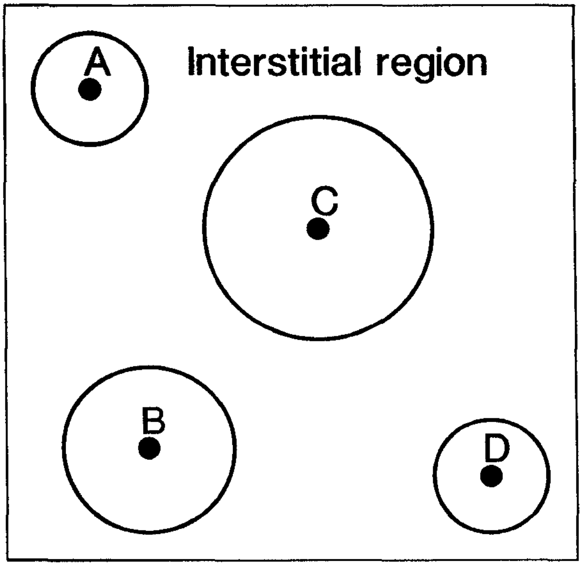

Figure 1. Schematic representation of a hypothetic four-atomic molecule. *A*, *B*, *C*, and *D* denote the nuclei, the circles are the muffin-tin spheres, and outside all spheres we have the interstitial region. (Reproduced from Springborg (1989*a*).)

occupy the centres, as shown in figure 1. The interstitial region is defined as the region outside all spheres. Inside the spheres we replace the total potential

$$V(\mathbf{r}) = V_N(\mathbf{r}) + V_C(\mathbf{r}) + V_{xc}(\mathbf{r}) \tag{4}$$

by its spherically symmetric component. The Kohn–Sham equations (1) become thereby one-dimensional and can be solved numerically whereby the ϵ_i are chosen reasonable (i.e. in the energy region where the resulting function is of interest). We thereby arrive at a numerically given function, which subsequently is matched continuously and differentiably on a spherical Hankel function. This function is inside any other sphere augmented continuously and differentiably with the numerical functions of that sphere.

As an example we show in figure 2 results for a CO molecule. The interatomic distance is set equal to 2·6 a.u. and the radii of the muffin-tin spheres to 1·2 a.u. for the carbon sphere and 1·0 a.u. for the oxygen sphere. Moreover, the molecular axis is assumed parallel to the z axis.

In figure 2(*a*) and 2(*b*) we show the full potential inside the spheres as well as its spherically symmetric parts. It is seen that the latter do constitute good approximations to the exact potential. This means that LMTO basis functions, which are eigenfunctions to the spherically symmetric potentials, are good approximations to the exact solutions to (1), especially in the region close to the nuclei, where the largest parts of the total energy originate. In carrying this argument through it might be useful to notice that a Gaussian basis set corresponds to replacing the potentials by harmonic ones, whereas the potentials for plane waves are constants and those for Slater-type orbitals are proportional to $1/r$. Finally, the s and p_z basis functions of the CO molecule are shown in figure 2(*c*)–(*f*).

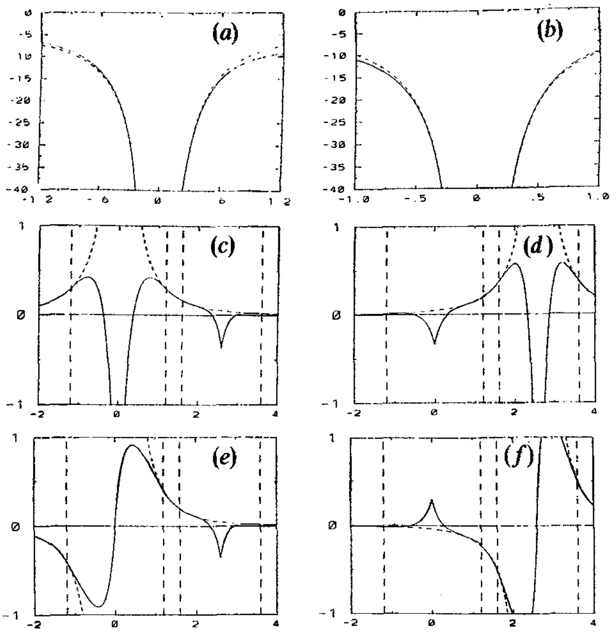

Figure 2. Various properties of a CO molecule along the molecular axis. (*a*) and (*b*) show the potential inside the muffin-tin spheres with the full line being the full potential and the dashed line being its spherically symmetric part. (*c*) and (*d*) show *s* basis functions and (*e*) and (*f*) show p_z basis functions. Here, the dashed curves are the Hankel functions and the vertical dashed lines represent the boarders of the muffin-tin spheres. (*a*), (*c*), and (*e*) show functions centred on the C atom; (*b*), (*d*), and (*f*) functions centred on the O atom. The carbon atom is placed at the origin and the oxygen atom at $z = 2{\cdot}6$ a.u. All quantities are given in Ry atomic units.

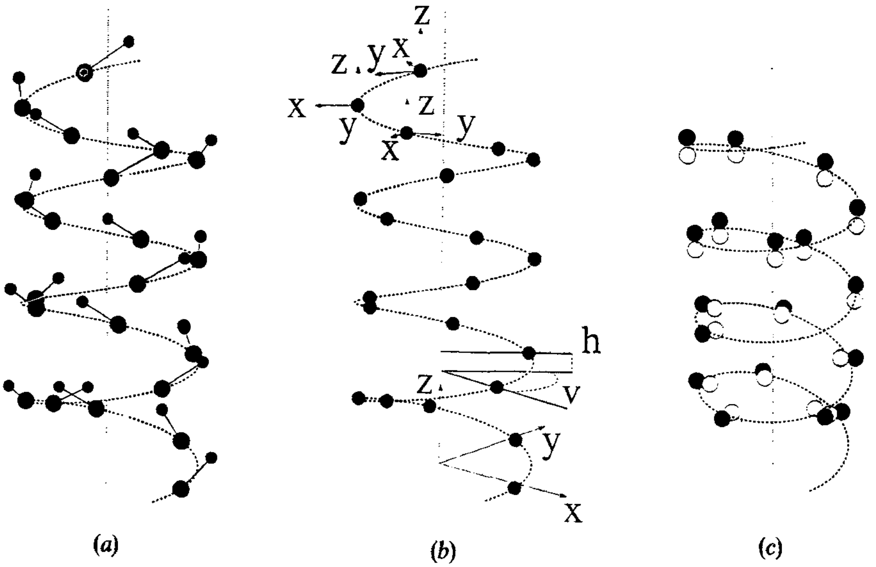

Figure 3. (*a*) A hypothetic helical polymer with two atoms per repeated unit. (*b*) Definition of the parameters *h* and *v* describing the structure of the polymer as well as local atom-centred coordinate systems. (*c*) Local p_z (upper part) and p_x (lower part) functions. (Reproduced from Springborg (1989 a).)

As soon as the basis set is defined one may determine Hamilton and overlap matrices as described in detail elsewhere. From these the eigenfunctions ψ_i can be calculated. These define a new density, which in turn leads to a new set of equations (1). This procedure is repeated until self-consistency is achieved. Once this is the case various quantities like the total energy E_{tot}, the electron density $\rho(\mathbf{r})$, the single-particle energies ϵ_i, Mulliken populations, optical spectra, densities of states, etc., can be extracted (see, e.g., Springborg *et al.* (1991 *b*) and references therein).

For the polymers satisfying the properties (i)–(vii) one may explicitly make use of the symmetry in defining symmetry-adapted Bloch-waves of the atom-centred orbitals. This may lead to substantial computer-time savings. In figure 3 (*a*) we show an example of a hypothetical helical polymer with two atoms per unit. The screw-axis symmetry of the system can be described by the combined translation of h and rotation of v shown in figure 3 (*b*). In figure 3 (*b*) we also show local, atom-centred, right-handed coordinate systems, which have the z axis parallel to the polymer axis and the x axis pointing away from it. In these one may define local basis functions as shown in figure 3 (*c*). It is here seen that all locally defined functions are equivalent and we can thus form Bloch waves from them. In doing so we will use a dimensionless k variable with $k = 0$ and $k = 1$ being the zone centre and the zone edge, respectively. We finally mention that v does not need to be commensurate with 2π, and that $v = \pi$ and $v = 2\pi$ correspond to the zig–zag and translational symmetry, respectively.

3. Structural defects

Structural defects are important for some polymers and properties. Their occurrence breaks the symmetry such that the property (i) of Section 2 no longer is satisfied. It becomes accordingly much more difficult to apply a first-principles method in studying the electronic properties of the system: one must either assume a periodically repeated defect for which the periodicity is so large that the defect-induced orbitals do not interact, or one can apply a Green function approach. In both cases the computational demands are very large and to our knowledge there exists only three density-functional studies of such defects, i.e. those of Kutzler *et al.* (1986) and of Vogl and Campbell (1989, 1990) on periodically repeated defects, and that of Ye *et al.* (1989 *b*) on a finite defect-containing molecule. As a simpler alternative we have chosen to map the results of first-principles calculations on chains obeying (i)–(vii) of Section 2 on model Hamiltonians with which we subsequently study the defect-containing chains. Two examples shall illustrate this approach.

The currently large research activity in conducting polymers (see, e.g., Roth *et al.* (1991)) was initiated about 15 years ago when it was reported (Chiang *et al.* 1977) that polyacetylene shows a very large doping-induced increase in electrical conductivity. In the meanwhile it has been demonstrated that many other conjugated polymers possess similar properties and that the change in electrical conductivity is accompanied by changes in other physical properties (see, e.g., Roth *et al.* (1991)).

About two years after the discovery of Chiang *et al.*, Su *et al.* (1979, 1980) presented a model that qualitatively can explain the features. This model assumes solitons to be the charge carriers. The soliton is related to the so-called misfit proposed (Longuet-Higgins and Salem 1959) and observed (Nechtschein 1964) already about 30 years ago, and is a structural defect.

A single chain of trans polyacetylene has a planar nuclear backbone and consists of a zig–zag chain of carbon atoms with a single hydrogen atom attached to each carbon atom (see figure 10 of Section 5). The chemical bonds can easily be interpreted as being due to energetically low lying σ bonds between carbon sp^2 hybrids and hydrogen 1s functions plus π bonds formed by carbon p functions perpendicular to the plane of the nuclei. The π orbitals are those appearing closest to the Fermi level. For the periodic chain with all C–C bond lengths equal the polymer has a zig–zag symmetry and will be metallic with a half-filled π band. A bond-length alternation will lower the symmetry and open up a gap at the Fermi energy. It is now important to realize that the two structures—the so-called *A* and *B* phases—only differing in an interchange of the shorter and the longer C–C bonds are energetically degenerate. A soliton is a domain wall between two parts of the polymer with different phases. Due to the energetical degeneracy of the *A* and *B* phases the soliton can move almost freely along the chain, eventually carrying charge.

However, as mentioned above also other conjugated polymers show similar physical properties. For most of those the *A* and *B* phases are not energetically degenerate and solitons may therefore not exist. Instead the occurrence of polarons has been proposed (Brazovskiĭ and Kirova 1981, Brédas *et al.* 1981, Campbell and Bishop 1981). A polaron is a local lattice distortion induced by the presence of extra or less electrons. The existence of a polaron does not require that of two (meta-)stable phases.

Doping or photoexciting the polymer will change the occupation of the orbitals closest to the Fermi energy. As proposed by Su *et al.* (1979, 1980) (for a detailed discussion, see, e.g., Heeger *et al.* (1988) and Baeriswyl *et al.* (1991)) a useful model Hamiltonian therefore includes a tight-binding description of the π orbitals. The hopping integrals are assumed depending linearly on the bond lengths. The remaining part of the total energy of the system is finally written as a simple function of the bond lengths.

We thus have

$$\hat{H}=\hat{H}_\pi+\hat{H}_\sigma, \tag{5}$$

in which the tight-binding part is

$$\hat{H}_\sigma=\sum_n\sum_s \epsilon_n c^\dagger_{n,s} c_{n,s}+\sum_{n,m}\sum_s t_{n,m}(c^\dagger_{n,s}c_{m,s}+c^\dagger_{m,s}c_{n,s}). \tag{6}$$

Here, ϵ_n are on-site terms and $t_{n,m}$ are hopping integrals. $c^\dagger_{n,s}$ and $c_{n,s}$ are the creation and annihilation operators, respectively, of an electron with spin *s* on site *n*. Su *et al.* (1979, 1980) applied the model only on trans polyacetylene and considered accordingly exclusively carbon-centred orbitals, assumed ϵ_n to be independent of *n*, and included only nearest-neighbour hopping integrals.

With $d_{n,m}$ being the bond length between site *n* and site *m* we assume

$$t_{n,m}=t^{0\prime}_{|n-m|}-\alpha'_{|n-m|}(d_{n,m}-d^0_{|n-m|}), \tag{7}$$

where $d^0_{|n-m|}$ is a typical value of $|n-m|$th-nearest-neighbour bond lengths, and $t^{0\prime}_{|n-m|}$ and $\alpha'_{|n-m|}$ are constants.

The lattice energy, $\hat{H}_\sigma$, is approximated by

$$\hat{H}_\sigma=\sum_{n,m} f'_{|n-m|}(d_{n,m}-d^0_{|n-m|}), \tag{8}$$

with $f'_{|n-m|}$ a simple function of the bond lengths (e.g. harmonic).

As a simplification we assume that the position of each site (e.g. carbon atom for trans polyacetylene) can be described by one single parameter. For trans polyacetylene we—as Su *et al.*—choose displacements u_n parallel to the polymer axis relative to the positions in the hypothetic chain with all C–C bond lengths equal. For

$$|u_n-u_m|\ll d_{n,m}, \tag{9}$$

we may thereby replace equation (7) by

$$t_{n,m}=t^0_{|n-m|}-\alpha_{|n-m|}(u_n-u_m), \tag{10}$$

and equation (8) by

$$\hat{H}_\sigma=\sum_{n,m} f_{|n-m|}(u_n-u_m). \tag{11}$$

It finally turns out that it is convenient to introduce

$$x_n=(-1)^n u_n. \tag{12}$$

The periodic chains are characterized by x_n being constant:

$$x_n=x_0. \tag{13}$$

For the A and B phases we will let x_A and x_B, respectively, denote this constant.

A soliton can be modelled through

$$x_n=\frac{x_A+x_B}{2}+\frac{x_A-x_B}{2}\tanh\left(\frac{n+\delta}{L}\right), \tag{14}$$

where δ is the position and L the width of the soliton. Similarly, a polaron can be modelled through

$$x_n=\frac{x_A+x_B}{2}+\frac{x_A-x_B}{2}\tanh\left(\frac{n+\delta+\Delta}{L}\right)\tanh\left(\frac{n+\delta-\Delta}{L}\right), \tag{15}$$

or, alternatively, through

$$x_n=x_A\left[1-\kappa\,\mathrm{sech}\left(\frac{n+\delta+\Delta}{L}\right)\mathrm{sech}\left(\frac{n+\delta-\Delta}{L}\right)\right]. \tag{16}$$

Here, 2Δ is the width of the polaron, and in equation (14) κ is the relative amplitude of the distortion. Equation (15) is only applicable for systems containing two metastable phases, whereas equation (16) is generally valid.

In order to obtain the parameter values of the model Hamiltonian we perform first-principles calculations on periodic, neutral chains. The results of these are then fitted to results of similar model calculations. Subsequently the model Hamiltonian can be used in studying the defects. We thereby assume that the defect will not induce extra effects like, e.g., Coulomb forces that are absent for the periodic chains or correlation effects beyond those of a local approximation. Moreover, the approach relies upon the capability of knowing the changes in all the other geometrical coordinates than the x_n. This includes the assumption that the optimized values of these other parameters are independent on the presence or absence of defects. Since these approximations need not be fully justified, the results of the model calculations will be connected with some uncertainty.

The other class of materials we will discuss here is the hydrogen-bonded chains. For these each hydrogen atom is placed asymmetrically between its two nearest neighbours forming a stronger chemical bond to one and a weak hydrogen bond to the other. Interchanging all chemical and hydrogen bonds may lead to another (meta-)stable structure and in certain cases the two structures are energetically degenerate. In that case we may introduce solitons of the form (14), where x_n now describes the position of the nth hydrogen atom, and in all cases polarons may be introduced. These defects are often assumed responsible for the relatively large electrical conductivity in hydrogen-bonded systems and the charge-transport mechanism is closely related to the well-known one of the Grotthus presented already in the beginning of the last century.

For these systems we will not be interested in the electronic orbitals themselves but solely in the total energy which we will write as a simple function of the $\{x_n\}$. This function is then to be determined from first-principles calculations on periodic chains invoking the same approximations as for the conjugated polymers.

We finally mention that also other structural defects can be treated within a picture as that presented here. Among many others these include the twistons (Brazovsky and Kirova 1988) for which a part of the nuclei of the polymer backbone of a conjugated polymer has been lifted out of the otherwise common plane, the ring torsions proposed for polyaniline (Ginder *et al.* 1989), as well as the local changes in the dihedral angle suggested by Ikawa and Fukutome (1990) for selenium helices.

4. Helical versus planar polymers

As a first example of applications of the density-functional methods for periodic chains we study the structures of some simple systems. In the first two subsections we explore why some systems have a planar polymer backbone whereas that of others is helical. This question is related to long-range interactions: neither nearest-neighbour bond lengths nor bond angles (determined by next-nearest-neighbour interactions) need to be modified when changing the polymer from being planar to being helical; first the dihedral angle (i.e. the angle between two neighbouring planes of three neighbouring atoms) describes the difference in structure. Consequently, we will expect the helical polymers to be soft—the structure can easily be modified by varying the dihedral angle—and actually our first examples, sulphur and selenium helices, belong to the softest polymers known.

In the second subsection we discuss why polyethylene has a planar backbone whereas replacing all hydrogen atoms with fluorine atoms, thus arriving at polytetrafluoroethylene, gives a helical polymer.

In the last subsection we explore whether the calculations can reproduce a Peierls distortion in same simple linear chains. As is obvious from the discussion of the preceding Section, this question is of ultimate relevance for studies of the properties of the conjugated polymers like trans polyacetylene.

4.1. *Sulphur and selenium helices*

The structure of a general helical polymer with M atoms per unit can be completely specified by $3M$ geometrical parameters. Thus, for the simplest helices with one atom per unit we need three parameters, and we may, e.g., choose any three out of the following six: the nearest-neighbour bond length q_1, the bond angle α, the dihedral angle γ, the rotational angle v and translational length h describing the structure of the helix, and the distance r of the atoms from the helical axis.

For the helices consisting of either sulphur or selenium atoms we fixed α and optimized q_1 and γ. The resulting total-energy curves as functions of α are shown in figure 4 (Springborg and Jones 1986, 1988).

For the sulphur helices (figure 4 (*a*)) we notice two metastable structures. This agrees with the findings for the S_3 molecule (Jones 1986), but the existence of the metastable

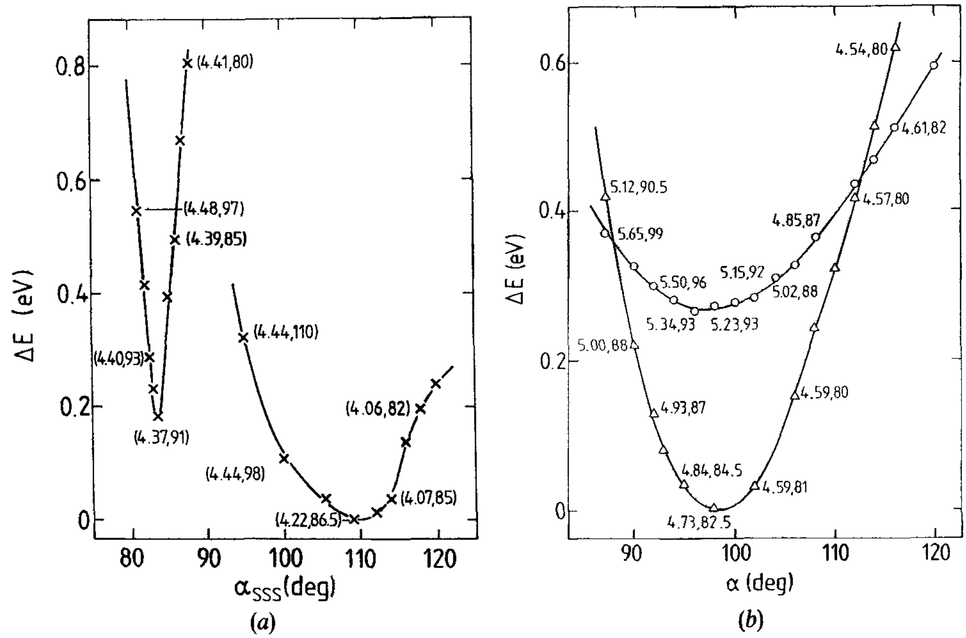

(*a*) (*b*)

Figure 4. Total energy per atom for (*a*) sulphur and (*b*) selenium helices as function of bond angle α. For selected values of α we also give the optimized values of the bond length q_1 and the dihedral angle γ. (Reproduced from Springborg and Jones (1986, 1988).)

structure with the smaller α value has not yet been confirmed by experimental or other theoretical studies.

Also for selenium we found two metastable structures, but their optimized α values are more similar to each other than for sulphur and they have a larger total-energy difference. We add that indications of the existence of a third minimum for $\alpha \simeq 75°$ were observed in the calculations.

Focusing on the minimum for $\alpha = 109°$ for sulphur and for $\alpha = 99°$ for selenium we see that the total energy as a function of α shows the smallest variations for selenium indicating this polymer to be the softest, which agrees with experimental findings.

The optimized structure for sulphur has $\alpha = 109°$, $q_1 = 4{\cdot}22$ a.u., $\gamma = 86{\cdot}5°$, and $v = 107{\cdot}3°$. About 40 years ago it was discussed (Pauling 1949, Prins *et al.* 1956), whether polymeric sulphur consisted of so-called 7/2 or 10/3 helices. Here, a n/m helix denotes a helix for which we have n repeated units (here atoms) along m full turns. An n/m helix has accordingly $v = 2\pi m/n$ and the two proposed helices correspond to $v = 103°$ and $v = 108°$, respectively; both close to the optimized value. As a curiosity it shall be added that using only translational symmetry and comparing 7/2 and 10/3 helices by performing equivalent calculations would require unit cells of 70 atoms. The use of the full helical symmetry is accordingly a very great computational simplification as we only need one atom per unit cell. Finally, the experimental structure of polymeric sulphur gives $\alpha = 106°$, $q_1 = 3{\cdot}90$ a.u., and $\gamma = 85{\cdot}3°$ (Donohue 1974). Except for an overestimate in q_1 our values agree well with those.

The optimized selenium helix has $\alpha = 99°$, $q_1 = 4{\cdot}66$ a.u., $\gamma = 81{\cdot}5°$, and $v = 109{\cdot}7°$. The smaller value of α for Se than for S may be explained as due to the larger importance of virtual d functions for Se than for S. We may compare the optimized values with those for crystalline, trigonal Se. Its crystal structure may be considered a distorted simple cubic crystal and looking along the (111) direction one may recognize parallel Se helices. However, non-negligible interchain interactions may obscure the comparison. This structure has $\alpha = 103{\cdot}1°$, $q_1 = 4{\cdot}49$ a.u., $\gamma = 100{\cdot}7°$, and—per definition—$v = 120°$, which differ somewhat from the values for the isolated helix.

In figure 5 (*a*) and 5 (*d*) we show the band structures for the optimized sulphur and selenium helices. In both cases we recognize well separated valence bands of which the lowest is mainly due to s functions whereas the other two plus the lowest conduction band have large p components. The structures are clearly semiconducting.

Restricting ourselves to zig–zag chains (i.e., fixing either $\gamma = 180°$ or $v = 180°$) we find the lowest total energy for $\alpha = 109{\cdot}5°$ and $q_1 = 4{\cdot}27$ a.u. for sulphur and for $\alpha = 124°$ and $q_1 = 4{\cdot}54$ a.u. for selenium. While the values for the zig–zag sulphur chains are very similar to those of the corresponding helix (in agreement with the discussion at the beginning of this Section) those of the planar and helical Se polymers differ significantly. It is interesting to notice that the calculations indicate the zig–zag chains

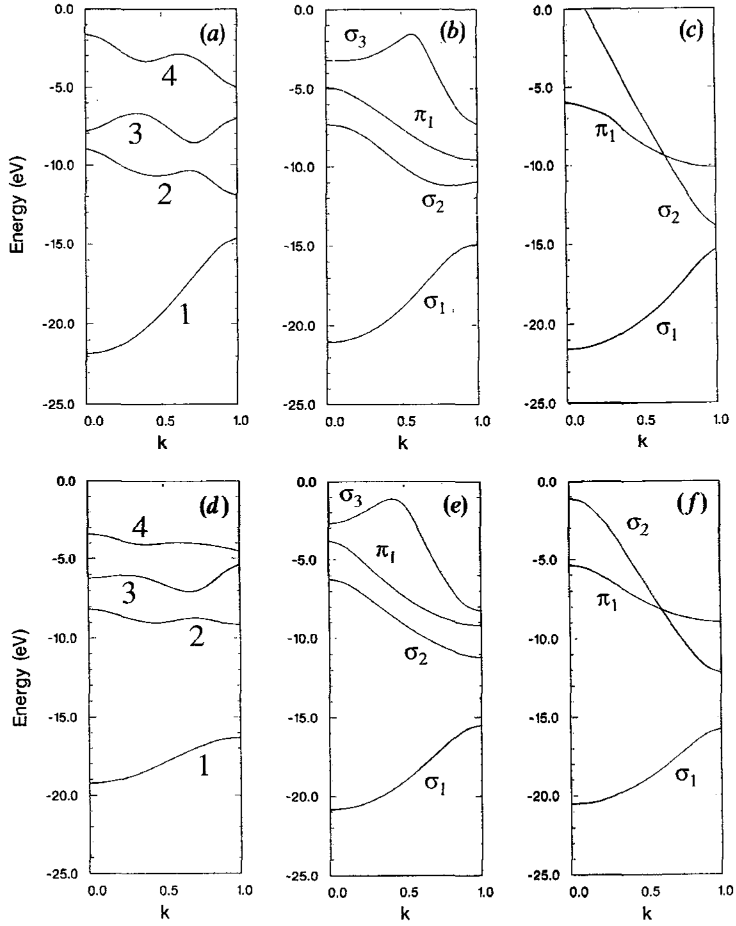

Figure 5. Band structures for (*a*)–(*c*) sulphur and (*d*)–(*f*) selenium chains. (*c*) and (*f*) are those of the optimized linear chains, (*b*) and (*e*) those of the zig–zag chains, and (*a*) and (*d*) those of the helices. The dashed lines represent the Fermi level. (Reproduced from Springborg (1989 *a*).)

and the helices to have comparable total energies. The band structures (figure 5 (*b*) and 5 (*e*)) show that in this case both chains become metallic with two bands crossing the Fermi level.

For the linear chains (i.e. restricting $v = 2\pi$ and $\alpha = \pi$) the lowest total energy was found for $q_1 = 4{\cdot}15$ a.u. for sulphur and for $q_1 = 4{\cdot}59$ a.u. for selenium. For these chains the total energy is significantly higher than for the zig–zag chains and the helices. Also the linear chains are metallic (figure 5 (*c*) and (5 (*f*)).

The metallic zig–zag chains have two types of bands crossing the Fermi level: one σ band which is formed by orbitals that are symmetric with respect to reflection in the plane of the nuclei and one π band constructed from antisymmetric orbitals. In a further study of planar selenium chains but of lower symmetry we found (Springborg *et al.* 1992) that the chains remained metallic with both σ and π bands crossing the Fermi level. However, for the non-planar polymer one can no longer separate the orbitals into σ and π orbitals and all bands will interact producing avoided crossings. Ultimately these will be so large that gaps may open up at the Fermi level as for the optimized helices. We therefore suggest that the occurrence of helical and not planar sulphur and selenium polymer chains is due to a ‘helical Peierls’ transition’.

It should finally be added that there exist more density-functional studies on crystalline Se, in which the full three-dimensional structure is included (see, e.g., Joannopoulos *et al.* (1975), Wendel *et al.* (1977), and Isomäki and von Boehm (1980)). We consider these, however, to be beyond the scope of the present review.

4.2. *Polyethylene and polytetrafluoroethylene*

The situation is different for polyethylene and polytetrafluoroethylene. Each chain consists of a zig–zag carbon backbone and to each carbon atom two hydrogen atoms for polyethylene and two fluorine atoms for polytetrafluoroethylene are attached, such that the carbon atoms become approximately tetrahedrally coordinated. The dihedral angle γ of the carbon backbone of polyethylene is 180°, whereas that of polytetrafluoroethylene is slightly smaller. Since both compounds are wide-gap insulators—independent of γ—we cannot hold a helical Peierls transition responsible for the difference.

Being insulators and having relatively small unit cells these compounds are fairly easy to study theoretically since the summations both in direct space and in reciprocal space converge fast. There exists therefore a number of theoretical studies of their electronic properties (see, e.g., Seki *et al.* (1986) and Springborg and Lev (1989)). Among these are the first density-functional studies on polymers by Falk and Fleming (1973, 1975), who, however, used a muffin-tin approximation for the potential (spherical symmetry inside the muffin-tin spheres; constant in the interstitial region). As demonstrated by Seki *et al.* (1986) this led to severe errors in the band structures for polyethylene.

In their work, Kasowski *et al.* (1980 *a*) included the full potential. Their calculations were, however, not self-consistent.

Our own calculations (Springborg and Lev 1989) on the other hand both were self-consistent and treated the full potential. The results of these suggest a simple explanation for the difference between the structure of the carbon backbones of the two compounds. In the computational scheme we split the three-dimensional space into atom-centred spheres and the interstitial region (see Section 2). This makes it possible to ascribe each atom a specific number of electrons (i.e. simply those inside the corresponding sphere), and when using the same sphere sizes for the same type of atoms but for different compounds these so determined numbers give qualitative insights into electronic distributions. For polyethylene and polytetrafluoroethylene we thus examine the number of electrons inside the carbon spheres. One should, however, be careful in doing so. As figure 2 shows, any wavefunction centred on one site contains a tail (and hence an electron density) inside the sphere of any other atom. Since we have more fluorine orbitals that hydrogen orbitals this simple argument will predict a larger number of electrons inside the carbon spheres for polytetrafluoroethylene than for polyethylene.

The calculations show the opposite trend. Therefore, an even stronger effect leads to a net electron flow from carbon to fluorine which is larger than that from carbon to hydrogen. This effect is due to the large electronegativity of fluorine and indicates the existence of substantial electrostatic interactions in polytetrafluoroethylene. It now turns out that for a helical chain the fluorine atoms of next-nearest carbon atoms become further apart than for the planar chain, thereby decreasing their electrostatic repulsion. The calculations indicate furthermore that upon reducing γ the electron transfer from carbon to fluorine is slightly decreased. We therefore believe differences in electrostatic forces between polarized units to be the reason for the structural difference between polyethylene and polytetrafluoroethylene. Finally, also the density-functional calculations of Kasowski *et al.* (1980*a*) predict large electron densities on the fluorine atoms for polytetrafluoroethylene.

It should be added that the most recent density-functional calculations on polyethylene (Mintmire 1991) predict a much weaker dependence of the total energy on γ than ours do, and bring the dependence into better agreement with results of other studies.

Polyethylene is interesting for one further reason. It is the first organic polymer for which experimental valence band structures have been reported (Seki *et al.* 1986, Fujimoto *et al.* 1987). In figure 6 we show the experimental band structures together with the calculated ones. In order to make a comparison directly possible, the bands correspond to a translational symmetry with two CH_2 units per unit cell. Except for a constant shift of about 2 eV the agreement between theory and experiment is very good. Experimentally the absolute uppermost part of the valence bands is difficult to determine. The prediction of a very steep band determining the top of the valence bands was apparently in conflict with other studies but was later verified experimentally (Ueno *et al.* 1990).

The theoretical band structures of polytetrafluoroethylene calculated with one CF_2 unit per cell are shown in figure 7 for $\gamma = 180°$ and for $\gamma = 165°$. Experimental X ray photoelectron spectroscopy (XPS) spectra have been reported by Pireaux and coworkers (Pireaux *et al.* 1974, Delhalle *et al.* 1977). The total valence-band width was measured to be 27–30 eV, whereas we find 25–26 eV. That of the uppermost seven bands and that of the lowest two bands was 14 and 3·7 eV, respectively, according to the experiments, and 13 and 3·3–4·5 eV according to figure 7. The agreement is thus seen to be good.

Seki *et al.* (1986) made a detailed comparison between their experimental band structures and those of a number of theoretical studies. They demonstrated that the Hartree–Fock approximation led to up to 50% too wide bands, in agreement with the results of other comparisons for other systems.

We finally add that Mintmire *et al.* (1987) have calculated the photoelectron spectrum of polyvinylidene fluoride using their density-functional method. In some sense this polymer is intermediate between polyethylene and polytetrafluoroethylene.

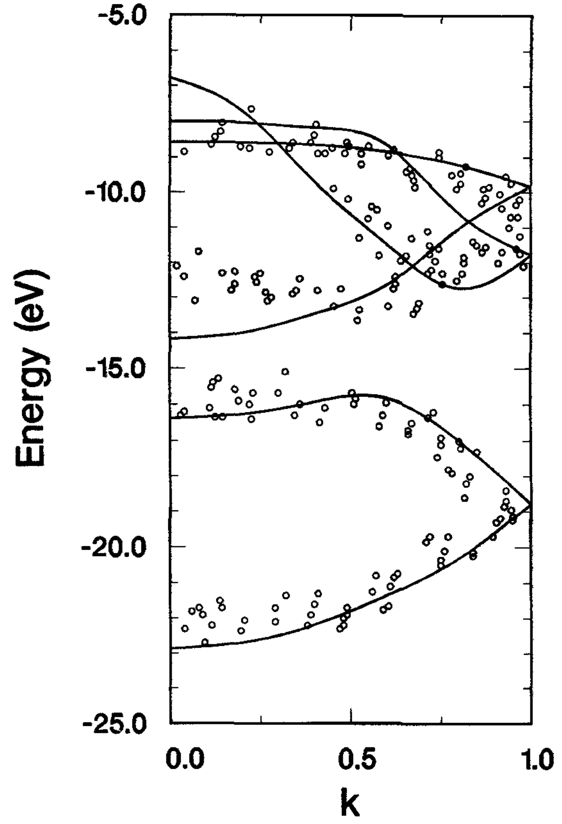

Figure 6. Theoretical (full curve) and experimental (points; from Seki *et al.* (1986)) band structures of polyethylene. The latter have been shifted upwards by 2 eV. (Reproduced from Springborg and Lev (1989).)

4.3. *Some simple, linear chains*

Ashkenazi *et al.* (1989) presented results of density-functional calculations on crystalline trans polyacetylene. Their calculations gave the lowest total energy for a structure lacking a C–C bond-length alternation in conflict with the simplest picture presented in Section 3 in which a Peierls mechanism is held responsible for a C–C bond-length alternation. They suggested that their results showed that strong correlation effects beyond those included in the local-density approximation are responsible for the experimentally observed bond-length alternation. Since their conclusion has been questionned (Mintmire and White 1989, Springborg *et al.* 1990 *a*, 1991 *b*), their findings call for further studies of the so-called dimerization of polymers.

In order to be able to perform many accurate calculations and simultaneously explore the structural properties in detail we decided (Eriksson *et al.* 1993) to study linear, monoatomic chains. We studied chains of hydrogen, lithium, boron, carbon, or nitrogen atoms and focused on whether the total energy could be lowered upon a bond-length alternation.

In the discussion of the results it is useful to consider a simple model that includes correlation effects, like the Hubbard Hamiltonian

$$\hat{H} = t\sum_{n,s}(c^{\dagger}_{n+1,s}c_{n,s} + c^{\dagger}_{n,s}c_{n+1,s}) + U\sum_{n}c^{\dagger}_{n,\alpha}c^{\dagger}_{n,\beta}c_{n,\beta}c_{n,\alpha}, \qquad (17)$$

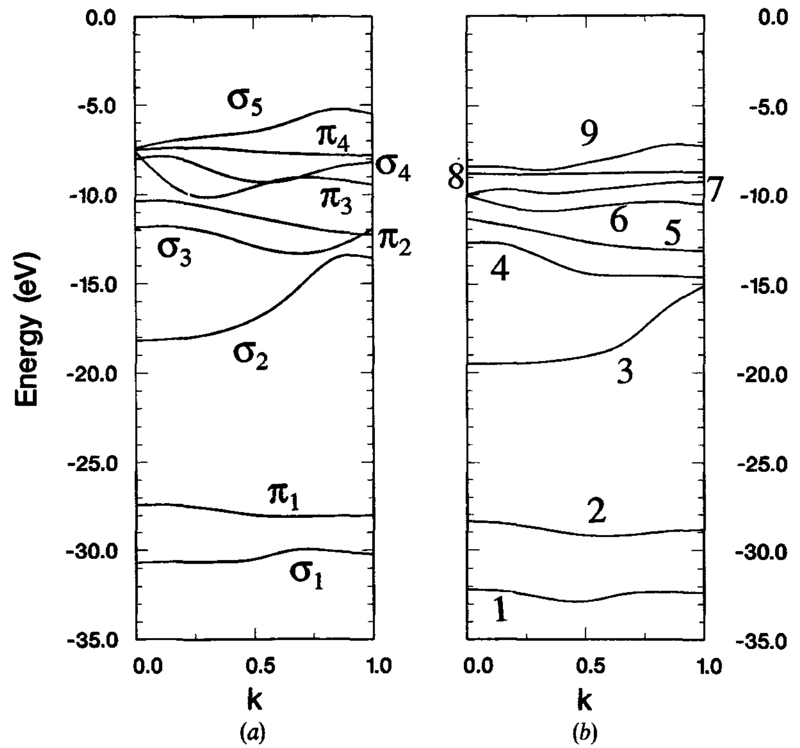

Figure 7. Band structures of polytetrafluoroethylene for (*a*) $\gamma = 180°$ and (*b*) $\gamma = 165°$. (Reproduced from Springborg and Lev (1989).)

which is related to $\hat{H}_\pi$ of equation (6) but which considers constant on-site terms and nearest-neighbour hopping integrals, excludes more distant interactions, and includes an extra term due to on-site correlation. The ratio $r = U/(4t)$ describes whether correlation ($r \gg 1$) or single-particle ($r \ll 1$) effects dominate.

Hydrogen has one electron per atom and lithium has one valence electron per atom. We will thus expect both these systems to prefer a structure with a bond-length alternation. The calculations confirm this. For Li the optimized undimerized chain (the chain without bond-length alternation) has bond lengths of 4·95 a.u., and those of the dimerized chain are 4·75 and 5·30 a.u. The band structures of the two chains are shown in figure 8 (*d*) and 8 (*e*) and the occurrence of a gap at the Fermi level when dimerizing is clearly noticed. For the undimerized H chain the lowest total energy occurred for bond lengths of 2·1 a.u. Keeping the unit-cell length fixed the total energy was then lowest for bond lengths of 1·5 and 2·7 a.u., but allowing both bond lengths to relax the system preferred to split into isolated H_2 units. The band structures for these three structures are shown in figure 8 (*a*)–8 (*c*). Compared with those of the Li chain we notice that the bands are much wider for the H chain, such that the ratio $U/(4t)$ may be much smaller for H than for Li. Therefore, correlation effects (as given by U) play only a minor role and will not prevent the system from splitting into isolated units with localized electrons.

For B, C, and N chains we will expect deep lying σ valence bands formed by *sp* hybrids. Closest to the Fermi level we will have π bands from the *p* orbitals perpendicular to the chain direction. Since the π bands are doubly degenerate and

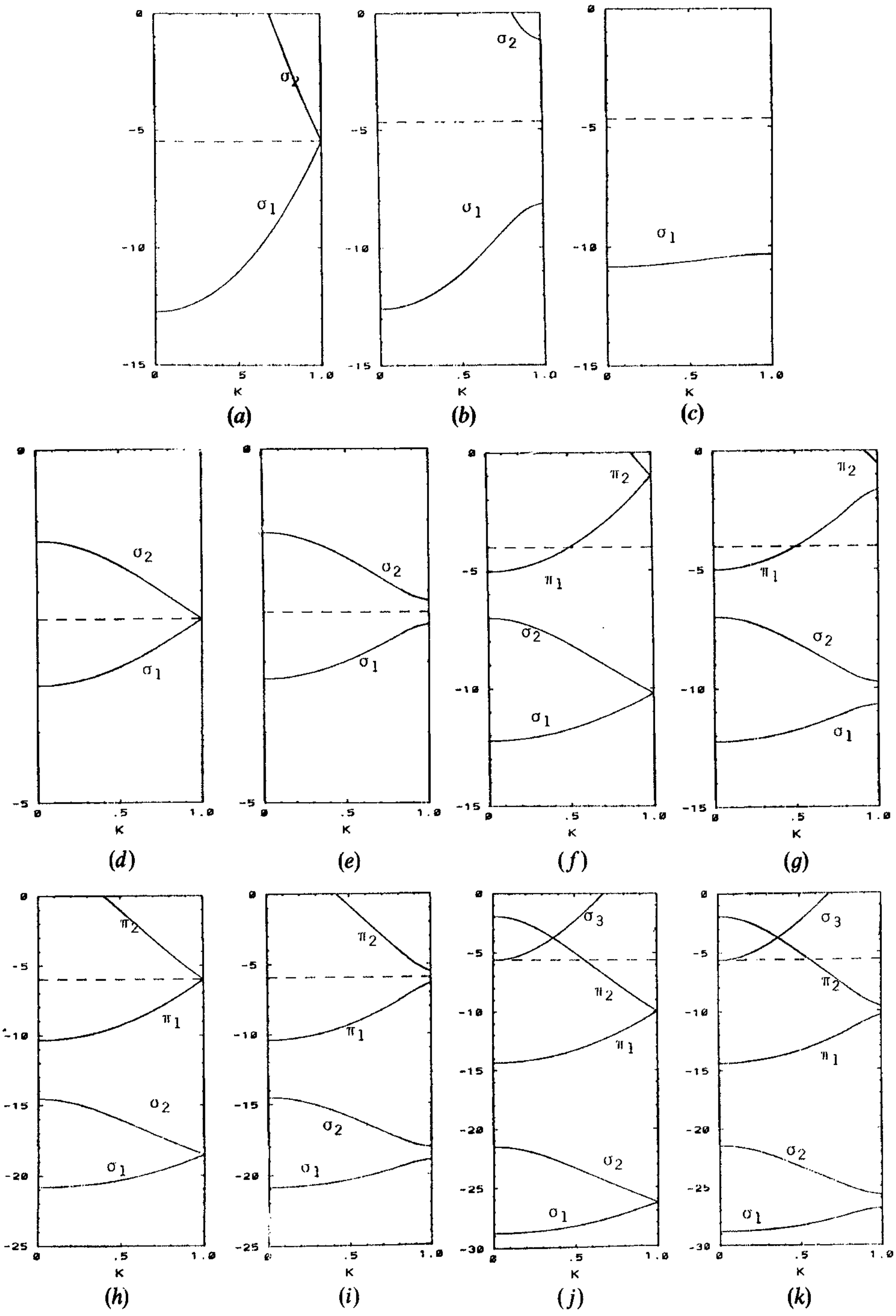

(*a*) (*b*) (*c*)

(*d*) (*e*) (*f*) (*g*)

(*h*) (*i*) (*j*) (*k*)

Figure 8. Band structures for various linear chains with two identical atoms per unit cell. The chains are (*a*)–(*c*) H, (*d*) and (*e*) Li, (*f*) and (*g*) B, (*h*) and (*i*) C, and (*j*) and (*k*) *N* chains, and the two nearest-neighbour bond lengths are (*a*) (2·1,2·1), (*b*) (2·7,1·5), (*c*) (5·0,1·5), (*d*) (4·95,4·95), (*e*) (4·75,5·30), (*f*) (2·90, 2·90), (*g*) (3·10,2·80), (*h*) (2·55,2·55), (*i*) (2·60,2·45), (*j*) (2·35,2·35), and (*k*) (2·30,2·40) a.u. The dashed lines are the Fermi levels and all energies are in eV.

hence can contain four electrons per atom, we will expect band fillings of 1/4, 1/2, and 3/4 for undimerized B, C, and N chains, respectively. Only the carbon chains should accordingly be expected to show the preference of a dimerization (B and N chains may lower their total energy upon a tetramerization; this was, however, not examined here). This prediction is confirmed by the calculations. For B the optimized bond lengths became $d_1 = 2{\cdot}90$ a.u., and for N $d_1 = 2{\cdot}35$ a.u. For the carbon chains the lowest total energy for undimerized chains was found for $d_1 = 2{\cdot}55$ a.u., and the global minimum for bond lengths of $d_1 = 2{\cdot}60$ and $d_2 = 2{\cdot}45$ a.u.

The band structures for these three types of chains (figure 8) show that the simplest picture to a large extent is correct, except that the N chains have low-lying σ conduction bands. The bond-length alternations lead in all cases to the occurrence of gaps but only for the carbon chains this changes the material from metallic to semiconducting.

The calculations thus indicate that we do find a bond-length alternation in the cases where such is to be expected and in no other cases. Although being the only density-functional study explicitly devoted to this topic, this gives confidence in applying density-functional methods in studying structural properties of polymers; including the conjugated polymers to be discussed next.

5. Trans polyacetylene

As mentioned in Section 3, trans polyacetylene is the prototype of the conjugated polymers. It is moreover the polymer for which most density-functional studies exist. We will therefore discuss this material in some detail and give only a brief discussion of some other conjugated polymers in Section 6.

Falk and Fleming (1975) applied their LMTO-based density-functional method on polyacetylene even before the large interest in that material developed. Their results are, however, at variance with almost all other later results giving two bands crossing the Fermi level. We will therefore not comment further on those.

Kasowski *et al.* (1980 *a*) presented both band structures and electron densities for different isomers of polymers, including the trans isomer. Although being non-selfconsistent they are pioneering in the sense that they gave the first correct band structures for trans polyacetylene as obtained with a density-functional method.

Since the dramatic changes in the properties of trans polyacetylene are a consequence of doping or photoexcitation, Kasowski *et al.* (1980 *b*) studied also the band structures of trans polyacetylene doped with various smaller molecules. We shall return to that paper in this section.

The first density-functional optimization of structural parameters of trans polyacetylene is due to Mintmire and White (1983 *a*). They did find a bond-length alternation for the optimized structure, although slightly smaller than experiments predicted. As is common within density-functional methods, the energy gap separating valence and conduction bands was roughly 50% too small.

In a series of later papers, Mintmire and coworkers have extended their density-functional study of the electronic properties of trans polyacetylene. They have thereby demonstrated a good agreement between their calculated data and the experimental ones. The properties they have studied include dielectric properties (Mintmire and White 1983 *b*, *c*) and photoelectron spectra (Mintmire and White 1983 *b*, *d*, Mintmire *et al.* 1987). We have later calculated many of the same properties using the LMTO-based method (Springborg *et al.* 1991 *b*). Since the results only show smaller differences, we will here concentrate on our own results.

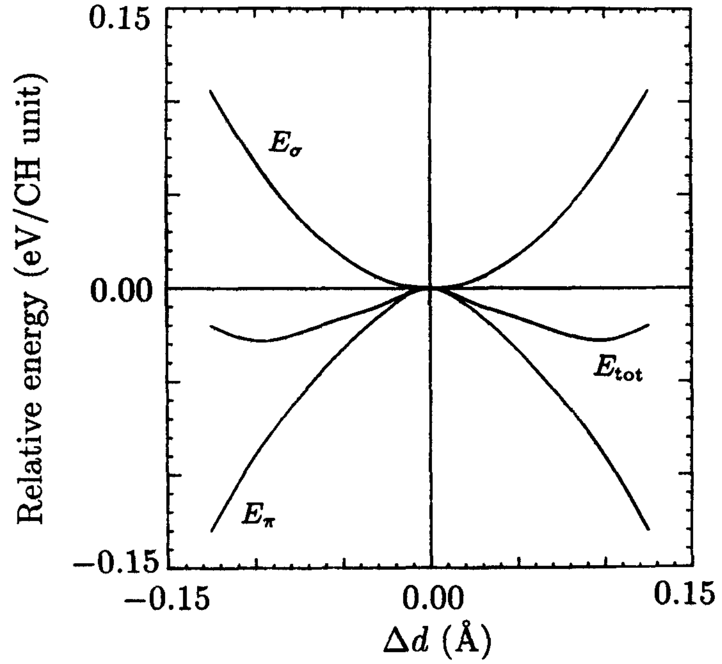

Figure 9. Total energy (E_{tot}), π electron energy (E_π), and the remainder (E_σ) in eV per CH unit for periodic trans polyacetylene as a function of the difference in C–C bond lengths $\Delta d = d_2 - d_1$. (Reproduced from Springborg *et al.* (1991 *b*).)

von Boehm *et al.* (1987) have used their Gaussian-based density-functional method in calculating band structures, densities of states, and electron densities of trans polyacetylene, giving results in good agreement with those of other studies.

In 1989 two density-functional studies of structural properties of trans polyacetylene were published in which the material was considered a three-dimensional solid. Ashkenazi *et al.* (1989) whose results already have been mentioned found both for realistic and for increased interchain distances the lowest total energy for a structure with no bond-length alternation. These results were interpreted as showing that density-functional calculations with a local approximation were not sufficiently accurate for those materials. The results of Vogl and Campbell (1989, 1990) gave, on the other hand, a non-vanishing bond-length alternation, although being smaller than experimentally observed. Due to the results of the preceding Section as well as those on a number of other conjugated polymers we suggest the following explanation for the surprising results of Ashkenazi *et al.* Three-dimensional effects may tend to decrease the bond-length alternation. Moreover, the plane-wave basis set used by Ashkenazi *et al.* may not be sufficiently accurate when the interchain distances are large such that there are both regions with almost no electrons and regions with localized electrons.

Before turning to our own results two more density-functional studies shall be mentioned. Ye *et al.* (1989 *a*) studied a finite C_nH_{n+2} molecule with *n* up to 20. They did find a C–C bond-length alternation. Using a Slater-transition-state description in calculating the optical gap they found a value of about 1·9 eV in good agreement with experiments and in contrast to the usual failure of the local-density approximation.

Finally, Zemach *et al.* (1989*a*, *b*) studied optical properties of crystalline trans polyacetylene applying a LMTO basis set. Their results give a surprisingly large difference dependent on neighbouring chains being parallel or antiparallel. This is in contrast to common expectations as well as to the more recent results of Vogl and Campbell (1990).

We shall now give a more detailed discussion of our own results, mentioning others where appropriate.

We first consider a periodic chain with alternating C–C bond lengths d_1 and d_2. The H atoms are assumed placed along the negative C–C–C bond-angle bisectors, and from calculations on chains with $d_1 = d_2$ it was found that C–H bond lengths of 2·10 a.u. were realistic. Denoting the C–C–C bond angle γ we found (Springborg *et al.* 1991 *b*) the lowest total energy for $d_1 = 2{\cdot}58$ a.u., $d_2 = 2{\cdot}76$ a.u., and $\gamma = 128°$. Experimental studies have given $d_1 = 2{\cdot}57$ a.u. and $d_2 = 2{\cdot}72$ a.u. (Yannoni and Clarke 1983), and our values agree thus well with the experimental findings.

We will ultimately be interested in studying solitons and polarons and follow accordingly the strategy outlined in Section C. The two metastable structures are the above-mentioned optimized one and that obtained by interchanging d_1 and d_2 (see figure 10). Each carbon atom defines a site and we need to ascribe a structural parameter x_n to the nth site. Keeping the hydrogen atoms placed relative to the carbon atoms as above it turned out that the smallest variations in the total energy were found for displacements of the carbon atoms parallel to the polymer axis. As suggested in Section 3, x_n is thus to be related to this displacement u_n through equation (12).

The total energy varies then as shown in figure 11 for the periodic structures (13) as a function of $\Delta d = d_1 - d_2 = 4\sin(\gamma/2)x_0$. We have split the total energy into E_π being the integral of the π valence energies and the remainder (the elastic energy) E_σ.

The π valence-band structures as functions of x_0 determine most of the parameters of $\hat{H}_\pi$ of equations (6) and (10). We will, however, add one more effect. Referring to figure 10(*c*) and 10(*d*) we notice that the carbon atoms closest to the solitons or polarons have nearest-neighbour bond orders which totally add up to less than the

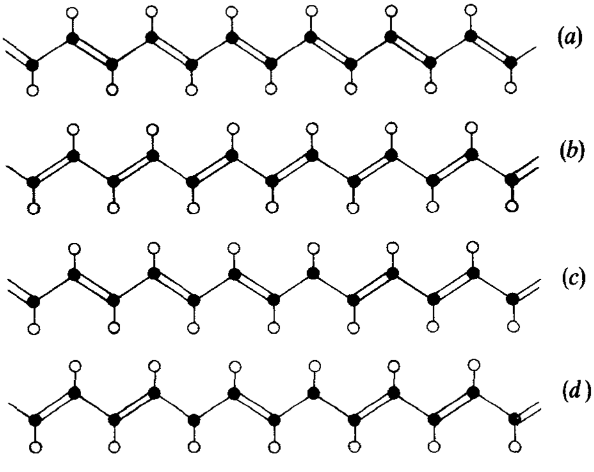

Figure 10. Schematic representation of (*a*), (*b*) the two energetically degenerate structures of trans polyacetylene, (*c*) a soliton, and (*d*) a polaron. (Reproduced from Springborg *et al.* (1991 *b*).)

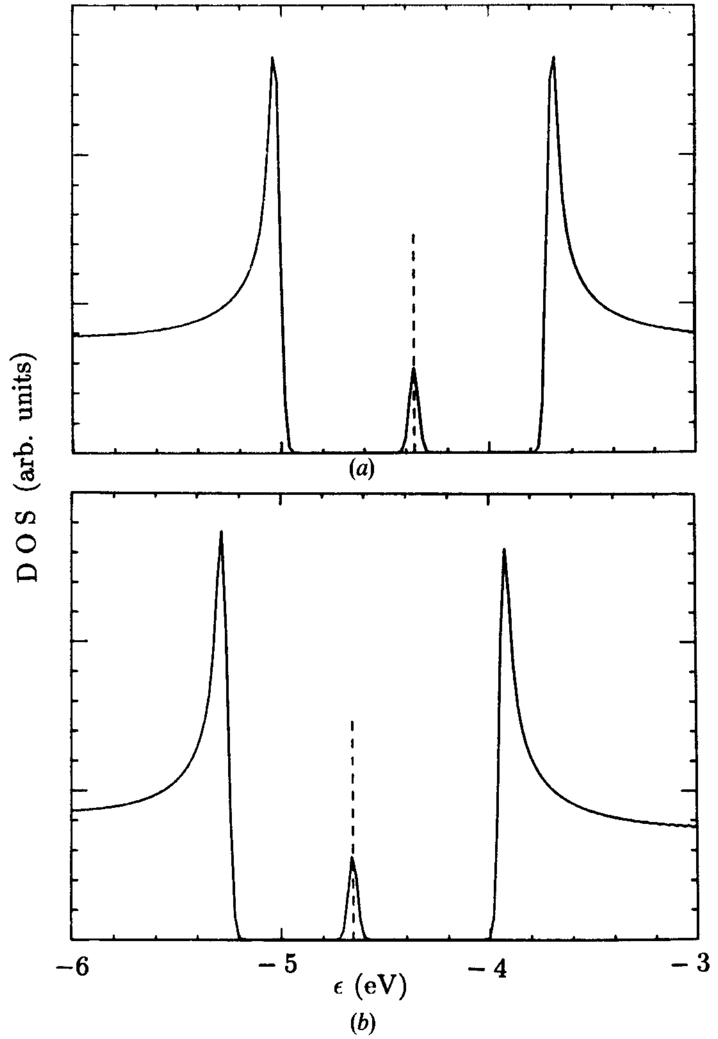

Figure 11. The π electron density of states around the gap for a trans polyacetylene chain with two solitons. In (*a*) we have used the parameters of Su *et al.* (1979, 1980), in (*b*) ours. The vertical dotted lines are the Fermi level for the neutral system. (Reproduced from Springborg *et al.* (1991 *b*).)

ideal value of four. We consider these atoms to be more naked and hence to attract electrons. This effect can be modelled through on-site terms ϵ_n which depend on the sum of the nearest-neighbour bond lengths. We have estimated this dependence by performing first principles calculations on periodic, undimerized chains for which the CH units were displaced perpendicular to the polymer axis. This is described in detail elsewhere (Springborg *et al.* 1991 *b*) and defines an extra so-called ionicity term in $\hat{H}_\pi$.

The resulting π electron model Hamiltonian H_π is related to that of Su *et al.* (1979, 1980) with, however, some important differences. Su *et al.* do not include the above-mentioned ionicity term and have accordingly constant on-site terms. Furthermore, they only consider nearest-neighbour hopping integrals, whereas we also have next-nearest-neighbour interactions. Finally, we find the nearest-neighbour hopping integrals to depend stronger on the bond lengths as Su *et al.* do.

E_σ of figure 9 is to determine $\hat{H}_\sigma$ of equation (11). Keeping only nearest-neighbour terms (all next-nearest-neighbour distances were constant in the first-principles calculations) it turned out that the function f_1 was to be a fourth-order polynomial, whereas Su *et al.* assume it to be harmonic.

According to the model of Su *et al.* solitons of the form (14) are stable when adding or removing an electron from the chain or when changing the spin of one electron (i.e., corresponding to exciting one electron from the top of the valence band to the bottom of the conduction band). The parameter L is found to be the same in all three cases and the soliton induces a state exactly at the mid-gap position (see figure 11 (*a*)). Moreover, this soliton-induced orbital has non-vanishing components only on every second site (see figure 12 (*a*)). Deviations from these predictions are often taken as indications of the importance of correlation effects as, e.g., described by U of equation (17). Thus, the fact

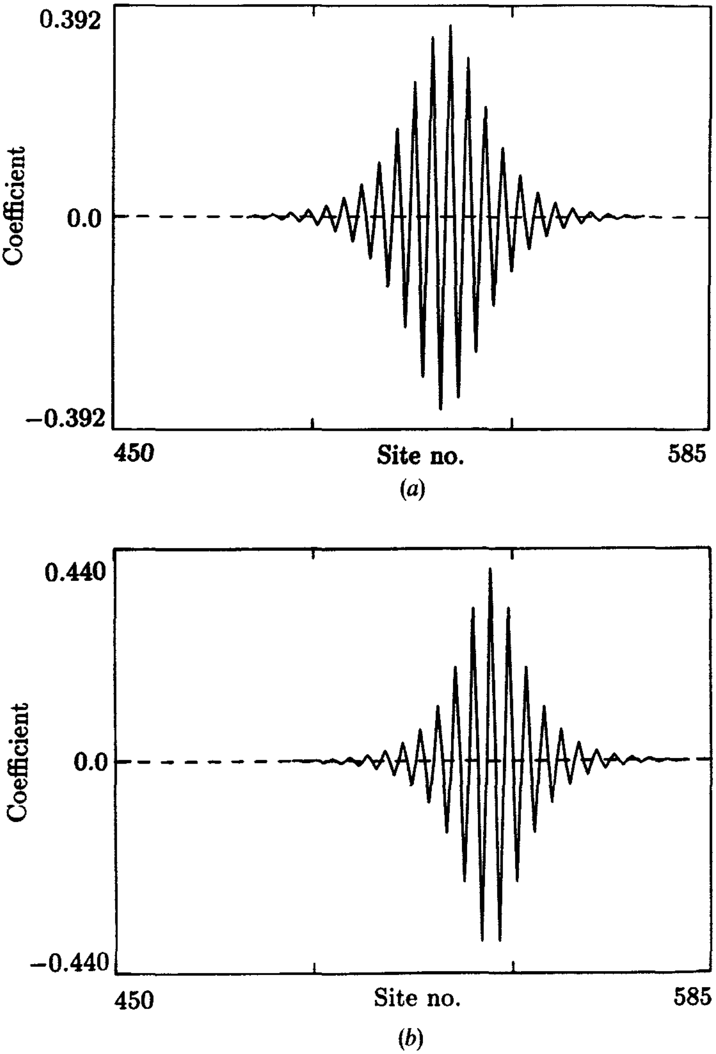

Figure 12. The coefficient to the carbon-centred basis functions as a function of site for the soliton-induced gap states. (*a*) and (*b*) corresponds to (*a*) and (*b*) in figure 11. (Reproduced from Springborg *et al.* (1991 *b*).)

that the gap states have been found $\Delta\epsilon = 0{\cdot}1$–$0{\cdot}2$ eV off the mid-gap position towards the valence-band edge depending on spin and charge (Tanaka *et al.* 1980 *a*, *b*, Feldblum *et al.* 1982, Vardeny *et al.* 1983 *a*, *b*, Chung *et al.* 1984) has been used in estimating large values of U (Baeriswyl *et al.* 1986):

$$\Delta\epsilon = U/(3L), \tag{18}$$

with L being the width of the soliton (see equation (14)).

Using our parameters we find gap-states away from the mid-gap position (see figure 11 (*b*)), which position moreover depends weakly on charge and spin of the system. The optimized values of L are reduced by more than 50% compared with those of the model of Su *et al.* Our single-particle model can thus account for about half the observed shifts of the gap states. Moreover, L is significantly smaller than usually assumed and using equation (18) this in total means that the Hubbard U is far smaller than normally considered realistic.

Our model does, however, only lead to small (compared with identically vanishing in the model of Su *et al.*) components of the soliton-induced states on every second site (see figure 12 (*b*)), which are not as large as those that are observed experimentally.

A further difference between the predictions of our model and those of the model of Su *et al.* is that our model does not support the existence of polarons, whereas that of Su *et al.* does. However, the experimental observations of only one gap state support the existence of solitons and not of polarons.

Our approach for studying the properties of solitonic and polaronic defects is based on parametrizing the results of density-functional calculations on periodic, neutral, undistorted chains within a suitable model Hamiltonian and subsequently applying this in studying the defects. There exists, however, some few attempts of applying density-functional calculations directly in investigating the defects.

For a periodically repeated neutral soliton for which the lattice distortion was assumed obeying equation (14), Kutzler *et al.* (1986) found the solitons to induce states placed asymmetric in the gap in agreement with experiments and our results. Ye *et al.* (1989 *b*) studied a finite, neutral and singly charged molecule. They found a neutral soliton to give a gap state almost exactly at mid-gap, whereas for positively (negatively) charged molecules the gap state appeared closer to the valence (conduction) band edge. Experimentally, the states for the charged systems appear closer to the valence band edge independent of the charge in agreement with the model calculations, but in contrast to the density-functional results of Ye *et al.* The difference may, however, be related to the problems of density-functional calculations in describing unoccupied orbitals.

Vogl and Campbell (1989, 1990) studied also defects in their density-functional calculations on crystalline trans polyacetylene, but had to restrict the width (i.e., the parameters L and Δ of equations (14–16)) of these to be very small. Their results predict a decreasing stability of those due to interchain interactions. Since the existence of the defects appears to be established, these results are somewhat surprising and might be due to the tendency of the local approximation to overestimate the strength of any chemical bond and thus also of interchain bonds (see, e.g., Jones and Gunnarsson (1989)) as well as to the small width of the defect. But also the fact that the real materials are not as crystalline as assumed by Vogl and Campbell as well as temperature effects may be reasons for the difference.

We shall finally demonstrate that the first-principles calculations also can be used in providing useful information on the periodic, defect-free chain. In figure 13 we show the

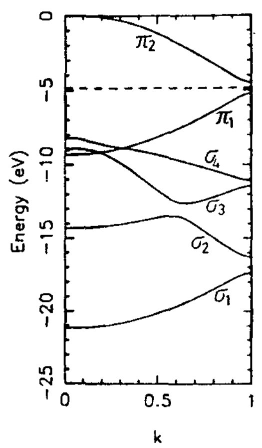

Figure 13. The band structures of the optimized trans polyacetylene chain. The dashed line represents the Fermi level. (Reproduced from Springborg *et al.* (1991 *b*).)

band structures of the optimized structure. Ignoring the avoided crossings between the σ bands as well as the band gaps at the zone edge we may form one hypothetical broad σ band between -20 and -7 eV and a narrower between -14 and -8 eV. The former is due to σ bonds between carbon sp^2 hybrids and the latter to σ bonds between carbon sp^2 hybrids and hydrogen 1*s* functions. Finally, we notice the π bands closest to the Fermi level.

A careful comparison between density-functional bands, Hartree–Fock bands, and experimental information on the band structures (Springborg 1986) shows that the Hartree–Fock bands often are much too broad, whereas the density-functional bands agree well with experimental findings. On the other hand, the gap is underestimated by the density-functional calculations and overestimated by the Hartree–Fock calculations.

The band structures of figure 13 give the density of states shown in figure 14 (*a*). A density of states is related to the spectra provided by photoelectron experiments and including the appropriate photoelectron cross-sections (Springborg *et al.* 1991 *b*) we obtain the XPS and ultraviolet photoelectron spectroscopy (UPS) spectra of figure 14 (*b*) and 14 (*d*). As expected, these are seen to be modulations of the density of states. Furthermore, we recover the well-known fact that UPS is better than XPS in studying orbitals with large *p* components (i.e. here those closest to the Fermi level), whereas XPS should be used in studying orbitals with large *s* components. For comparison we also show the experimental UPS spectra of Rasmusson *et al.* (1991) in figure 14 (*c*). We observe a very good agreement between theory (figure 14 (*d*)) and experiment (figure 14 (*c*)). Moreover, our results agree very well with the earlier density-functional results of Mintmire and coworkers (Mintmire and White 1983 *b*, *d*, Mintmire *et al.* 1987), who presented the first density-functional calculations on optical properties of polymers.

Valence to conduction-band transitions can be measured by electron energy loss spectroscopy (EELS), such that both energy and momentum transfer ($\Delta\epsilon$ and q, respectively) can be determined. For highly crystalline samples one may distinguish between transitions of different symmetries (e.g., π to σ against σ to σ transitions). In figure 15 we show the onsets and maxima for the different types of transitions as function of momentum transfer q. A comparison between the experimental data of Fink and coworkers (Fink and Leising 1986, Fritzsche *et al.* 1989) shows a good agreement

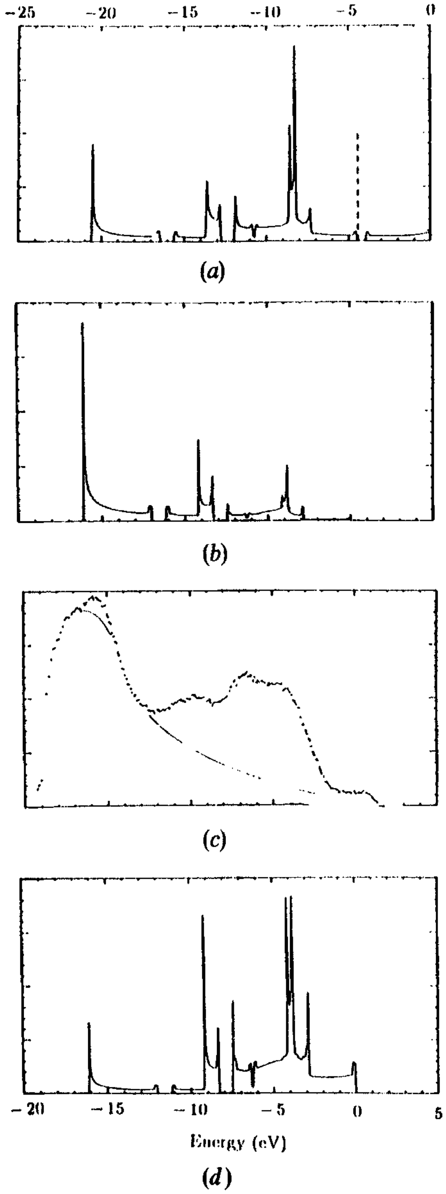

Figure 14. Theoretical (*a*) density of states, (*b*) XPS, and (*d*) UPS spectra. The dashed line in (*a*) is the Fermi energy, which in (*b*) and (*d*) has been chosen as origin. (*c*) is an experimental UPS spectrum from Rasmusson *et al.* (1991). The lower curve here is the background.

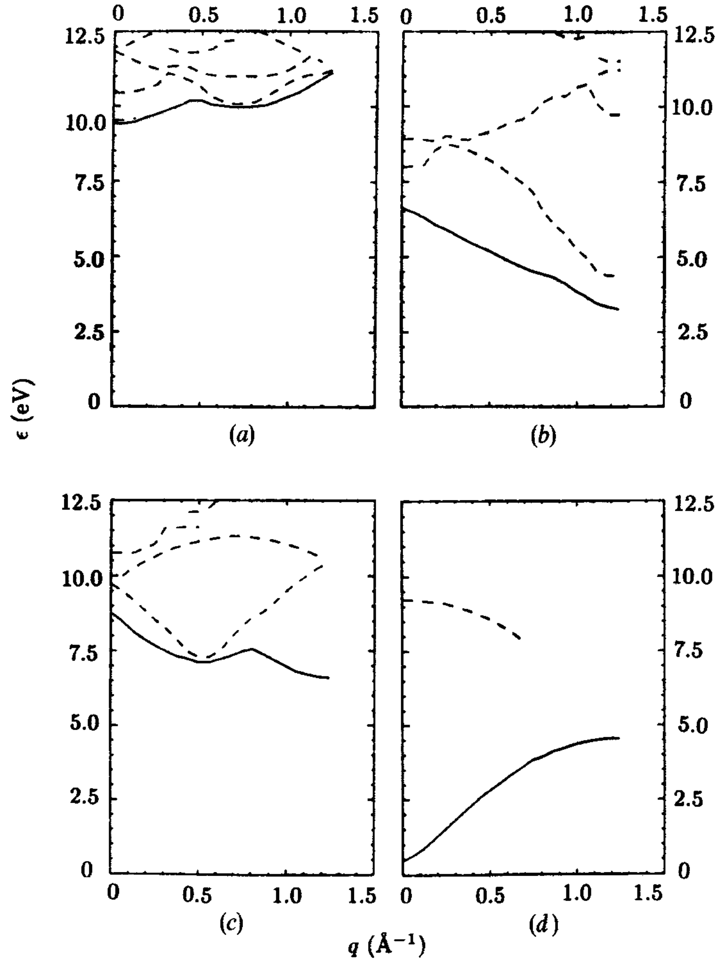

Figure 15. Onsets (full curves) and maxima (dashed curves) for various valence to conduction-band transitions as functions of momentum transfer q. Shown are (*a*) $\sigma \to \sigma$, (*b*) $\sigma \to \pi$, (*c*) $\pi \to \sigma$, and (*d*) $\pi \to \pi$ transitions, with v and c in $v \to c$ labelling the symmetries of the valence and conduction orbitals, respectively. (Reproduced from Springborg *et al.* (1991 *b*).)

except that the onsets generally appear at too low energies (Springborg *et al.* 1991 *b*). However, in figure 15 only single-particle band-to-band transitions are included, and, moreover, matrix-element effects have been ignored. A more complete description can be obtained by calculating the full dielectric function as put forward by Mintmire and White (1983 *b*, *d*). Thereby also the plasmons will be captured, which are responsible for some low-energy features in the spectra. But otherwise the results of figure 15 agree well with those of Mintmire and White.

Compton scattering experiments can be used in determining the electron density in momentum space. We show this density in figure 16, but as is seen this is relatively structureless and only little information is directly extractable. Only a peak for $p_z \simeq 1{\cdot}2$ a.u. may be recognized. This peak can be related to a standing wave along the chain.

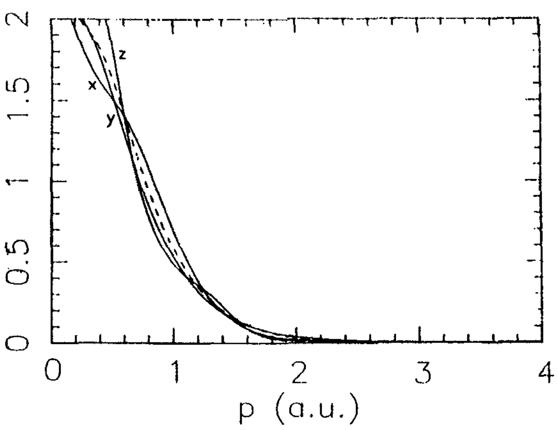

Figure 16. The total electron density in momentum space. x, y, and z is the density along the p_x, p_y, and p_z axis, respectively, and the dashed line is the spherical average. The polymer is assumed placed in the (x, z) plane with the z axis parallel to the polymer axis. (Reproduced from Springborg (1992*c*).)

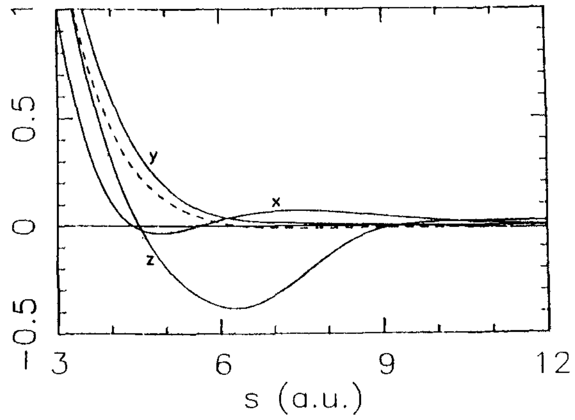

Figure 17. The total reciprocal form factor $B(\mathbf{r})$. x, y, and z is the function along the x, y, and z axis, respectively, and the dashed line is the spherical average. The polymer is assumed placed in the (x, z) plane with the z axis parallel to the polymer axis. (Reproduced from Springborg (1992*c*).)

However, Fourier transforming this density gives the so-called reciprocal form factor $B(\mathbf{r})$. It can be shown (Pattison and Williams 1976, Pattison *et al.* 1977) that $B(\mathbf{r})$ is related to auto-correlation functions in position space:

$$B(\mathbf{r}) = \sum_{i=1}^{\text{occ}} \int \psi_i^*(\mathbf{s}+\mathbf{r})\psi_i(\mathbf{s})\,d\mathbf{s}, \qquad (19)$$

and it thus gives thus information about extension, nodes, and shape of the wavefunctions in position space.

We show in figure 17 the calculated $B(\mathbf{r})$. The considerably more structured z component than the other components demonstrates the delocalization of the electrons in this direction and the difference between this component and the others may be used in experimentally studying chain alignment.

In closing this Section we finally mention that the substantial interest in trans polyacetylene largely is due to the changes in its physical properties upon doping. Our studies have so far mainly considered the dopants as a passive electron reservoir. However, their presence may lead to more changes than just a change in the total number of electrons. In order to explore this question we are currently studying the interactions between a trans polyacetylene chain and periodically distributed dopants. These results (Springborg *et al.* 1991 *a*, Eriksson and Springborg 1992) indicate that dopant orbitals appear very close to the Fermi level such that the dopants should be incorporated in a more complete model. This is in agreement with the early density-functional results of Kasowski *et al.* (1980 *b*). The results indicate furthermore polymer–dopant hopping integrals of the order of 0·5 eV; i.e. certainly non-negligible. This value may, however, be considered reasonable when remembering that the dopant-induced electrical conductivities are very large (up to 10^5 S cm^{-1}) and that the polymer chains do not have macroscopic lengths such that some charge transfer has to take place between different chains; may be assisted by the dopants. These results agree with the electron spin resonance (ESR) results of Bernier and coworkers (El-Khodary and Bernier 1986, Rachdi and Bernier 1986, Fite *et al.* 1987).

6. Other conjugated polymers

The model of Su *et al.* (1979, 1980) provides a useful phenomenological framework for describing the properties of the conjugated polymers. However, any quantitative statements about a specific material as well as detailed comparisons between different related compounds require more detailed, quantitatively correct, descriptions of the materials of interest. In this spirit we have studied a number of conjugated polymers of which some are shown in figure 18. We will here summarize the main findings with special emphasis on a comparison with trans polyacetylene.

6.1. *Cis polyacetylene*

Cis polyacetylene (figure 18 (*a*)) resembles trans polyacetylene and has as the only difference a slightly more complicated carbon backbone. As a consequence of this difference, cis polyacetylene without C–C bond-length alternation has two CH units per unit cell, when making use of the full (zig–zag) symmetry, whereas the equivalent trans polyacetylene has a higher symmetry and may be described with only one CH unit per repeated unit. A further consequence is that the two forms differing in the alternation of the C–C bond lengths (i.e. the cis-trans isomer with the shorter double-bonds parallel to the polymer axis and the trans-cis isomer for which the longer single-bonds are parallel to the polymer axis) need not be energetically degenerate.

Another consequence is that the bands will not meet pairwise at the zone edge for the undimerized chain (which has non-alternating C–C bond lengths). This can be seen in figure 19 in which we show the band structures of the undimerized, the cis-trans, and the trans-cis isomers of cis polyacetylene (Springborg 1986). Comparing the bands of figure 19 with those for trans polyacetylene (figure 13) we notice first of all that the π valence bands have for cis polyacetylene the maximum for $k=0$ but that it appears at $k=1$ for trans polyacetylene. This is solely a consequence of the formalism in which we define basis functions in local coordinate systems such that the p functions of π symmetry in neighbouring unit cells are antiparallel for cis and parallel for trans polyacetylene. This difference can accordingly *not* be measured experimentally.

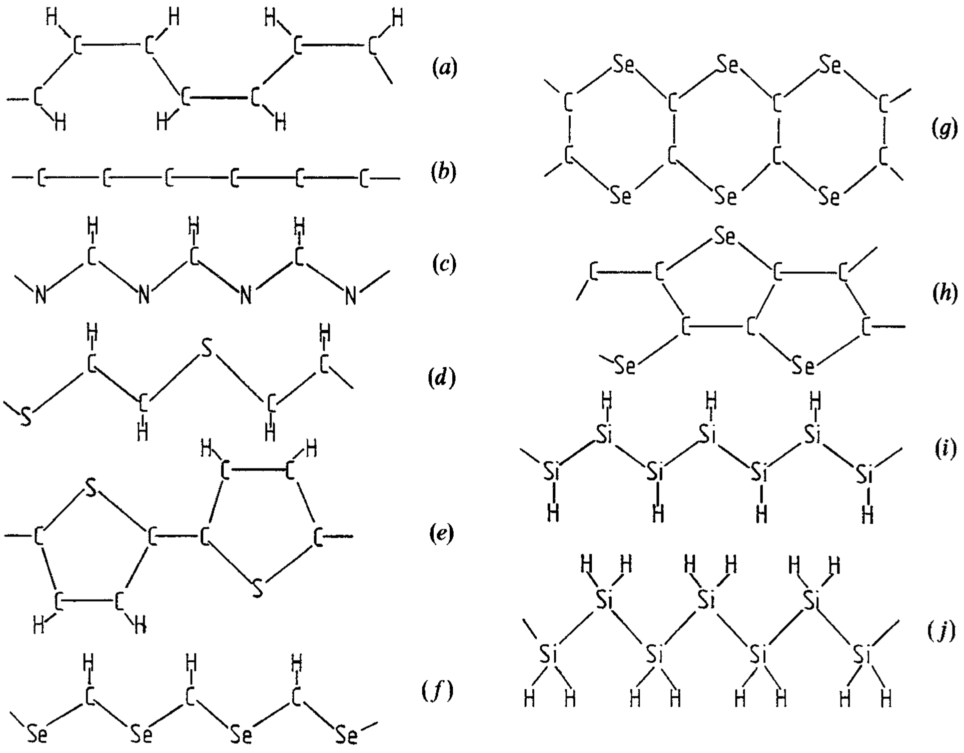

Figure 18. Schematic representation of (*a*) cis polyacetylene, (*b*) polyyne, (*c*) polycarbonitrile, (*d*) polyvinylene sulphide, (*e*) polythiophene, (*f*)–(*h*) three carbon selenium polymers, (*i*) polysilene, and (*j*) polysilane.

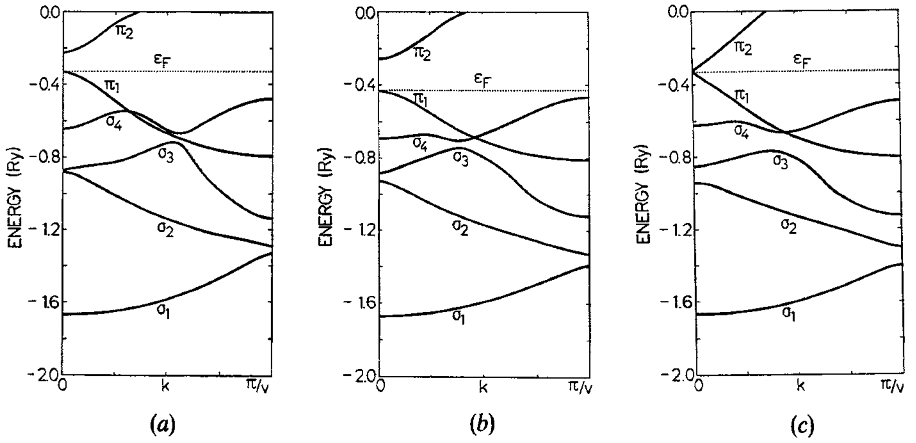

(*a*) (*b*) (*c*)

Figure 19. Band structures of (*a*) the ‘undimerized’, (*b*) the cis-trans, and (*c*) the trans-cis isomer of cis polyacetylene. The dashed lines are the top of the valence bands. (Reproduced from Springborg (1986).)

However, an observable difference that may be used experimentally in distinguishing between cis and trans polyacetylene is the avoided crossing between the σ_2 and σ_3 bands for trans polyacetylene which appears between the σ_3 and σ_4 bands for cis polyacetylene. The resulting peaks in the densities of states should provide fingerprints of the isomers, that may be observed in, e.g., photoelectron spectroscopy.

We have not made a detailed first-principles study of cis polyacetylene and are accordingly lacking parts of the information required for deriving a complete model Hamiltonian for the study of solitons and polarons. However, we have made some preliminary studies of the π electron density of states that should be expected for cis polyacetylene (Springborg 1986, 1989 *b*, Springborg *et al.* 1989). These studies indicate first of all that the nearest-neighbour hopping integrals are to be separated into two types: those for the C–C bonds not parallel to the polymer axis and those for the C–C bonds parallel to the polymer axis. The former bonds have local surroundings as the C–C bonds in trans polyacetylene and it is therefore not surprising that the hopping integrals are as for trans polyacetylene. The other hopping integrals, however, are significantly larger.

One out of two situations may occur: either the gap closes under the transition between the trans-cis and the cis-trans isomer, or it does not. In the unrealistic, hypothetical case that the two isomers are energetically degenerate solitons may exist. It now turns out that only in the case of a band-gap closure under the trans-cis to cis-trans transition will a soliton induce a state close to the mid-gap position. This finding as well as related findings for other polymers have made us propose the following approximate rule (Springborg 1991 *a*). Referring to Section 3 we introduce one configuration coordinate x_n per site. A structural defect makes x_n deviate from one or two constant values in a limited region such that

$$x_l \leqslant x_n \leqslant x_u. \tag{20}$$

The proposition states then that one may only find a state at a specific energy ϵ if there exists a periodic structure (13) with

$$x_l \leqslant x_0 \leqslant x_u, \tag{21}$$

for which state(s) occur(s) at ϵ. This can explain why a band-gap closure under the transition between the energetically equivalent *A* and *B* phases is a requirement for the occurrence of a soliton-induced state close to mid-gap.

A polaron is often considered two interacting solitons (see figure 10). As such one explains the two polaron-induced gap states as the bonding and the antibonding combinations of the soliton-induced gap states. Within this picture one may therefore not expect polaron-induced gap states for cis polyacetylene. However, a polaron may alternatively be considered a finite segment of one isomer inserted into the other, and accordingly, when inserting a polaron into the cis-trans isomer (which is the wide-gap isomer and which is believed to be the stable form of cis polyacetylene) one does find polaron-induced gap states independent of the occurrence of a band-gap closure under the transition between the trans-cis and the cis-trans isomers.

To our knowledge there exists only one other density-functional study on cis polyacetylene, namely that of Ye *et al.* (1989 *b*) on a finite molecule containing two solitonic defects. It is surprising to notice that their results predict two non-interacting solitons to induce states close to mid-gap. This is in marked contrast to our proposition but might be due to finite-size or end effects. It demonstrates that further studies on cis polyacetylene are required.

6.2. *Polyyne*

A linear carbon chain, polyyne, may be considered the simplest conjugated polymer. Synthesizing this material is however not trivial and the resulting material is not completely characterized (see, e.g., Kavan *et al.* (1990)). But as we shall see, polyyne possesses properties that make it an interesting system. First of all, in contrast to most other conjugated polymers the C–C bond alternation is not between single and double bonds but between single and triple bonds. Moreover, the π bands are doubly degenerate, such that when the polymer backbone remains linear the π bands can contain up to four electrons compared with two for the more common conjugated polymers. This leads to a particularly rich spectrum of metastable structures (see, e.g., Rice *et al.* (1983)). Finally, from a theoretical point of view the structural simplicity of polyyne makes it an excellent system for detailed studies.

As far as we know, polyyne has only been studied by the present author using density-functional methods. The results of these studies shall now be summarized.

The band structures of polyyne were already presented in figure 8. We here clearly notice that the bands split into π bands close to the Fermi level and energetically deep lying σ bands. Therefore, a model that includes a detailed description of solely the π orbitals is even more justified for polyyne than for trans polyacetylene. Using the strategy of Section 3 we parametrized a large number of first-principles calculations within a model Hamiltonian. This model Hamiltonian resembles that of equations (5), (6), and (11) with the only modification that the spin index s is to be generalized such that it also includes the double degeneracy of the p_x and p_y orbitals.

It turned out (Springborg *et al.* 1990 *a*) that the next-nearest-neighbour interactions were very small. One reason for this is that since all nuclei lie along one line there is an effective screening of more distant interactions. Another result of the first-principles calculations was that the function f_1 describing $\hat{H}_\sigma$ was an anharmonic function, as also was the case for trans polyacetylene. We finally estimated the size of the ionicity term in $\hat{H}_\pi$ but did not include it in the model calculations. Consequently only the next-nearest neighbour interactions break the electron–hole symmetry. Therefore, soliton and polaron induce states almost symmetric in the gap and, moreover, the results of the model calculations depend only marginally on the sign of the total charge of the chain.

The anharmonic terms in $\hat{H}_\sigma$ led for trans polyacetylene to the lack of stable polarons. For polyyne the anharmonic terms have the opposite effect. We find for polyyne a very rich variety of (meta-)stable polarons. In figure 20 we show the energy gain per added or removed electron for a number of those as well as for solitons. We have here used a notation of the form P_q^x with q being the charge of the system and x labelling different polarons of the same charge. The symbol S denotes solitons. The

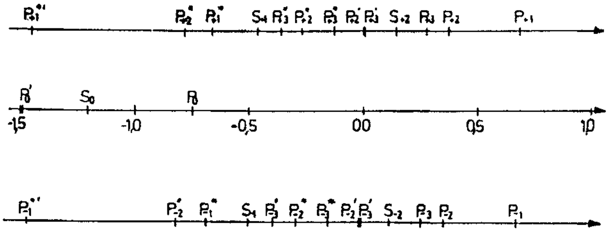

Figure 20. Energy gain per added or removed electron for positively (upper axis) and negatively (lower axis) charged linear carbon chains, as well as energy gain for neutral chains (middle axis). The energy unit is eV. (Reproduced from Springborg *et al.* (1991 *c*).)

energy gain is defined as the difference in the total energy of the undistorted system of charge q minus that of the polaron (or soliton), and is thus positive for stable distortions and negative for metastable distortions when comparing with the undistorted system.

In figure 20 we see that the singly charged polarons are the stablest defects followed by doubly and triply charged polarons. Then solitons are found. It is moreover noticed that the ground state of the neutral, spin-containing system is the undistorted chain, and that solitons and polarons in that case only are metastable. This hierarchy is different from what we observed for trans polyacetylene.

Many conjugated polymers have a planar nuclear backbone defined by the sp^2 hybrids of the carbon atoms. Twistons in which a local part of the polymer backbone is lifted out of the otherwise common plane have been proposed as possible charge-carrying defects (Brazovsky and Kirova 1988). A twiston for the sp-bonded polyyne corresponds to a region in which the polymer is not linear. This will break the symmetry of the polymer such that the doubly degenerate π bands will split into one of π symmetry and one of σ symmetry. A model for describing this system must therefore include two tight-binding parts; one for each of the two π-derived bands.

We derived such a model (Springborg *et al.* 1990 *a*) by parametrizing results of first-principles calculations on periodic zig-zag chains for which the nearest-neighbour bond lengths were kept constant (but alternating) and the bond angles were varied in unison. In figure 21 we show the resulting total energy (E_{tot}), the integral over the π-derived σ band (E_{π}^{σ}), that over the π-derived π band (E_{π}^{π}), and the remainder (E_{σ}) as functions of the common bond angle. We see how the two π contributions become more and more different as the bond angle is reduced. We moreover notice that the polymer appears to be very soft against bending. This will become of importance later in this subsection.

With the resulting model we subsequently studied twistons. It was, however, found that these were not (meta-)stable. The twiston-induced gap states appeared so close to the band edges that the energy gains upon populating or depopulating those when doping the system could not compensate the costs in elastic energy related to their creation. Moreover, since they appear so close to the band edges, a proposed soliton–twiston interaction (Brazovsky and Kirova 1988) can only be of minor importance.

Polyyne is an excellent system for theoretical studies of the role of interchain interactions. Although these may be small such that they in most cases can be ignored they may have crucial impacts on the stability of solitons. If, e.g., two neighbouring chains have a lower total energy when they are antiparallel than when they are parallel, the creation of a soliton in one of the two chains will cost energy and the soliton will move in that direction which leads to an increase in the antiparallel segment of the two chains. For polyyne this can easily be studied since the complexity due to relative orientations of neighbouring polymer planes is lacking. Results of first-principles calculations on two interacting chains (Springborg 1989 *c*) indicated that there is a noteworthy interchain interaction. The total energy difference for two chains being parallel or antiparallel was found to be of the order of 0·1 eV per two C_2 units with the antiparallel arrangement being preferred. The band splittings were of comparable size.

These results are a further indication of the stability of polarons over solitons for polyyne since the stability of polarons is much less sensitive to interchain interactions. They moreover propose that for those systems for which solitons are believed to exist (e.g. trans polyacetylene) the solitons will be less localized to single chains but be more three-dimensional objects eventually also involving the dopants. This is in accordance with our results on doped trans polyacetylene.

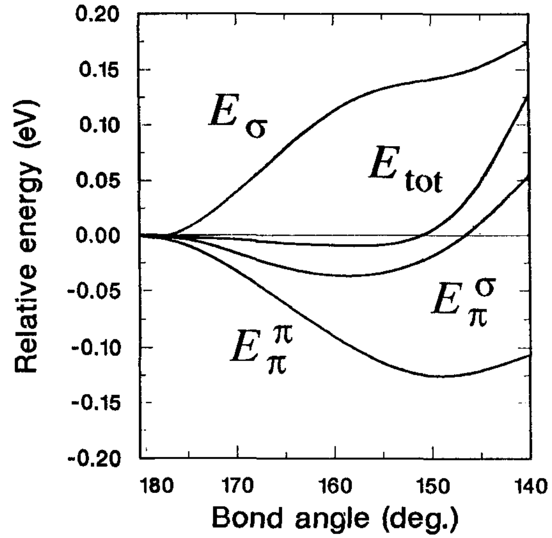

Figure 21. Relative total energy E_{tot}, the π electron energies E_π^σ and E_π^π, and the remainder E_σ for a zig–zag carbon chain as functions of the bond angle. All energies are in eV per C_2 unit. (Reproduced from Springborg *et al.* (1990*a*).)

Kavan *et al.* (1990) have studied polyyne experimentally. They proposed that upon ageing the compound will change and the single chains will interact ultimately forming graphite-like complexes. The results in figure 21 indicate that the polyyne chains are easy to bend, such that the change from *sp*-bonded to sp^2-bonded chains only will cost little energy. However, sp^2-bonded zig–zag chains will have dangling bonds and may tend to bond together. This process will then ultimately lead to the graphite-like compound observed by Kavan *et al.* Actually, density-functional studies on two chains bonded together support this picture (Springborg and Kavan 1992).

6.3. *Polycarbonitrile*

Polycarbonitrile (figure 18 (*c*)) was synthesized more than 20 years ago (Wöhrle 1971), but has to the author's knowledge not yet been studied experimentally in the context of a conjugated polymer. It has the same structure and number of electrons as trans polyacetylene and the only difference is the atom alternation along the polymer backbone for polycarbonitrile. However, due to this so-called site alternation the chain with constant C–N bond lengths has a non-vanishing gap around the Fermi level. This can, e.g., be seen in figure 22 where we show the band structures for an optimized chain without bond-length alternation (Springborg 1991 *b*). The important question is thus whether the total energy can be lowered upon a bond-length alternation. In that case solitons may exist. But before exploring this question we will compare the band structures of figure 22 with those of figure 13 for trans polyacetylene.

As for trans polyacetylene we can form a hypothetical broad σ valence band formed by σ bonds between carbon and nitrogen sp^2 hybrids and a hypothetical, narrower band at higher energies. However, the latter has a large band gap for $k=1$ and is essentially split into two branches of which one (the lower) is due to σ bonds between carbon sp^2 hybrids and hydrogen 1*s* functions and the other is due to nitrogen lone-pairs. Also the wider hypothetical band has a band gap at $k=1$ but this is considerably

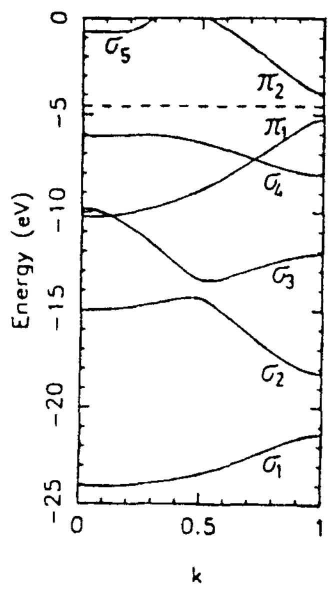

Figure 22. The band structures for the optimized structure of polycarbonitrile with constant C–N bond lengths. The dashed line is the Fermi level. (Reproduced from Springborg (1991 *b*).)

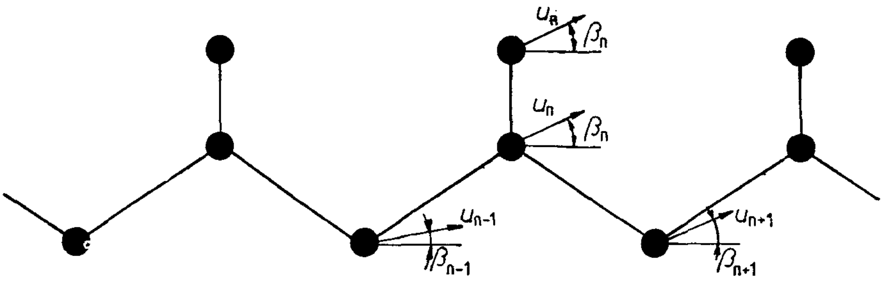

Figure 23. Definition of the configuration coordinates u_n and β_n describing the structure of polycarbonitrile. (Reproduced from Springborg (1991 *b*).)

smaller. Finally, the two π bands are split into the lower (valence) band mainly formed by nitrogen *p* functions and the upper (conduction) band from carbon *p* functions. This difference can be explained from the difference in nuclear charge or electronegativity.

In studying whether a bond-length alternation could lower the total energy we kept the unit-cell length fixed and moved the CH units rigidly as well as the N atoms as shown in figure 23. Comparing with the prescription of Section 3 we thus ascribe two parameters (u_n and β_n) to each site (i.e. carbon or nitrogen atom). We define x_n as in equation (12) and assume both $\{x_n\}$ and $\{\beta_n\}$ to follow equations (13), (14), (15), or (16) for the undistorted chain, for solitons, and for the two types of polarons, respectively.

The results of the first-principles calculations were subsequently mapped on to a model Hamiltonian of the form (5) in which all terms were to depend both on $\{x_n\}$ and on $\{\beta_n\}$. Due to the site alternation both the on-site terms ϵ_n and the nest-nearest-neighbour hopping integrals $t_{n,n+2}$ are alternating but were otherwise assumed constant. Moreover, $\hat{H}_\sigma$ was found to contain anharmonic terms in bond-length variations—as was the case for trans polyacetylene and polyyne.

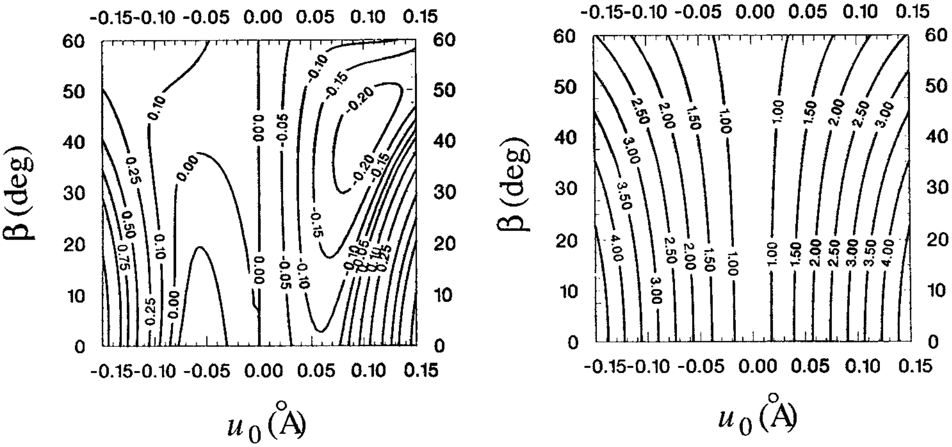

(a) (b)

Figure 24. (a) Total energy in eV per CHN unit and (b) the band gap in eV as functions of $u_n = u_0$ and $\beta_n = \beta$ for periodic chains of polycarbonitrile. (Reproduced from Springborg (1991 b).)

In figure 24 we show the total energy and the band gap for the periodic chain as functions of $x_n = x_0$ and $\beta_n = \beta$. We see that there is a substantial energy gain upon bond-length alternation. Moreover, any bond-length alternation is accompanied by an increase in the band gap. Finally, the lowest total energy is found for a structure with $\beta \neq 0$, which is in contrast to the results for trans polyacetylene for which $\beta = 0$.

Since the structure without bond-length alternation is semiconducting a Peierls transition cannot directly be held responsible for the observed preference of a bond-length alternation. But as found by Rice and Mele (1982), if the electron–phonon coupling (as given by the dependence of the hopping integrals on the bond lengths) is sufficiently large and dominating over the alternation in on-site terms, one may find a bond-length alternation. This is obviously the case for polycarbonitrile.

As a consequence of the non-vanishing bond-length alternation solitons may exist. And according to the model calculations (Springborg 1991 b) they are stable for the charged or spin-containing chain. But in contrast to trans polyacetylene they induce two and not one gap state. These appear very close to the positions of the band edges, for the chain with no bond-length alternation. This finding agrees with the results of Rice and Mele (1982) as well as with our proposition (Section 6.1.) for possible energies of defect-induced orbitals.

Finally, the model calculations indicate polarons to be unstable. We will ascribe this result the anharmonic effects in $\hat{H}_\sigma$.

6.4. *Polyvinylene sulphide*

Polyvinylene sulphide (figure 18 (*d*)) resembles trans polyacetylene but has every third CH unit replaced by one S atom. Within the simplest chemical picture one would expect C–C double bonds and C–S single bonds. This would indicate the existence of only one (meta-)stable structure and fairly localized π electrons, and polyvinylene sulphide should thus have little interest as a synthetic metal. But the polymer has been synthesized (Ikeda *et al.* 1983) and it has been shown to possess a large doping-induced increase in electrical conductivity (Ikeda *et al.* 1983). It appeared therefore interesting to study the properties of polyvinylene sulphide in more detail (Springborg 1989 *d*).

The first question to be answered was whether the prediction of the existence of only one (meta-)stable structure was correct. But the first-principles calculations did not give any indication of any but one structure. For this partially optimized structure we show in figure 25 the band structures. With some goodwill one may consider those a trimerized version of those of undimerized trans polyacetylene (see figure 13). We recognize furthermore three π bands of which two are occupied and one is empty. The π bands determine the orbitals around the gap.

As a second result of the first-principles calculations it turned out that the frontier orbitals were not localized to the C–C bonds but had significant components on the sulphur atoms indicating that the orbitals are not strongly localized. We therefore examined whether polarons—i.e. local distortions—were stable and eventually could be the charge carriers in the doped system. To this end we defined a model Hamiltonian as that described in Section 3 including both carbon and sulphur π orbitals as well as C–C and C–S bond-length variations (Springborg 1989 *d*).

The π electron density of states will for the neutral, undistorted system split into three separate bands and the Fermi level will fall in the uppermost gap (see figure 25). It now turned out that polarons that were related to increases in the C–C bond lengths and decreases in the C–S bond lengths led to states in the gap around the Fermi level. These gap states could with advantage be populated or depopulated upon doping thereby making the polarons stable for charged chains. Moreover, the polaron-induced orbitals were spread out over a larger part of the chain and are thus mobile. However, when the polarons were associated with decreases of the C–C bond lengths and increases of the C–S bond lengths, the gap states appeared in the other, lowest, gap and such polarons were not stable.

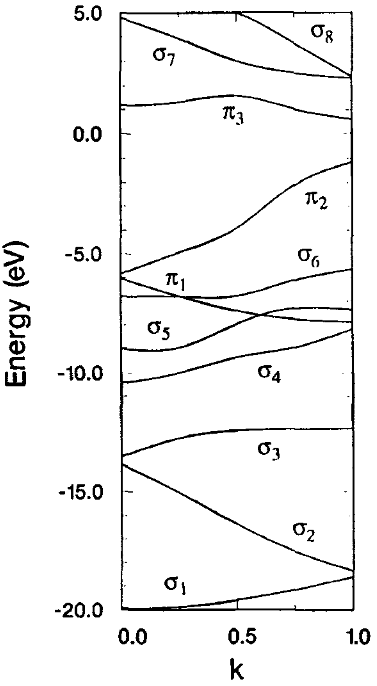

Figure 25. The band structures for the optimized structure of polyvinylene sulphide. The dashed line is the Fermi level. (Reproduced from Springborg (1989 *d*).)

6.5. *Polythiophene*

Polythiophene (figure 18 (*e*)) is one of the currently most intensively studied conjugated polymers. This is partly due to its excellent stability against the atmosphere (Waltman *et al.* 1983) and heat (Yumoto and Yoshimura 1986) as well as the possibility of synthesizing crystalline (Kobayashi *et al.* 1984) and soluble (Elsenbaumer *et al.* 1986) derivatives. These properties are not shared by the prototype of the conjugated polymers, trans polyacetylene, and make therefore polythiophene attractive.

The carbon backbone of polythiophene may be related to those of the isomers of polyacetylene and has as such a slightly more complicated structure than those of trans and cis polyacetylene. From this point of view one arrives at polythiophene by replacing certain pairs of hydrogen atoms by single sulphur atoms. This description proposes that the role of the sulphur atoms is minor, and that the conducting properties can be described by models including solely the carbon atoms.

As for cis polyacetylene, two metastable forms of polythiophene exist only differing in the alternation of the C–C single and double bonds. Of these, the aromatic isomer with single bonds connecting neighbouring C_4SH_2 pentagons is the stable form (Yumoto and Yoshimura 1986), whereas the other, quinoid, form has a higher total energy.

In the first-principles study of polythiophene (Springborg 1992 *a*) we focused on the π electron density of states and its modifications when passing from the quinoid to the aromatic structure. The polymer has too large a unit cell for us to make a detailed study of the total-energy variations connected with this transition and we thus focused on the π electrons believing their density of states to be less sensible to smaller structural variations.

The results indicated that sulphur-centred functions were important over the whole valence-band range, thus also in describing the π electrons. This could also be seen from the total width of the π valence bands which was about 50% larger than those of trans and cis polyacetylene. Since trans and cis polyacetylene have similar π valence-band widths, one would expect that of polythiophene to have the same size, *if* the sulphur atoms did not play any noteworthy role.

The band structures suffered from estimating the σ bands to lie too high (about 1 eV) relative to the π bands (Springborg 1992 *a*). Adjusting this the band structures were in excellent agreement with experimental photoelectron spectra. This can be seen in figure 26 where we compare the calculated (adjusted) density of states with the experimental XPS spectra of Wu *et al.* (1987).

A further result of the first-principles calculations was that the band gap did not close under the transition between the quinoid and the aromatic isomer. Mapping the results on a model Hamiltonian of the form (6) (including sulphur-centred π functions) and subsequently studying solitons (for the hypothetical case that the aromatic and quinoid isomers are energetically degenerate) we therefore found no near-mid-gap states. This agrees well with the proposed criterion presented in Section 6.1.

Using the model Hamiltonian in studying polarons inserted in the (wide-gap) aromatic isomer we observed two gap levels which were placed asymmetrically in the gap. That we found them to be placed asymmetrically is an important finding since most single-particle studies assume them to be symmetrical and ascribe any deviation from this to correlation effects. For reasonable values of Δ of equation (15) (i.e. $\Delta < 15$–20) the gap levels appeared close to the band edges. By comparing with experimental optical spectra on doped (Harbeke *et al.* 1986) or photoexcited (Colaneri *et al.* 1987, Kaneto *et al.* 1987, Rühe *et al.* 1990) the results indicate that the experiments do not

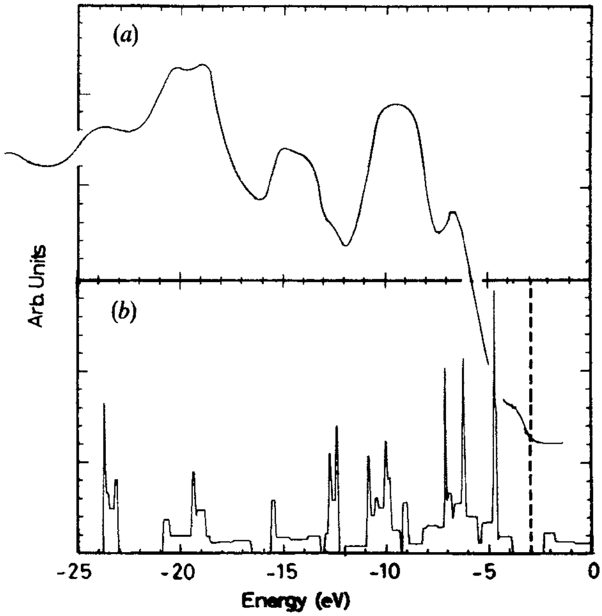

Figure 26. (*a*) Experimental XPS spectra of Wu *et al.* (1987) and (*b*) adjusted calculated density of states for polythiophene. (Reproduced from Springborg (1992*a*).)

observe transitions between the two gap levels. This means that both gap levels are either filled or empty, and thus that the defects are so-called bipolarons and not polarons. Similar conclusions were reached by Colaneri *et al.* (1987) based on their experimental results.

To our knowledge the only other density-functional study on polythiophene is due to Mintmire *et al.* (1988). However, polythiophene is obviously a system that deserves more studies since the results of the two sets of calculations differed in more respects. Thus, the results of Mintmire *et al.* were not obscured by a shift of the σ bands relative to the π bands, but they found a significantly smaller π valence-band width than we did. Both differences might be due to sulphur *d* functions which we have included but Mintmire *et al.* did not. On the other hand, the two sets of calculations give very similar sizes and positions of the band gap of the two isomers.

Related to polythiophene is polyfuran with the sulphur atoms replaced by oxygen atoms and polypyrrole with NH groups instead of the S atoms. Both polymers were studied by Mintmire *et al.* (1987, 1988), who included a comparison between theoretical and experimental UPS spectra for polypyrrole. Equivalent to the results of figure 26, the agreement was found to be good.

6.6. *Carbon–selenium polymers*

Linear CSe_2 molecules may be polymerized but the resulting material is not yet completely characterized and the structure and composition have been the subject of some debate (Kobayashi *et al.* 1985, Iqbal *et al.* 1986, 1988, Okamoto *et al.* 1986). We have analysed a number of the proposed intermediates and final products using the first-principles method (Springborg 1989 *e*, *f*) but will here concentrate on the results of relevance in the context of conjugated polymers. As far as we know, our results are the only density-functional results on C–Se polymers.

Replacing the hydrogen atoms in the CSeH polymer of figure 18 (*f*) by selenium atoms we arrive at a CSe_2 polymer with the structure as that of the analogue CS_2 polymer. For this we found, however, a repulsive interaction between the carbon atoms and the attached selenium atoms, indicating this polymer to be unstable. Independent of our study and parallel to it, Iqbal *et al.* (1988) found experimentally that the CSe_2 polymer could not be the product of their synthesis.

Removing the attached Se atoms we arrive at a CSe polymer that was found to be stable according to the first-principles calculations. However, it was also found to be highly reactive and could, e.g., attract hydrogen atoms resulting in the polymer of figure 18 (*f*). The band structures of a realistic but not completely optimized structure are shown in figure 27. We notice both σ and π bands around the Fermi level but we believe that a detailed structure optimization may change this. One could then imagine a situation in which the π band becomes exactly half-filled, such that the compound will be as undimerized trans polyacetylene but with an extra Se atom per CH unit. This material would then undergo a Peierls transition and doping it may lead to the formation of solitons or polarons. But a further study of this should await experimental confirmations that the material can be synthesized.

We may also let two chains of the above-proposed CSe polymer interact giving the structure of figure 18 (*g*). For this, typical band structures are shown in figure 28. There are very many bands and it is not obvious that the polymer will have relevance as a conducting polymer. However, we may speculate that a lower total energy can be obtained by allowing the C–Se bond lengths to alternate. They may then do so either in parallel or in antiparallel on the two chains constituting the polymer. Defects related to these two structures may ultimately be charge carriers. But it should be stressed that this reflects only speculations.

The C_2Se polymer of figure 18 (*h*) was proposed by Iqbal *et al.* (1986) as a stable compound although it could not account for their extended X-ray absorption fine

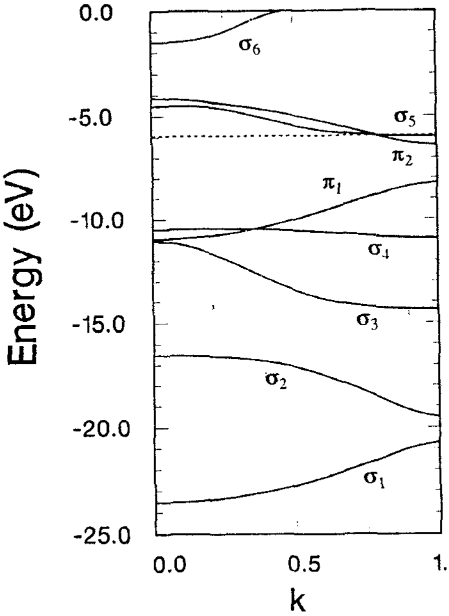

Figure 27. Band structures of the CSeH polymer of figure 18 (*f*). The Fermi level is marked by the dashed line. (Reproduced from Springborg (1989 *e*).)

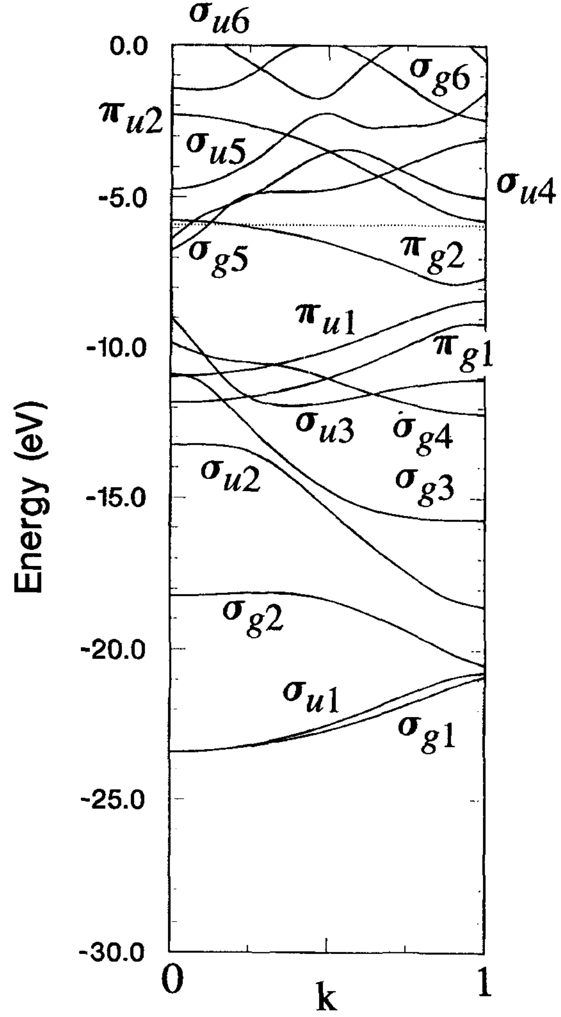

Figure 28. Band structures of the C_2Se_2 polymer of figure 18 (*g*). The Fermi level is marked by the dashed line. (Reproduced from Springborg (1989*f*).)

structure data. It is similar to cis polyacetylene (figure 18 *a*) with each pair of hydrogen atoms replaced by a single selenium atom. Keeping all geometrical parameters fixed at reasonable values except for the C–C bond-length alternation we found the total energies shown in figure 29 (*a*) as a function of difference in the two C–C bond lengths. As is the case for cis polyacetylene, we find the cis-trans isomer to be stable and the trans-cis isomer to be metastable. The band structures (figure 29 (*b*)) show π bands close to the Fermi level, but in contrast to cis polyacetylene there are two (instead of one) π valence bands. The positions of the energies of the frontier orbitals (figure 29 (*c*)) show that the cis-transisomer is the small-gap isomer (which is opposite to the case for cis polyacetylene) and contour curves of their electron densities (figure 29 (*d*)–(*f*)) clearly demonstrate that selenium-centred functions are required in a proper description of these. We have, however, not yet derived any model Hamiltonian or performed any model calculations for this compound.

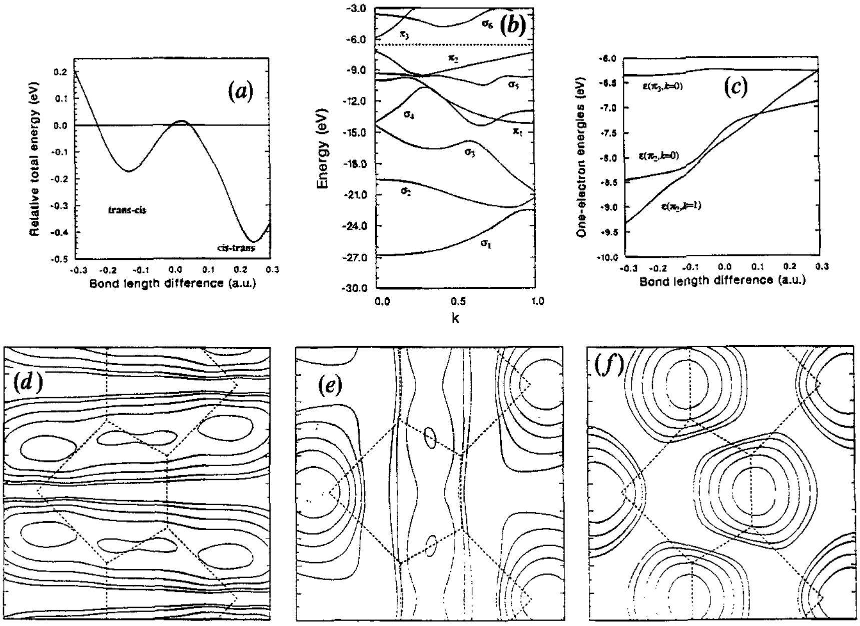

Figure 29. Various properties of the C_2Se polymer of figure 18 (*h*): (*a*) Relative total energy per C_2Se unit as a function of difference Δd in C–C bond lengths. (*b*) The band structures for $\Delta d = 0$. The dashed line represents the Fermi level. (*c*) Energies of the frontier orbitals (i.e., the π_2 orbital at $k=0$ and $k=1$ and the π_3 orbital at $k=0$) as functions of Δd. (*d*)–(*f*) Contour curves of the electron densities of the frontier orbitals in a plane parallel to but 2 a.u. away from the nuclear plane. The orbitals are (*d*) π_2 at $k=0$, (*e*) π_2 at $k=1$, and (*f*) π_3 at $k=0$. (Reproduced from Springborg (1989 *e*).)

6.7. *Polysilene and polysilane*

In closing the discussion of the conjugated polymers we consider some obtained by replacing carbon by silicon.

The silicon-analogue of trans polyacetylene is polysilene (figure 18 (*i*)) and—except for a general narrowing—the band structures of undimerized polysilene (figure 30) resemble those of undimerized trans polyacetylene. There is, however, the remarkable difference that polysilene possesses a low-lying σ conduction band which is partially occupied. We could relate this difference to low-lying virtual *d* functions for silicon absent for carbon (Springborg 1989 *g*).

In spite of this it is somewhat surprising that further calculations indicated that the total energy could be lowered upon a Si–Si bond-length alternation, although the compound stayed metallic with both σ and π bands crossing the Fermi level (Springborg 1989 *g*).

It is relevant to the present study to mention that these calculations indicated a strong dependence of the total-energy variations on the way the bond-lengths were allowed to alternate. Similar results might be found for other conjugated polymers indicating that care must be taken when studying the effects of a bond-length alternation.

Polysilene may, however, not be synthesized, as the synthesis of compounds with Si–Si double bonds is difficult (Gusel'nikov and Nametkin 1979). Indications of the

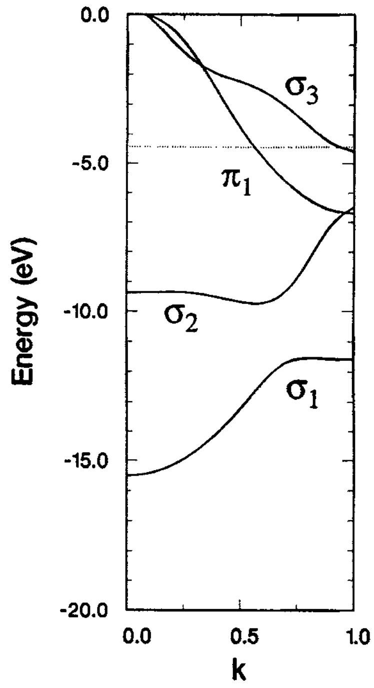

Figure 30. Band structures of undimerized polysilene. The dashed line is the Fermi level. (Reproduced from Springborg (1989*g*).)

lacking stability of polysilene were obtained by studying (Springborg 1989*g*) a reaction between polysilene and hydrogen atoms ultimately leading to the polysilane of figure 18 (*j*).

The band structures of polysilane are shown in figure 31 and they demonstrate that compared to its carbon-analogue, polyethylene, the band gap is significantly reduced. In fact, the polysilane of figure 18 (*j*) may be considered a prototype of a number of silicon-based polymers related to that of figure 18 (*j*) but for which the hydrogen atoms have been replaced by other, often organic, sidegroups. Since these possess properties similar to those of the carbon-based conjugated polymers (see, e.g., Aldissi (1988–1989)), Rice and coworkers (Rice and Phillpot 1987, Jeyadev *et al.* 1988) proposed polarons to be stable defects for the charged system. A polaron is here to be related to displacements of the silicon atoms perpendicular to the polymer axis and in their model they described two orbitals per Si atom within a tight-binding picture. These two orbitals were the two sp^3 hybrids pointing towards the neighbouring Si atoms.

We used the first-principles results in deriving a model related to that of Rice and coworkers. It turned out, however, that the model did not support the existence of polarons in contrast to the results of Rice and coworkers. The polaron-induced gap states appeared so close to the band edge that the energy gain upon populating or depopulating these could not compensate the costs in lattice energy due to the formation of the polaron.

Almost parallel to our own study of polysilane, Mintmire (1989) studied both the $(SiH_2)_x$ polymer as well as an organosilane polymer in which the hydrogen atoms were replaced by methyl groups. He furthermore realized that the synthesized polysilanes

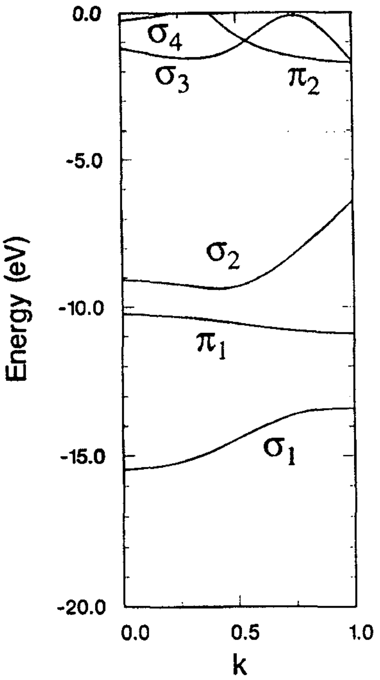

Figure 31. Band structures of polysilane. The dashed line is the Fermi level. (Reproduced from Springborg (1989*g*).)

often have a helical and not planar silicon backbone and studied therefore both planar and helical structures. His results show that the electronic densities of states depend crucially on the structure of the backbone. Moreover, although the frontier orbitals might be strongly localized to the Si atoms, their energies (including the band gap) are influenced by the sidegroups. Finally, where a comparison between the two sets of calculations was possible, the agreement was good.

Also at that time Takeda and Shiraishi (1989) studied $(SiH_2)_x$ using a density-functional method. They concentrated on the (small) modifications in the band structures due to interchain interactions. Their results otherwise resemble those of the other density-functional calculations on polysilane.

7. Hydrogen halides

Compared with other hydrogen-bonded systems, hydrogen fluoride has an unusually short and strong hydrogen bond. This may be ascribed a partially covalent character of the hydrogen bond (Springborg 1987) and hydrogen fluoride can accordingly not be considered the prototype of hydrogen-bonded systems. However, crystalline hydrogen fluoride consists of parallel, weakly interacting chains of the form shown in figure 32 (Atoji and Lipscomb 1954, Habuda and Gagarinsky 1971, Johnson *et al.* 1975), and by making use of the zig–zag symmetry one unit cell has only two atoms making $(HF)_x$ an excellent compound for theoretical studies. Under the further assumptions that the chain is planar and that the hydrogen atoms are placed along the lines connecting neighbouring fluorine atoms, the structure can be completely described by the three parameters shown in figure 32: the F–F–F bond angle α, the F–F

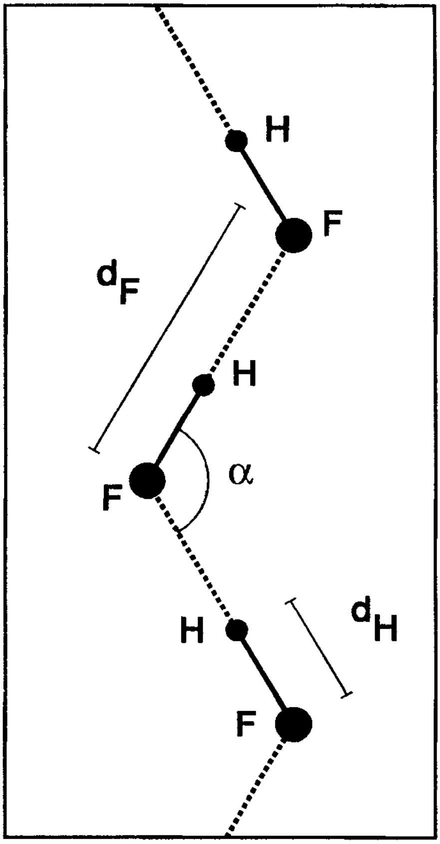

Figure 32. Schematic representation of one $(HF)_x$ chain. The full and the dashed lines represent the chemical and the hydrogen bonds, respectively. (Reproduced from Springborg (1987).)

nearest-neighbour distance d_F, and the length of the covalent F–H bond d_H. The hydrogen-bond length becomes then $d_F - d_H$, and it is important to notice that the structure with d_H replaced by $d_F - d_H$ has the same total energy.

We made a detailed study for two fixed values of α: $\alpha = 120°$ (labelled the zig–zag chain) and $\alpha = 180°$ (the linear chain), as well as a study where all three geometrical parameters were allowed to relax and a study of the isolated monomer (Springborg 1987, 1988).

For the isolated monomer ($d_F \rightarrow \infty$; α irrelevant) we found the relative total energies shown in figure 33. The minimum occurs for $d_H = 1{\cdot}70$ a.u., which compares well with the experimental values of 1·71–1·73 a.u. (Di Lonardo and Douglas 1973, Huber and Herzberg 1979) and with other theoretical values (1·70 a.u.; Yarkony *et al.* 1974).

The total-energy curve of figure 33 is well fit with a Morse potential as can be seen in the figure. This can subsequently be used in giving frequencies of bond-stretch vibrations, resulting in 3865, 7506, 11 034, 14 118, and 17 088 cm^{-1} for the five lowest modes. These compare well with experimental values of Di Lonardo and Douglas (1973): 3961, 7750, 11 372, 14 831, and 18 130 cm^{-1}, respectively. We notice both in our values and in the experimental values the importance of anharmonicities that make the frequencies unevenly spaced.

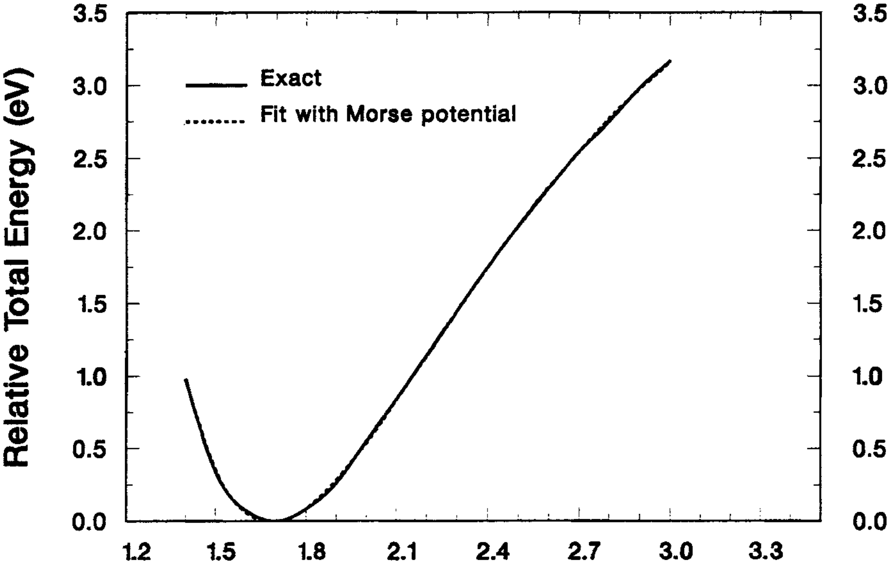

Figure 33. Relative total energy of the isolated HF monomer as a function of d_H as well as a fit with a Morse potential. (Reproduced from Springborg (1988).)

Relaxing all three parameters of figure 32 for the polymer resulted in the lowest total energy for $\alpha = 125°$, $d_F = 4{\cdot}72$ a.u., and $d_H = 1{\cdot}85$ a.u. These agree very well with the experimental values of Atoji and Lipscomb (1954) and Habuda and Gagarinsky (1971): $\alpha = 120{\cdot}1°$, $d_F = 4{\cdot}71$ a.u., and $d_H = 1{\cdot}80$ a.u., as well as with those of Johnson *et al.* (1975): $\alpha = 116°$, $d_F = 4{\cdot}72$ a.u., and $d_H = 1{\cdot}83$ a.u. On the other hand, the *ab initio* Hartree–Fock calculations by Karpfen and coworkers (Karpfen 1980, Karpfen *et al.* 1981, Beyer and Karpfen 1982) gave $\alpha = 129{\cdot}7°$, $d_F = 4{\cdot}91$ a.u., and $d_H = 1{\cdot}74$ a.u.

In figure 34 we show contour curves of the total energy for $\alpha = 120°$ and $\alpha = 180°$. For the zig–zag chains we have marked the position of the experimentally observed structure, and this is seen to lie very close to the optimized structure. For the linear chains the calculations predict the existence of two minima, which, however, are separated by a barrier that is so low that we consider its existence beyond the numerical accuracy.

The local-density calculations tend to overestimate the strength of chemical bonds (see, e.g., Jones and Gunnarsson (1989)), which makes a comparison between total energies of different compounds difficult. However, comparing those of the $(HF)_x$ polymers and the HF monomer we obtain energies of the hydrogen bonds of 0·6 eV and 0·3 eV for the zig–zag and the linear chain, respectively. As discussed elsewhere (Springborg 1988) these energies are realistic.

Jansen *et al.* (1987) have presented density-functional calculations on solid HBr. This material is closely related to HF, but Jansen *et al.* restricted themselves to linear chains ($\alpha = 180°$). Our results and those of Jansen *et al.* show many similar features. Among those is the tendency for the barrier for the collective shift of all protons to the symmetrically equivalent position to decrease upon decreased d_F. This can be considered a theoretical manifestation of the experimentally observed pressure-induced phase transition (Pinnick *et al.* 1989).

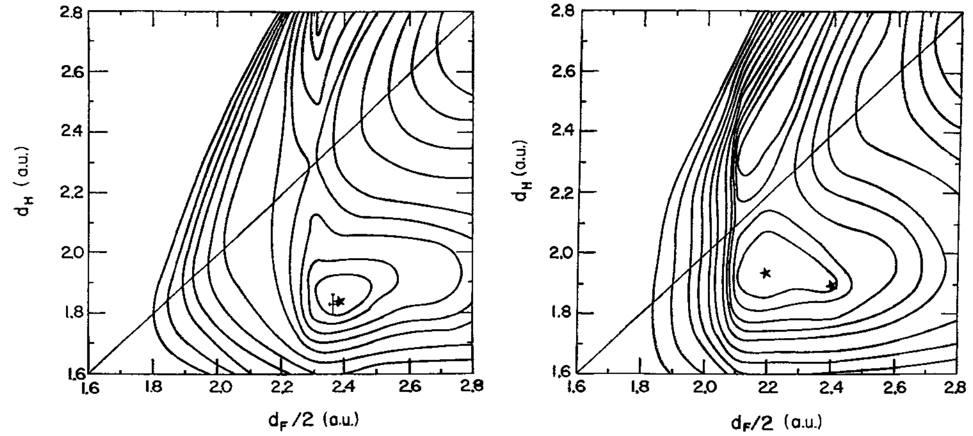

(*a*) (*b*)

Figure 34. The relative total energy per monomer for (*a*) the zig–zag and (*b*) the linear $(HF)_x$ chains. The stars mark the local minima and the cross the experimental structure with error bars. The total-energy zero in (*a*) is 0·3 eV below that in (*b*), and the contour values are 0·05, 0·1, 0·2, 0·3, 0·4, 0·5, 0·75, 1·0, 1·25, 1·5, and 2·0 eV. (Reproduced from Springborg (1987).)

Figure 35 shows the band structures for the optimized zig–zag chain. We notice that the bands are fairly narrow, but widths up to about 1 eV indicate, nevertheless, some electronic interactions. Similar results were found for HBr (Jansen *et al.* 1987).

Assuming a harmonic approximation valid for the total energy around the minimum in figure 34 (*a*) gives a frequency of 3535 cm^{-1} for the bond-stretch, in-plane Γ phonon. This value is in good agreement with the experimental values of 3360–3404 cm^{-1} (Kittelberger and Hornig 1967, Anderson *et al.* 1980, Desbat and Huong 1983). But the potential is strongly anharmonic due to the existence of two energetically degenerate structures only differing in the alternation of covalent and hydrogen bonds. Since the barrier height for the collective shift of the protons from one minimum to the other $[(\alpha, d_F, d_H) \rightarrow (\alpha, d_F, d_F - d_H)]$ is comparable to the frequency of the lowest bond-stretch mode, the anharmonicities will be important.

We made a simple qualitative model (Springborg 1988) for a quantum-mechanical description of the protons in a one-dimensional double-well. This resulted in Γ modes at roughly 500, 2000, and 4000 cm^{-1}. The latter corresponds reasonably well to that found in the harmonic approximation, whereas the first falls in a region where many modes are observed. Only the middle one appears in a 'new' region and has not yet been observed. We believe, however, it to have a small cross-section and thus to be difficult to observe experimentally.

Jansen *et al.* (1987) made a much more detailed study of the vibrational properties of the hydrogen halides, for which they got the parameters for the model potentials by fitting to experimental results. The results of the density-functional calculations were subsequently used in demonstrating the validity of the model. However, they made use of a harmonic approximation in studying the phonons.

The total energies of figure 34 may also be used in studying liquid and gaseous hydrogen fluoride. Both these phases consist of $(HF)_n$ oligomers (Maybury *et al.* 1955, Smith 1958, Ring and Egelstaff 1969) and theoretical studies of thermodynamical, statistical, and dynamical properties of $(HF)_x$ thus require interaction potentials that

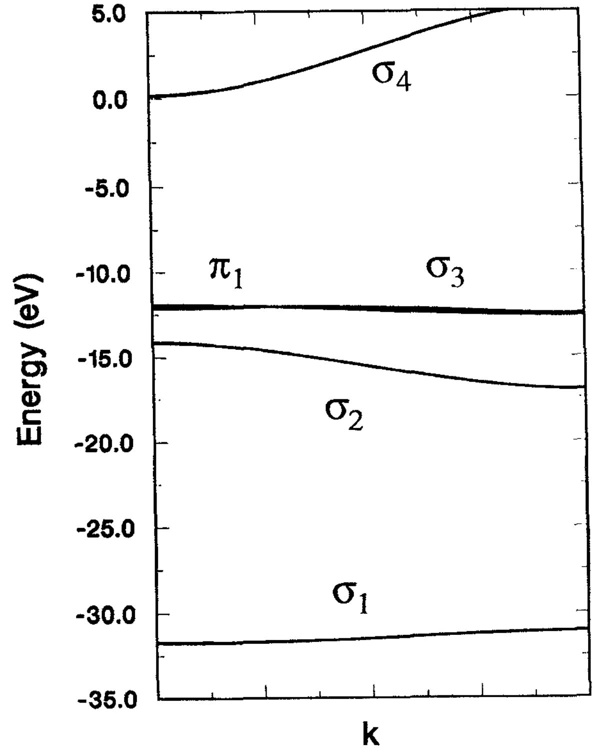

Figure 35. The band structures for the optimized zig–zag $(HF)_x$ chain. All bands except for the uppermost are occupied. (Reproduced from Springborg (1988).)

describe the properties of the oligomers and polymers well. Independent of this most potentials have been derived from *ab initio* calculations on the $(HF)_2$ dimer for which it furthermore is assumed that the length of the chemical F–H bond is as for the isolated monomer. Figure 34 clearly shows that this assumption is not justified for the polymer, and is therefore not to be expected to be a good approximation for $(HF)_n$, with n medium-sized. We compared moreover the total-energy variations as functions of d_F (under relaxation of d_H) as extracted from figure 34 with those predicted by the model potentials. It turned out (Springborg 1988, 1989 *a*) that none of the potentials could describe the properties of the polymers satisfactorily, and thus that improvements are strongly required.

By studying the collective shifts of all the protons from one total-energy minimum to the energetically degenerate one can obtain a model potential with which solitons subsequently can be investigated. Instead of focusing solely on the total energies we included a description of the electronic single-particle energies (Springborg 1988). For a soliton we found then that it had a vanishing width (i.e. L of equation (14) becomes vanishing) and that the soliton gave rise to extra electronic states just outside the band regions. These extra peaks or shoulders may provide an experimental indication on the existence of solitons although also other effects (excitons, colour centres, interchain interactions, finite chain lengths, etc.) can be held responsible for such features.

The model so derived is lacking more aspects and may only be considered a first approximation. It has thus been proposed (see, e.g., Laedke *et al.* (1985)) that there

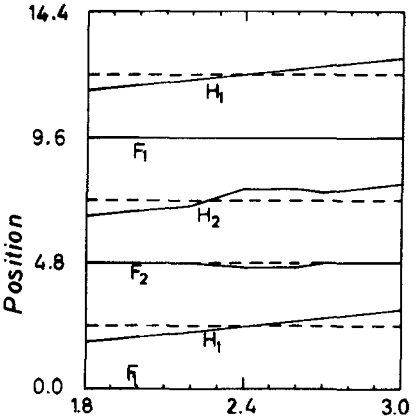

Figure 36. Positions of various atoms for a linear chain of periodically repeated $(HF)_2$ units as functions of the position *d* of every second H atom. The fluorine atoms at 0 and 9·6 a.u. are fixed whereas that at roughly 4·8 a.u. is allowed to move. The hydrogen atoms between 0 and 4·8 a.u. and between 9·6 and 14·4 a.u. are those being moved, wheres that between 4·8 and 9·6 a.u. is allowed to relax its position. The dashed lines are placed with intervals of 2·4 a.u. and mark the positions of the fluorine atoms and the mid-points between those for the undistorted system. (Reproduced from Springborg (1992*b*).)

should be a coupling to the heavier sublattice. This means that under the propagation of a soliton in which the protons are moved also the heavier atoms (i.e. the fluorine atoms) will move. Since the linear and the zig-zag $(HF)_x$ chains possess similar properties (see figure 34) we felt that the coupling to the heavier sublattice could be studied on the linear chains.

We considered a linear chain with fixed F–F next-nearest-neighbour distances of 9·6 a.u., and moved every second hydrogen atom in unison from being closest to the fixed fluorine atoms to being closest to the other fluorine atoms (Springborg 1992*b*). The other (i.e. every second) H and F atoms were allowed to relax.

In figure 36 we show the position of the various atoms as functions of the distance (*d*) between the fixed fluorine atoms and the hydrogen atoms being shifted. For *d* close to half the F–F nearest-neighbour distance (i.e., $d \simeq 2{\cdot}4$ a.u.) we notice that the not-fixed F atoms (i.e. that at $\sim 4{\cdot}8$ a.u. in figure 36) move towards the moving H atoms (that at $\sim 2{\cdot}4$ a.u. in figure 36). Simultaneously, the other H atoms jump towards the fixed F atoms. In some sense this corresponds to the creation of HFH^+ and F^- ions, although this interpretation should be taken with some care. According to the first-principles calculations the hydrogen atoms are carrying charge; about 0·5 electron as given by the Mulliken populations. Compared with shifting *all* hydrogen atoms simultaneously the barrier upon shifting from the one structure to the energetically degenerate structure is roughly halved when allowing the atoms to move as in figure 36.

Finally, also Jansen *et al.* (1987) studied solitons in the hydrogen halides. They, however, invoked a continuum approximation which is justified when the lattice distortion of the soliton is much larger than the lattice spacing. Since this is not the case for the hydrogen halides, their relatively large creation energy of a soliton (some few eV; compared with our values of some 0·1 eV) may be a result of this approximation.

In Section 6.2. we studied, among others, the interaction between two linear, parallel polyyne chains and argued that this interaction could have crucial effects on the stability of solitons. Similar arguments can be carried through for the $(HF)_x$ chains, and we therefore studied two linear, parallel $(HF)_x$ chains (Springborg 1989 *c*). It turned out that the electronic interactions were less important and the electrostatic interactions more important than for the carbon chains. Therefore, the band splittings were significantly smaller, and the antiparallel arrangement was consequently preferred almost independent of the relative arrangement of the two chains. As for polyyne these results indicate that the interactions do need to be included in a complete description of solitons in hydrogen-bonded chains, although other effects like temperature-induced fluctuations or solvation effects may decrease the importance of the interchain interactions.

8. Other hydrogen-bonded polymers

As mentioned above, hydrogen fluoride (and the other hydrogen halides) may not be considered the prototypes of hydrogen-bonded systems. Therefore, the overall good agreement between the theoretical values and experimental values does not need to imply that this will be found for any hydrogen-bonded system.

Hydrogen cyanide represents an excellent system for further theoretical studies on hydrogen-bonded systems. In the solid phase hydrogen cyanide consists of weakly interacting, linear chains of linear, hydrogen-bonded HCN monomers (Dulmage and Lipscomb 1951). Compared with the hydrogen halides, hydrogen cyanide has the further interesting property that it has only one ground-state structure and shifting the hydrogen atoms from being closest to one of their two nearest neighbours (carbon atoms) to being closest to the other (nitrogen atoms) results in a structure with another total energy. In the context of the structural defects discussed in Section 3 this implies that polarons but not solitons may be metastable quasi-particles. As such hydrogen cyanide can serve as a prototype for the many biologically important systems with hydrogen-bonding hydrogen atoms asymmetrically placed between two different types of nearest neighbours. Of those, the α-helix and the double-helix are two well known examples.

The study of hydrogen cyanide (Springborg 1991 *b*) was motivated by one further reason. The unit cell of hydrogen cyanide consists of exactly the same three atoms as that of polycarbonitrile discussed in Section 6.3. Thus, we can compare the results for those two compounds and thereby obtain interesting information about the differences and similarities between hydrogen-bonded and conjugated polymers.

We first studied isolated, linear HCN and CNH molecules. The optimized bond lengths were $d_{HC} = 1{\cdot}93$ a.u. and $d_{CN} = 2{\cdot}22$ a.u. for HCN and $d_{CN} = 2{\cdot}21$ a.u. and $d_{NH} = 1{\cdot}75$ a.u. for CNH. Experimental values are $d_{HC} = 2{\cdot}01$ a.u. and $d_{CN} = 2{\cdot}18$ a.u. for HCN (Suzuki *et al.* 1966, Winnewisser *et al.* 1971) and $d_{CN} = 2{\cdot}21$ a.u. and $d_{NH} = 1{\cdot}88$ a.u. for CNH (Creswell and Robiette 1978). The chemical bonds between hydrogen and its nearest neighbour are accordingly too short, whereas we reproduce the C–N bond length accurately. *Ab initio* Hartree-Fock calculations, on the other hand, give too short C–N bond lengths but accurate H–C bond lengths (Karpfen 1983, Hennico *et al.* 1988). The calculations indicate furthermore the CNH monomer to have a lower total energy than the HCN monomer, which is wrong. As already mentioned, the density-functional calculations with a local approximation are known to overestimate the strength of chemical bonds with up to some few eV per bond (see, e.g., Jones and Gunnarsson (1989)). Since the total-energy difference between HCN and CNH is of that order of magnitude, these inaccuracies, which depend on the type of chemical bonds, exclude us from making any reliable statements about the relative stability of these two monomers.

We believe the same overestimate in the strength of chemical bonds to be responsible for the too short hydrogen bonds we find for the polymers. For a linear $(HCN)_x$ chain we found the lowest total energy for $d_{HC} = 1{\cdot}83$ a.u. and $d_{CN} = 2{\cdot}28$ a.u. The hydrogen-bond length was found to be $d_{NH} = 3{\cdot}51$ a.u. giving a unit-cell length of $D = 7{\cdot}62$ a.u., whereas experiments (Dulmage and Lipscomb 1951, Maroncelli *et al.* 1985) have given $D = 8{\cdot}20$ a.u. The *ab initio* Hartree–Fock values of Karpfen (1983) are in this case in better agreement with the experiments. We are lacking experimental and other theoretical information about the structure of linear $(CNH)_x$ chains, for which we find $d_{CN} = 2{\cdot}23$ a.u., $d_{NH} = 1{\cdot}78$ a.u., and $d_{HC} = 3{\cdot}67$ a.u. giving $D = 7{\cdot}68$ a.u. It is remarkable that D is almost the same for the two compounds. As for the monomers, the calculations indicate the CNH-based compounds to be stable than the HCN-based compounds. Moreover, we find the polymers to be only metastable compared with dissociation into isolated monomers.

In figure 37 we show the band structures for the two optimized structures together with those of a transition state. This latter is obtained by considering a transition between the two polymers in which it is assumed that all bond lengths vary linearly as functions of positions of the hydrogen atoms. The structure of figure 37 (*c*) is then that for which the hydrogen atoms are about halfway between the two nearest neighbours. For all three we notice the deep-lying σ_1 band at almost constant energy. This band is formed by strong σ bonds between C and N. The σ_2 bands are due to the σ bonds between hydrogen and its nearest neighbour and thus approaches a hydrogen 1s orbital for the transition state. The σ_3 band is formed by orbitals that to some extent can be characterized as lone-pair orbitals. This label is most justified for $(HCN)_x$ (in which case the orbitals are lone-pairs on nitrogen) and less for $(CNH)_x$ (lone-pairs on carbon). Finally, the doubly degenerate π_1 band is formed by the bonding combination of carbon and nitrogen p functions perpendicular to the molecular axis. This interpretation explains why the σ_2 and σ_3 bands are those changing most under the transition between the two structures.

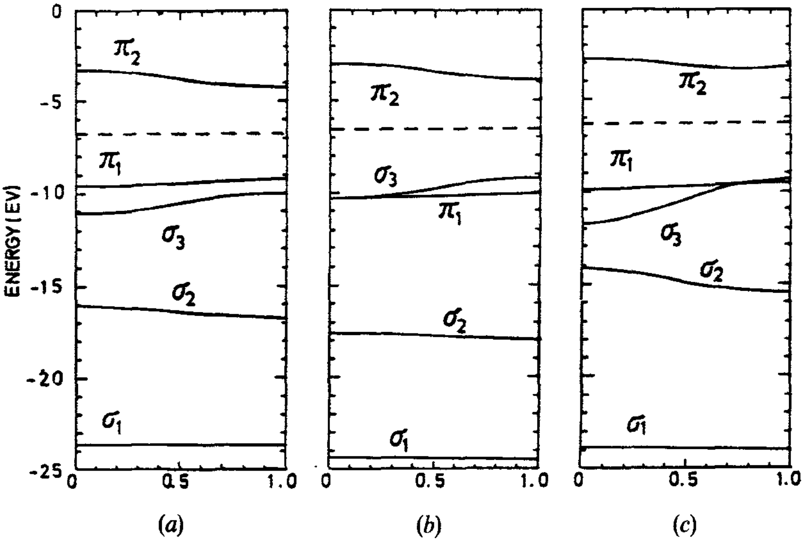

(*a*) (*b*) (*c*)

Figure 37. Band structures of (*a*) $(HCN)_x$, (*b*) $(CNH)_x$, and (*c*) the 'transition state' between the other two. The dashed lines are the Fermi levels. (Reproduced from Springborg 1992*b*.)

Comparing the bands of figure 37 with those of the conjugated polymer (figure 22) it is obvious that the conjugated polymer is covalently bonded with relatively delocalized electrons resulting in wide bands, whereas the electrons of the hydrogen-bonded systems are localized and only produce narrow bands. As discussed elsewhere (Springborg 1992 *c*) this difference is recovered in other properties like photoelectron and electron-energy-loss spectra, momentum distributions, and reciprocal form factors.

Due to the inaccuracies of the total energies as calculated within the local-density approximation we have not studied solitons or polarons in detail. However, the calculations indicate that the energy barrier for the transition between $(HCN)_x$ and $(CNH)_x$ is relatively high, such that the lattice distortion related to solitons or polarons is expected to be very localized. But it should be stressed that this does not imply that the defect-induced electron densities are strongly localized (Springborg 1991 *b*), and using the proposal of Section 6.1. as well as figure 37 we believe the defects to induce states just outside the band regions. Most significant will these be for the σ_2 and σ_3 bands, and these may provide an experimental possibility of identifying the occurrence of the structural defects.

The results on hydrogen cyanide indicate that structural properties on hydrogen-bonded systems as calculated with present density-functional methods may be related with some inaccuracy. Those on hydrogen halides, on the other hand, show that they may also be accurate. Since there are very few density-functional studies on extended hydrogen-bonded systems, these constitute obviously a class of materials that should be further studied with related methods. We are thus planning to investigate linear chains of water molecules (which is of importance in many biological systems; see Bountis (1992)) as well as the α-helix in the near future. However, some very recent density-functional studies of finite systems containing hydrogen bonds have indicated that replacing the local approximation for exchange and correlation effects by a so-called non-local approximation (see Section 2) may improve the reliability of the calculated parameters (Sim *et al.* 1992).

9. Some further systems

Except for the materials discussed in Section 4, we have concentrated on hydrogen-bonded and conjugated polymers. However, there are many other materials that naturally can be examined with the methods discussed in the present review. In this Section we will discuss some of those for which first-principles studies exist. Some other systems that could by the subjects of future studies will form a part of the discussion in Section 10.

9.1. *Sulphur nitride*

Although sulphur nitride was synthesized already in the beginning of this century (Burt 1910), it was first in 1975 that its crystal structure was determined (Boudelle 1975). This was partly a result of an enormous increase in the interest in this compound due to the reports that the material stayed metallic down to unusually low temperatures (Walatka *et al.* 1973) and that it became superconducting at $T_c \simeq 0{\cdot}26 \pm 0{\cdot}03$ K (Greene *et al.* 1975).

$(SN)_x$ consists of weakly interacting chains of the form shown in figure 38 and is one of the first real quasi-dimensional materials for which an intensive study of its electronic properties was undertaken. One of the intensively discussed issues was (see, e.g., Springborg (1989 *h*)) why the compound was superconducting instead of showing a

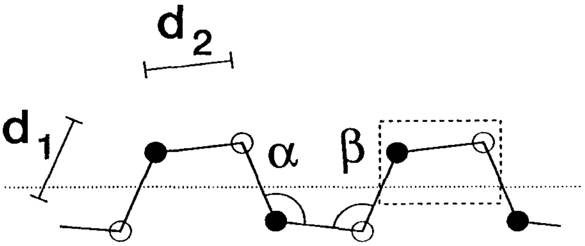

Figure 38. Structure and structural parameters of a single sulphur nitride chain. The dashed lines show the unit cell and the polymer axis, and the black and white circles indicate the sulphur and nitrogen atoms, respectively. (Reproduced from Springborg (1989 *h*).)

Peierls distortion. As one possible explanation it was proposed that two bands and not one were crossing the Fermi level but as pointed out by Berlinsky (1976) any truly one-dimensional compound with two bands crossing the Fermi level can always lower its total energy upon a periodic, symmetry-lowering distortion that produces a gap at the Fermi level. The other explanation that was put forward and that currently is believed to be the correct one (Causá *et al.* 1988) proposes that it is more correct to consider sulphur nitride as a highly anisotropic three-dimensional material instead of a quasi-one-dimensional one, such that interchain interactions suppress the Peierls transition.

Although the current interest in conjugated polymers and charge-transfer salts to some extent has replaced that in sulphur nitride, we felt that there still was a need for a further first-principles study of $(SN)_x$; partly because there had been no attempt at calculating structural or vibrational properties using first-principles methods and partly because the material had not been the subject of any density-functional study. We will here review the results of the study (Springborg 1989 *h*).

For the structure of figure 38 with one SN unit per unit cell we found the lowest total energy for $\alpha = 122°$, $\beta = 112°$, $d_1 = 3{\cdot}20$ a.u., and $d_2 = 3{\cdot}45$ a.u. These values are to be compared with experimental values of $\alpha = 113{\cdot}5$, $\beta = 112{\cdot}5°$, $d_1 = 3{\cdot}25$ a.u., and $d_2 = 2{\cdot}99$ a.u. (Boudelle 1975), $\alpha = 120°$, $\beta = 106°$, $d_1 = 3{\cdot}08$ a.u., and $d_2 = 3{\cdot}01$ a.u. (Mikulski *et al.* 1975), and $\alpha = 120°$, $\beta = 107°$, and $d_1 = d_2 = 3{\cdot}00$ a.u. (Heger *et al.* 1978). The bond angles are thus realistic but the finding of $d_1 < d_2$ is at variance with the experimental findings. However, *ab initio* Hartree–Fock calculations on finite segments of $(SN)_x$ terminated with hydrogen atoms (Haddon *et al.* 1980) have given results indicating $d_1 < d_2$ for the isolated molecules, and we may thus relate the difference to interchain interactions. In addition, the calculated total-energy difference between the optimized structure and the experimental structure of Boudelle (1975) is 1·4 eV per SN unit which may be considered a realistic value of the interchain bond energy.

Figure 39 shows that the optimized and experimental structures have very similar band structures and have both only one (π) band crossing the Fermi level. It turns out that the orbital at the Fermi level has large sulphur components. This will become of importance later.

The calculated total energy as a function of structural parameters can be used in calculating frequencies of in-plane Γ phonons. These were, however, only in qualitative agreement with experimental values. The disagreement may be a further consequence of the lacking interchain interactions.

According to the conventional BCS theory of superconductivity (Bardeen *et al.* 1957), the important ingredient for superconductivity is the coupling between phonons

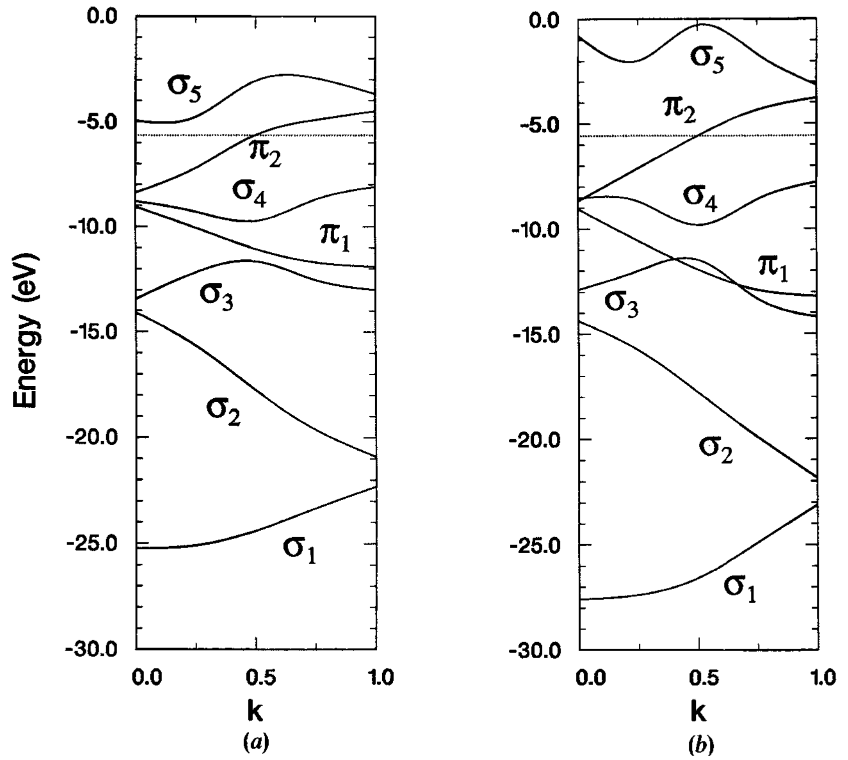

Figure 39. Band structures of (*a*) the optimized structure and (*b*) the experimental structure (Boudelle 1975) of $(SN)_x$. The dashed lines correspond to the Fermi level. (Reproduced from Springborg (1989 *h*).)

and electronic orbitals at the Fermi level. We have only one such orbital, and have moreover a single, isolated chain such that the position of the energy of that orbital refers to a common energy zero. Therefore, shifts in the Fermi energy measure couplings of the orbitals at the Fermi level. Exciting the chains with the above-mentioned Γ phonons shows then that the phonons involving mainly displacements of the sulphur atoms perpendicular to the chain axis are those that cost least energy and lead to the largest changes in the Fermi energy. One part of an explanation for this is the large sulphur component for this orbital. A further part is that the perpendicular displacements do only modify the S–N bonds approximately perpendicular to the polymer axis, whereas displacements parallel to this axis would modify both S–N nearest-neighbour bonds and S–N next-nearest-neighbour quasi-bonds. Moreover, the phonons mainly involving displacements of the nitrogen atoms perpendicular to the chain direction are those leading to the smallest changes in the Fermi level but the largest changes in the total energy.

9.2. *A charge-transfer salt*

Shortly after the discovery of the superconductivity in sulphur nitride and of the large doping-induced increase in electrical conductivity in polyacetylene, unusual properties were discovered in another class of quasi-one-dimensional compounds. For the $(TMTSF)_2X$ salts with TMTSF being tetramethyltetraselenafulvalene and $X = PF_6$, AsF_6, SbF_6, TaF_6, NC_3, BF_4, ReO_4, ClO_4, ..., were metal–insulator transitions at unusuallly low temperatures (Bechgaard *et al.* 1980), as well as superconductivity (Jérome *et al.* 1980, Bechgaard *et al.* 1981) discovered. These discoveries have led to a large research activity in these and related so-called charge-transfer salts (see, e.g., Aldissi (1988–1989), Roth *et al.* (1991)).

A typical charge-transfer salt A_nB_m (n and m being small integers) consists of parallel, weakly interacting chains of either A or B molecules. Most often at least one of the A and B molecules is organic, and the energies of the frontier orbitals of the two are comparable such that a small charge-transfer may take place. This leads often to two bands crossing the Fermi level of which the orbitals of each band are concentrated on one of the two subsystems. The molecules of one chain are only weakly interacting such that bandwidths are small. For some systems the interchain interactions are sufficiently strong to suppress Peierls distortions.

A Hubbard Hamiltonian of the form (17) is often applied in studying the properties of the charge-transfer salts and since the hopping integrals t are small (0·1–1 eV), the Hubbard U easily becomes dominating. It is therefore often assumed that accurate studies of these materials require detailed descriptions of correlation effects. We will here, however, argue that structural properties may be understood from simpler descriptions.

A typical charge-transfer salt is TTF–TCNQ (tetrafulvalene–tetracyanoquinodimethane, $C_6S_4H_4$–$C_{12}N_4H_4$). It has 34 atoms per formular unit and is thus far too large for a detailed first-principles study of the structure. There exists accordingly only one density-functional study on a charge-transfer salt, namely that of Kübler *et al.* (1987) on β-(BEDT–TTF)$_2$I$_3$ [BEDT–TTF = Bis(ethylenedithio)tetrathiafulvalene, $C_{10}S_8H_8$], which actually has 55 atoms per unit cell. Kübler *et al.* concentrated on the band structures as obtained for the full three-dimensional structure. These did give small bandwidths as well as a complicated Fermi surface. Moreover, the local densities of states showed non-vanishing components at the Fermi level both for the organic molecules and for the I_3 molecules in agreement with the picture above.

However, in order to study structural properties one might have to look at smaller systems. The largest atoms of the mentioned systems are the sulphur atoms, and if interactions between electronic orbitals can be held responsible for the properties of the salts, these must be mediated through sulphur-centred orbitals.

A model system which contains sulphur and consists of two subsystems with comparable first ionization potentials (such that a smaller charge transfer may take place) is H_2S–S shown in figure 40. We examined the total energy as a function of the two parameters D and d shown in figure 40 (Springborg *et al.* 1990 *b*), and found a stable structure for the type of figure 40 (*a*) for $D \simeq 3{\cdot}6$ Å and $d \simeq 2{\cdot}6$ Å, but none for the type of figure 40 (*b*). It is remarkable that the optimized D value compares well with typical intermolecular distances in the sulphur-based charge-transfer salts (see, e.g., Aldissi (1988–1989), Roth *et al.* (1991)) indicating that simple orbital interactions are partly responsible for the structural stability of these salts. However, also ionic interactions are required as could be shown by removing the single S atoms and thus considering stacked H_2S molecules. These were found not to be stable. In fact, it turned out that the H_2S and S subsystems interacted strongly, which may explain why some salts have molecules that are tilted relative to being perpendicular to the stacking direction: thereby the electronic interactions between the A and B subsystems may be increased.

It should finally be pointed out that the model system cannot account for all properties of the charge-transfer salts: thus it is found to be semiconducting and accordingly not superconducting.

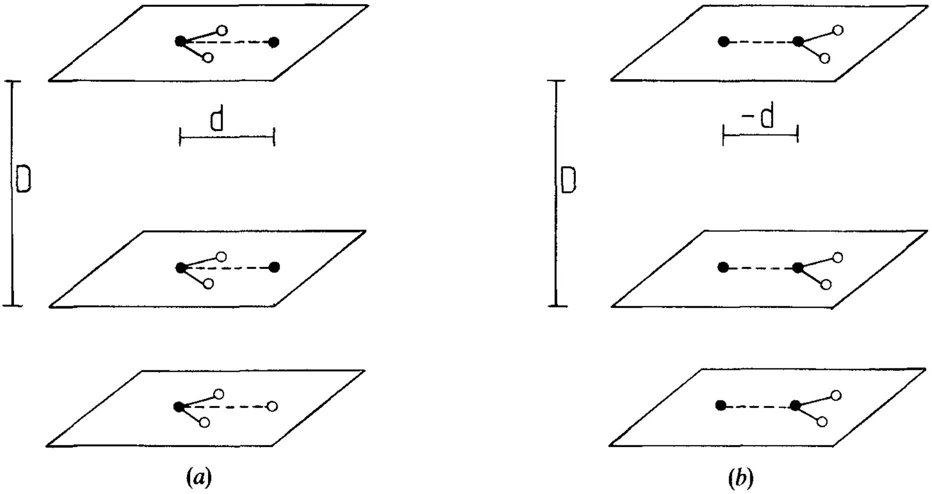

Figure 40. Schematic representation of two types of stacks of H_2S–S units. Black and white circles represent sulphur and hydrogen atoms, respectively. All atoms of one unit are supposed placed in one common plane perpendicular to the stacking direction and the single S atoms are placed along the bond-angle bisectors of the H_2S molecules. (Reproduced from Springborg *et al.* (1990*b*).)

9.3. *A* MX *chain*

A class of materials that has received much attention recently is the so-called halogen-bridged, transition-metal, linear-chain, mixed-valence (actually, a better word is alternating-valence) MX compounds (see Aldissi (1988–1989), Roth *et al.* (1991)). Neglecting for the moment side-ligands, these consist of linear chains of alternating metal ($=M$, being Ni, Pd, or Pt) and halogen ($=X$, being Cl, Br, or I) atoms. The X atoms tend to move pairwise closer to one half part of the M atoms leaving the other half part more isolated. This results effectively in an alternation in the valence of the M atoms. There exist two energetically degenerate structures only differing in this alternation. This has led Baeriswyl and Bishop (1988) to propose the existence of defects like solitons and polarons similar to the case of the conjugated polymers. One aspect that makes these materials interesting is that many of the properties can be tuned by varying the M or X atoms, by applying pressure, or by changing the side-ligands.

One of these compounds consists of $M=\text{Pt}$ and $X=\text{Br}$ along the polymer axis. To each M atom two further Br atoms and two NH_3 molecules are attached as side-ligands. In a first study, Albers and coworkers (Albers 1988, Albers *et al.* 1991) used the LMTO method for three-dimensional crystals in order to explore the band structures. Their results indicate frontier orbitals defined by p_z functions on the Br atoms and d_{z^2} functions on the Pt atoms when assuming the MX chains to lie along the z axis. This study, however, did not include optimization of structural parameters.

In order to explore structural properties we have first studied the naked chain consisting solely of the Pt and Br atoms along the polymer axis. The lowest total energy was found for a Pt–Pt distance of 9·15 a.u., which is significantly smaller than the experimental value of 10·49 a.u. for the full chain including side ligands (Keller *et al.* 1981). Further calculations gave no sign of a lowering of the total energy upon moving the Br atoms pairwise closer to one half of the Pt atoms in disagreement with experimental findings on the complete system (Keller *et al.* 1981). That this is so may be

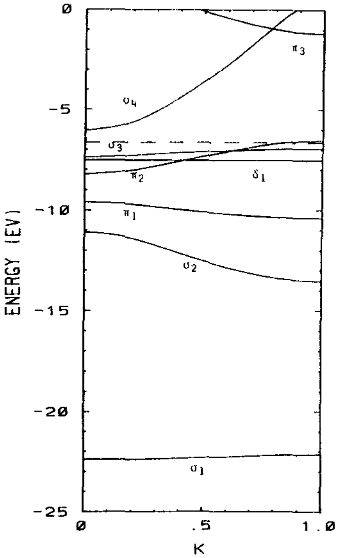

Figure 41. Band structures of the optimized PtBr chain.

understood from the band structures (figure 41) of the undimerized chain. Here, a doubly degenerate π band is seen to cross the Fermi level, such that it becomes 3/4 filled and such that no gap will appear at the Fermi level upon dimerization.

By lowering the symmetry, the double degenerate π bands can be split into single degenerate ones, which in turn might lead to a half-filled band at the Fermi level such that a Peierls dimerization becomes favourable. Including the Br ligands is one obvious way of achieving this but density-functional calculations on three-dimensional materials showed (Alouani *et al.* 1992), that although the NH_3 molecules are closed-shell systems (in contrast to the Br atoms) also their presence was required in order to remove states from the Fermi level. Without those ligands (but with the Br ligands), more bands would cross the Fermi level excluding a Peierls dimerization.

In figure 42 we show the calculated total energies as functions of the dimerization ratio ζ both for chains without the NH_3 ligands and for chains with those. ζ is defined as the shift of the Br atoms of the backbone away from the symmetric position towards the Pt atoms measured in units of half the Pt–Pt interatomic distance. Figure 42 shows clearly that the NH_3 ligands are required in order to be able to theoretically reproduce the experimentally observed dimerization. Finally, since the inclusion of the NH_3 ligands leads to a half-filled band for the undimerized chain, the dimerization results in a gap at the Fermi level, which is calculated to be about 1·2 eV (Alouani *et al.* 1992).

9.4. *Fullerene tubules*

The present intense research activity in the C_{60} and C_{70} fullerenes is well-known and has been reviewed several times despite the young age of the field. Of relevance to the present discussion is that it has been proposed (see, e.g., Dresselhaus *et al.* (1992)) that one might also synthesize so-called fullerene tubules. One may imagine these by considering a strip of a graphite sheet of finite width folded such that the dangling bonds at each side of the strip get bonded together. Eventually the tubes might be of finite length and closed by caps (see Dresselhaus *et al.* (1992)).

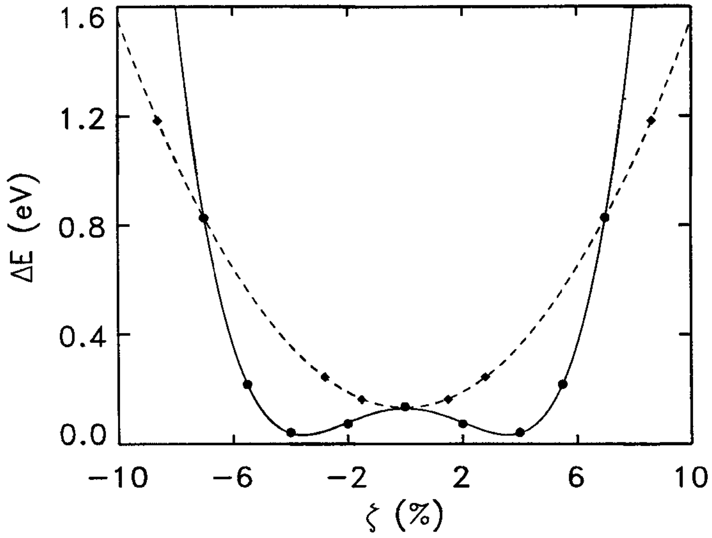

Figure 42. Relative total energy of the $Pt_2Br_6(NH_3)_4$ chain (full curve) and of the Pt_2Br_6 chain (dashed curve) as a function of the dimerization ratio. (Reproduced from Alouani *et al.* (1992).)

Mintmire *et al.* (1992) have presented the first and so far only density-functional study of these. They calculated the band structures of one of these that contained ten atoms per unit cell and that possessed the highest possible symmetry. This was found to lead to a metal with two bands crossing the Fermi level, proposing interesting properties for those materials. It is however not clear whether this result is a consequence of a specific geometry and whether other fullerene tubules possess similar properties. These questions should be addressed by further density-functional studies.

10. Extensions and improvements

Over the last decade a number of quasi-one-dimensional systems have been studied using density-functional methods as those described in Sections 2 and 3 and giving the results presented in the preceding Sections. There are, however, still many further systems that could be studied as well as limitations that should be removed. In this Section we will address these points.

Polyaniline which backbone consists of alternating phenyl rings and nitrogen atoms is currently one of the most intensively studied conjugated polymers (see, e.g., Roth *et al.* (1991)). It differs from those of Sections 5 and 6 in two important aspects. First of all, the polymer possesses the extra, partly controllable, degree of freedom that the number of hydrogen atoms attached to the nitrogen atoms of the polymer backbone may be varied. Furthermore, the backbone is not planar but neighbouring phenyl rings make an angle $\phi \neq 0$. Therefore, structural defects related to local variations in ϕ have been proposed (Ginder *et al.* 1989, Ginder and Epstein 1990). These two extra features make polyaniline an interesting candidate for future studies.

In the study of solitonic defects in hydrogen-bonded chains not only ionic solitons, which were discussed in Section 7, but also the so-called Bjerrum defects (Bjerrum 1952) should be included. For $(HF)_x$ these correspond to F–F bonds with either none or two hydrogen atoms. Both types of defects should actually be described within the same model as, e.g., proposed by Pnevmatikos (1988), since both are required in describing proton transfer through hydrogen-bonded systems (see, e.g., Bountis (1992)). Finally, further studies on more hydrogen-bonded systems should address the reliability of the density-functional methods in describing the properties of these systems as discussed in Section 8.

There exist also totally different classes of materials for which the density-functional methods have definite advantages over, e.g., Hartree–Fock based methods. Among those are the transition metal trichalcogenides MX_3 (M = Ta, Nb, Hf, Zr, Ti; X = S, Se, Te) and the transition metal tetrachalcogenides MX_4 which all show interesting charge-density-wave properties (see, e.g. Barišić 1985). The large degeneracy of the d orbitals makes a Hartree–Fock approximation poor, and a density-functional approach is an obvious alternative. The charge-density waves have actually been observed experimentally (Dai *et al.* 1991).

Among the experimentally relevant systems for which density-functional methods should be applied are systems containing more different materials. These include heterojunction between metals and semiconductors where the semiconductor could be a conjugated polymer and the metal Al, Ag, or Au (see, e.g., Gupta *et al.* (1991)). Such systems are extremely important for any device application of the conjugated polymers (see, e.g., Salaneck *et al.* (1991)).

The currently applied density-functional methods are suffering from a number of limitations of which the most serious ones are as follows.

Except for some few plane-wave based methods for crystalline materials, they are lacking the capability of calculating forces, i.e. the derivatives of the total energy with respect to structural parameters. This makes it tedious to optimize the structure for the simple systems, and for the more complicated systems we are forced to consider solely certain selected structures. But once forces can be calculated accurately we may ultimately combine the density-functional calculations with molecular-dynamics calculations, as proposed by Car and Parrinello (1985).

In our own study of electron-energy-loss spectra we have neglected matrix-element effects and considered solely band-to-band transitions. A much more detailed level of information about many more optical properties can be obtained by calculating the fulll dielectric matrix as has been done by Mintmire and coworkers.

We have everywhere assumed the eigenvalues to the Kohn–Sham equations (1) to be good approximations to electronic excitation energies, which may or may not be justified. An (computationally costly) improvement would be to calculate the quasi-particle energies as demonstrated by Hybertsen and Louie (1986) for crystalline semiconductors.

Further comparisons with experimental available information as well as important predictions could be obtained by calculating other properties like, e.g., nonlinear optical properties. It is presently assumed that also these properties will make the conjugated polymers technologically important. In addition, for a number of properties the linear-response methods as put forward by Baroni *et al.* (1987) and by Gunnarsson *et al.* (1989) could be useful, or the treatment of nonlinear responses presented by Gonze and Vigneron (1989) may be used. These approaches have, however, so far only been applied on three-dimensional solids.

Upon mapping the density-functional results on a suitable model Hamiltonian we depend crucially upon having defined a model that includes all effects of relevance to the problem of interest. Some of these are, however, difficult to evaluate. This includes, e.g., long-range electrostatic effects related to defects in the hydrogen-bonded chains. Determining these requires often calculations on systems with larger unit cells.

Another important quantity, but so far neglected in our approach, is the Hubbard U (as well as other correlation parameters in extended models). For these various approaches have been proposed for extracting them from first-principles calculations (McMahan *et al.* 1988, Hybertsen *et al.* 1989, Gunnarsson 1990). Such methods might be incorporated in the polymer calculations.

11. Conclusions

In this review we have presented a detailed study of the electronic properties of a number of quasi-one-dimensional systems. The results were based on parameter-free calculations on finite or periodic chains using density-functional methods. As demonstrated, the present density-functional methods offer an effective and most often accurate way of calculating electronic ground-state properties, but may for some systems be related with some inaccuracy. Compared with the Hartree–Fock methods, a density-functional method is computationally easier to apply, especially since the long-range exchange interactions are screened, since light and heavy atoms can be treated on approximately the same footing, since it does not have conceptional problems in describing metallic systems, and since correlation effects are included.

The results demonstrated that one can describe structural properties of a variety of systems accurately, with the weak hydrogen bonds of hydrogen cyanide representing an exception. For some systems the calculations could also be used in discriminating between possible outcomes of a synthesis, as was most clearly observed for the carbon–selenium polymers.

The conjugated polymers formed a major part of the presentation. We demonstrated how the first-principles calculations could provide experimentally accessible information and, furthermore, how they could be used in determining model Hamiltonians with which solitons and polarons could be studied. We showed that the solitons and polarons induced states in the gap, but that the details of the positions and relative stability of these structural defects required models that were specific for the systems of interest.

Another part of the presentation was devoted to hydrogen-bonded systems. These materials represent systems that are close to being not treatable within the present density-functional methods. For the hydrogen halides we thus observed calculated properties that were in good agreement with experiments whenever a comparison was possible, whereas the agreement was less good for hydrogen cyanide. Among the results for the hydrogen halides we mention in particular the anharmonic effects that showed up at two places: in the appearance of extra phonon modes, and in the possibility of soliton formation.

As discussed in the last parts of the review, many other systems can be treated with the methods presented here. We gave some few examples of systems that already have been considered and concluded by mentioning further systems that should be treated in the nearest future as well as possible improvements of the first-principles methods.

Acknowledgments

Without the assistance and encouragement of a number of colleagues and friends the present review would not have been possible. Among those are Robert C. Albers, Meb Alouani, Ole Krogh Andersen, Klaus Bechgaard, Thomas Bjørnholm, Jean-Louis Calais, Stefan-Ludwig Drechsler, Leif A. Eriksson, Osvaldo Goscinski, Per Hedegård, Detlev Hohl, Robert O. Jones, Ladislav Kavan, Helmuth Kiess, Milos Lev, Jiři Málek, Wolf Weyrich, and John M. Wills.

References

Albers, R. C., 1989, *Synth. Met.*, **29**, F169.

Albers, R. C., Alouani, M., Wills, J. M., and Springborg, M., 1991, *Synth. Met.*, **41–43**, 2739.

Aldissi, M. (editor), 1988–1989, *Proceedings of the International Conference on Science and Technology of Synthetic Metals 1988, Santa Fe, New Mexico, U.S.A. Synth. Met.*, **27–29.**

Alouani, M., Albers, R. C., Wills, J. M., and Springborg, M., 1992, *Phys. Rev. Lett.* (to be published).

Anderson, A., Torrie, B. H., and Tse, W. S., 1980, *Chem. Phys. Lett.*, **70**, 300.

André, J. M., Gouverneur, L., and Leroy, G., 1967, *Int. J. quant. Chem.*, **1**, 451.

Ashkenazi, J., Pickett, W. E., Krakauer, H., Wang, C. S., Klein, B. M., and Chubb, S. R., 1989, *Phys. Rev. Lett.*, **62**, 2016.

Atoji, M., and Lipscomb, W. N., 1954, *Acta crystallogr.*, **7**, 173.

Baeriswyl, D., and Bishop, A. R., 1988, *J. Phys.* C, **21**, 339.

Baeriswyl, D., Campbell, D. K., and Mazumdar, S., 1986, *Phys. Rev. Lett.*, **56**, 1509.

Baeriswyl, D., Campbell, D. K., and Mazumdar, S., 1992, *Conducting Polymers*, edited by H. Kiess (Heidelberg: Springer).

Bardeen, J., Cooper, L. N., and Schrieffer, J. R., 1957, *Phys. Rev.* **108**, 1175.

Barišić, S., 1985, *Electronic Properties of Inorganic Quasi-one-dimensional Compounds*, edited by P. Mondeau (Dordrecht: D. Reidel).

Baroni, S., Giannozzi, P., and Testa, A., 1987, *Phys. Rev. Lett.*, **59**, 2662.

von Barth, U., and Hedin, L., 1972, *J. Phys.* C, **5**, 1629.

Bechgaard, K., Jacobsen, C. S., Mortensen, K., Pedersen, H. J., and Thorup, N., 1980, *Solid St. Commun.*, **33**, 1119.

Bechgaard, K., Carneiro, K., Olsen, M., Rasmussen, F. B., and Jacobsen, C. S., 1981, *Phys. Rev. Lett.*, **46**, 852.

Berlinsky, A. J., 1976, *J. Phys.* C, **9**, L283.

Beyer, A., and Karpfen, A., 1982, *Chem. Phys.*, **64**, 343.

Bjerrum, N., 1952, *Science*, **115**, 385.

von Boehm, J., Kuivalainen, P., and Calais, J.-L., 1987, *Phys. Rev.* B, **35**, 8177.

Boudelle, M., 1975, *Crystal Struct. Commun.*, **4**, 9.

Bountis, T. T. (editor), 1992, *Proton Transfer in Hydrogen-Bonded Systems* (New York: Plenum).

Brazovskĭ, S. A., and Kirova, N. N., 1981, *Pis'ma Zh. Eksp. Teor. Fiz.*, **33**, 6. (*JETP Lett.*, **33**, 4).

Brazovsky, S. A., and Kirova, N. N., 1988, *Solid St. Commun.*, **66**, 11.

Brédas, J. L., Chance, R. R., and Silbey, R., 1981, *Molec. Crystals liq. Crystals*, **77**, 319.

Burt, F. P., 1910, *J. chem. Soc. London*, **97**, 1171.

Campbell, D. K., and Bishop, A. R., 1981, *Phys. Rev.* B, **24**, 4859.

Car, R., and Parrinello, M., 1985, *Phys. Rev. Lett.*, **55**, 2471.

Causá, M., Dovesi, R., Pisani, C., Roetti, C., and Saunders, V. R., 1988, *J. chem. Phys.*, **88**, 3196.

Chiang, C. K., Fincher Jr., C. R., Park, Y. W., Heeger, A. J., Shirakawa, H., Louis, E. J., Gau, S. C., and MacDiarmid, A. G., 1977, *Phys. Rev. Lett.*, **39**, 1098.

Chung, T.-C., Moraes, F., Flood, J. D., and Heeger, A. J., 1984, *Phys. Rev.* B, **29**, 2341.

Colaneri, N., Nowak, M., Spiegel, D., Hotta, S., and Heeger, A. J., 1987, *Phys. Rev.* **B**, **36**, 7964.

Creswell, R. A., and Robiette, A. G., 1978, *Molec. Phys.*, **36**, 869.

Dai, X., Slough, C. G., and Coleman, R. V., 1991, *Phys. Rev. Lett.*, **66**, 1318.

Del Re, G., Ladik, J., and Biczó, G., 1967, *Phys. Rev.*, **155**, 997.

Delhalle, J., Delhalle, S., André, J. M., Pireaux, J. J., Riga, J., Caudano, R., and Verbist, J. J., 1977, *J. electron Spectrosc.*, **12**, 293.

Desbat, B., and Huong, P. V., 1983, *J. chem. Phys.*, **78**, 6377.

Di Lonardo, G., and Douglas, A. E., 1973, *Can. J. Phys.*, **51**, 434.

Donohue, J., 1974, *The Structures of the Elements* (New York: Wiley).

Dresselhaus, M. S., Dresselhaus, G., and Saito, R., 1992, *Phys. Rev.* B, **45**, 6234.

Dulmage, W. J., and Lipscomb, W. N., 1951, *Acta crystallogr.*, **4**, 330.

El-khodary, A., and Bernier, P., 1986, *J. chem. Phys.*, **85**, 2243.

Elsenbaumer, R. L., Jen, K. Y., and Oboodi, R., 1986, *Synth. Met.*, **15**, 169.

Eriksson, L. A., and Springborg, M., 1992, *Phys. Rev.* B, (accepted).

Eriksson, L. A., Springborg, M., and Calais, J.-L., 1993, *New J. Chem.* (to be published).

Falk, J. E., and Fleming, R. J., 1973, *J. Phys.* C, **6**, 2954.

Falk, J. E., and Fleming, R. J., 1975, *J. Phys.* C, **8**, 627.

Feldblum, A., Kaufman, J. H., Etemad, S., Heeger, A. J., Chung, T.-C., and MacDiarmid, A. G., 1982, *Phys. Rev.* B, **26,** 815.

Fink, J., and Leising, G., 1986, *Phys. Rev.* B, **34,** 5320.

Fite, C., El Khodary, A., and Bernier, P., 1987, *Solid St. Commun.*, **62,** 599.

Fritzsche, H., Nücker, N., Scheerer, B., Fink, J., and Leising, G., 1989, *Synth. Met.*, **28,** D237.

Fujimoto, H., Mori, T., Inokuchi, H., Ueno, N., Sugita, K., and Seki, K., 1987, *Chem. Phys. Lett.*, **141,** 485.

Ginder, J. M., Epstein, A. J., and MacDiarmid, A. G., 1989, *Solid. St. Commun.*, **72,** 987.

Ginder, J. M., and Epstein, A. J., 1990, *Phys. Rev.* B, **41,** 10674.

Gonze, X., and Vigneron, J.-P., 1989, *Phys. Rev.* B, **39,** 13120.

Greene, R. L., Street, G. B., and Suter, L. J., 1975, *Phys. Rev. Lett.*, **34,** 577.

Gunnarsson, O., 1990, *Phys. Rev.* B, **41,** 514.

Gunnarsson, O., Gies, P., Hanke, W., and Andersen, O. K., 1989, *Phys. Rev.* B, **40,** 12140.

Gupta, R., Misra, S. C. K., Malhotra, B. D., Beladakere, N. N., and Chandra, S., 1991, *Appl. Phys. Lett.*, **58,** 51.

Gusel'nikov, L. E., and Nametkin, N. S., 1979, *Chem. Rev.*, **79,** 529.

Habuda, S. P., and Gagarinsky, Y. V., 1971, *Acta crystallogr.* B, **27,** 1677.

Haddon, R. C., Wasserman, S. R., Wudl, F., and Williams, G. R. J., 1980, *J. Am. chem. Soc.*, **102,** 6687.

Harbeke, G., Baeriswyl, D., Kiess, H., and Kobel, W., 1986, *Physica scripta*, **T13,** 302.

Heeger, A. J., Kivelson, S., Schrieffer, J. R., and Su, W.-P., 1988, *Rev. mod. Phys.*, **60,** 781.

Heger, G., Klein, S., Pintschovius, L., and Kahlert, H., 1978, *J. solid-st. Chem.*, **23,** 341.

Hennico, G. Delhalle, J., Raynaud, M., Reynaud, C., and Ellinger, Y., 1988, *Chem. Phys. Lett.*, **152,** 207.

Hohenberg, P., and Kohn, W., 1964, *Phys. Rev.*, **136,** B, 864.

Huber, K.-P., and Herzberg, G., 1979, *Constants of Diatomic Molecules* (New York: Van Nostrand Reinhold).

Hybertsen, M. S., and Louie, S. G., 1986, *Phys. Rev.* B, **34,** 5390.

Hybertsen, M. S., Schlüter, M., and Christensen, N. E., 1989, *Phys. Rev.* B, **39,** 9028.

Ikawa, A., and Fukutome, H., 1990, *J. phys. Soc. Japan*, **59,** 1002.

Ikeda, Y., Ozaki, M., and Arakawa, T., 1983, *J. chem. Soc. chem. Commun.*, **1983,** 1518.

Iqbal, Z., Khanna, Y., Murthy, N. S., Szobota, J. S., Maleysson, C., Baughman, R. H. Okamoto, Y., and Choi, L. S., 1986, *J. chem. Phys.*, **85,** 4019.

Iqbal, Z., Correale, S. T., Reidinger, F., Baughman, R. H., and Okamoto, Y., 1988, *J. chem. Phys.*, **88,** 4492.

Isomäki, H., and von Boehm, J., 1980, *J. Phys.* C, **13,** L485.

Jansen, R. W., Bertoncini, R., Pinnick, D. A., Katz, A. I., Hanson, R. C., Sankey, O. F., and O'Keeffe, M., 1987, *Phys. Rev.* B, **35,** 9830.

Jérome, D., Mazaud, A., Ribault, M., and Bechgaard, K., 1980, *J. Phys., Paris, Lett.*, **41,** L95.

Jeyadev, S., Phillpot, S. R., and Rice, M. J., 1988, *Molec. Crystals liq. Crystals*, **160,** 433.

Joannopoulos, J. D., Schlüter, M., and Cohen, M. L., 1975, *Phys. Rev.* B, **11,** 2186.

Johnson, M. W., Sándor, E., and Arzi, E., 1975, *Acta crystallogr.* B, **31,** 1998.

Jones, R. O., 1986, *J. chem. Phys.*, **84,** 318.

Jones, R. O., and Gunnarsson, O., 1989, *Rev. mod. Phys.*, **61,** 689.

Kaneto, K., Uesugi, F., and Yoshino, K., 1987, *J. phys. Soc. Japan*, **56,** 3703.

Karpfen, A., 1980, *Chem. Phys.*, **47,** 401.

Karpfen, A., 1983, *Chem. Phys.*, **79,** 211.

Karpfen, A., Beyer, A., and Schuster, P., 1981, *Int. J. quant. Chem.*, **19,** 1113.

Kasowski, R. V., Caruthers, E., and Hsu, W. Y., 1980*b*, *Phys. Rev. Lett.*, **44,** 676.

Kasowski, R. V., Hsu, W. Y., and Caruthers, E. B., 1980*a*, *J. chem. Phys.*, **72,** 4896.

Kavan, L., Dousek, F. P., and Micka, K., 1990, *J. phys. Chem.*, **94,** 5127.

Keller, H. J., Keppler, B., Ledezma-Sanchez, G., and Steiger, W., 1981, *Acta Crystallogr.* B, **37,** 674.

Kittelberger, J. S., and Hornig, D. F., 1967, *J. chem. Phys.*, **46,** 3099.

Kobayashi, A., Sasagawa, N., Sasaki, Y., Asakura, K., Yokoyama, T., Ishii, H., Kosugi, N., Kuroda, H., and Kobayashi, H., 1985, *Chem. Lett.*, **1985,** 1.

Kobayashi, M., Chen, J., Chung, T.-C., Moraes, F., Heeger, A. J., and Wudl, F., 1984, *Synth. Met.*, **9,** 77.

Kohn, W., and Sham, L., 1965, *Phys. Rev.*, **140,** A, 1133.

Kübler, J., Weger, M., and Sommers, C. B., 1987, *Solid St. Commun.*, **62**, 801.

Kutzler, F. W., White, C. T., and Mintmire, J. W., 1986, *Int. J. quant. Chem.*, **29**, 793.

Laedke, E. W., Spatschek, K. H., Wilkens Jr., M., and Zolotariuk, A. V., 1985, *Phys. Rev.* A, **32**, 1161.

Longuet-Higgins, H. C., and Salem, L., 1959, *Proc. R. Soc. Lond.* A, **251**, 172.

Maroncelli, M., Hopkins, G. A., Nibler, J. W., and Dyke, T. R., 1985, *J. chem. Phys.*, **83**, 2129.

Maybury, R. H., Gordon, S., and Katz, J. J., 1955, *J. chem. Phys.*, **23**, 1277.

McMahan, A., Martin, R. M., and Satpathy, S., 1988, *Phys. Rev.* B, **38**, 6650.

Mikulski, C. M., Russo, P. J., Saran, M. S., MacDiarmid, A. G., Garito, A. F., and Heeger, A. J., 1975, *J. Am. chem. Soc.*, **97**, 6358.

Mintmire, J. W., 1991, *Density Functional Methods in Chemistry*, edited by J. K. Labanowski and J. W. Andzelm (New York: Springer).

Mintmire, J. W., Dunlap, B. I., and White, C. T., 1992, *Phys. Rev. Lett.*, **68**, 631.

Mintmire, J. W., Kutzler, F. W., and White, C. T., 1987, *Phys. Rev.* B, **36**, 3312.

Mintmire, J. W., and White, C. T., 1983*a*, *Phys. Rev. Lett.*, **50**, 101.

Mintmire, J. W., and White, C. T., 1983*b*, *Phys. Rev.* B, **28**, 3283.

Mintmire, J. W., and White, C. T., 1983*c*, *Phys. Rev.* B, **27**, 1447.

Mintmire, J. W., and White, C. T., 1983*d*, *Int. J. quant. Chem. Symp.*, **17**, 609.

Mintmire, J. W., and White, C. T., 1989, *Phys. Rev. Lett.*, **63**, 2532.

Mintmire, J. W., White, C. T., and Elert, M. L., 1988, *Synth. Met.*, **25**, 109.

Nechtschein, M., 1964, *J. Polym. Sci.* C, **4**, 1367.

Okamoto, Y., Choi, L. S., Iqbal, Z., and Baughman, R. H., 1986, *Synth. Met.*, **15**, 281.

Pattison, P., Weyrich, W., and Williams, B., 1977, *Solid St. Commun.*, **21**, 967.

Pattison, P., and Williams, B., 1976, *Solid St. Commun.*, **20**, 585.

Pauling, L., 1949, *Proc. Natl. Acad. Sci. U.S.A.*, **35**, 495.

Pinnick, D. A., Katz, A. I., and Hanson, R. C., 1989, *Phys. Rev.* B, **39**, 8677.

Pireaux, J. J., Riga, J., Caudano, R., Verbist, J. J., André, J. M., Delhalle, J., and Delhalle, S., 1974, *J. electron spectrosc.*, **5**, 531.

Pisani, C., Dovesi, R., and Roetti, C., 1988, *Hartree–Fock Ab Initio Treatment of Crystalline Systems* (Heidelberg: Springer).

Pnevmatikos, S., 1988, *Phys. Rev. Lett.*, **60**, 1534.

Prins, J. A., Schenk, J., and Hospel, P. A. M., 1956, *Physica*, **22**, 770.

Rachdi, F., and Bernier, P., 1986, *Phys. Rev.* B, **33**, 7817.

Rasmusson, J., Stafström, S., Lögdlund, M., Salaneck, W. R., Karlsson, U., Swanson, D., MacDiarmid, A. G., and Arbuckle, G. A., 1991, *Synth. Met.*, **41–43**, 1365.

Rice, M. J., Bishop, A. R., and Campbell, D. K., 1983, *Phys. Rev. Lett.*, **51**, 2136.

Rice, M. J., and Mele, E. J., 1982, *Phys. Rev. Lett.*, **49**, 1455.

Rice, M. J., and Phillpot, S. R., 1987, *Phys. Rev. Lett.*, **58**, 937.

Ring, J. W., and Egelstaff, P. A., 1969, *J. chem. Phys.*, **51**, 762.

Roth, S., Hanack, M., and Schier, H., 1991, (editors), *Proceedings of the International Conference on Science and Technology of Synthetic Metals 1990, Tübingen, Federal Republic of Germany, Synth. Met.*, **41–43**.

Rühe, J., Colaneri, N. F., Bradley, D. D. C., Friend, R. H., and Wegner, G., 1990, *J. Phys.: Condens. Matt.*, **2**, 5464.

Salaneck, W. R., Clark, D. T., and Samuelson, E. J., 1991, (editors), *Science and Applications of Conducting Polymers* (Bristol: Adam Hilger).

Seki, K., Ueno, N., Karlsson, U. O., Engelhardt, R., and Koch, E.-E., 1986. *Chem. Phys.*, **105**, 247.

Sim, F., St-Amant, A., Papai, I., and Salahub, D. R., 1992, *J. Am. chem. Soc.*, **114**, 4391.

Smith, D. F., 1958, *J. chem. Phys.*, **28**, 1040.

Springborg, M., 1986, *Phys. Rev.* B, **33**, 8475.

Springborg, M., 1987, *Phys. Rev. Lett.*, **59**, 2287.

Springborg, M., 1988, *Phys. Rev.* B, **38**, 1483.

Springborg, M., 1989*a*, *J. Chim. phys.*, **86**, 715.

Springborg, M., 1989*b*, *Synth. Met.*, **28**, D, 527.

Springborg, M., 1989*c*, *Phys. Rev.* B, **40**, 5774.

Springborg, M., 1989*d*, *Synth. Met.*, **32**, 337.

Springborg, M., 1989*e*, *Synth. Met.*, **29**, F, 207.

Springborg, M., 1989*f*, *Phys. Rev.* B, **39**, 5327.

SPRINGBORG, M., 1989 *g*, *Phys. Rev.* B, **40,** 7839.

SPRINGBORG, M., 1989 *h*, *Phys. Rev.* B, **40,** 7928.

SPRINGBORG, M., 1991 *a*, *Physica* B, **172,** 225.

SPRINGBORG, M., 1991 *b*, *Ber. Bunsenges. phys. Chem.*, **95,** 1238.

SPRINGBORG, M., 1992 *a*, *J. Phys.: Condens. Matter*, **4,** 101.

SPRINGBORG, M., 1992 *b*, *Proton Transfer in Hydrogen-Bonded Systems*, edited by T. Bountis (New York: Plenum).

SPRINGBORG, M., 1992 *c*, *Z. Naturf.* A (to be published).

SPRINGBORG, M., and ANDERSEN, O. K., 1987, *J. chem. Phys.*, **87,** 7125.

SPRINGBORG, M., BECHGAARD, K., and BJØRNHOLM, T., 1990 *b*, *Phys. Rev.* B, **42,** 5784.

SPRINGBORG, M., CALAIS, J.-L., GOSCINSKI, O., and ERIKSSON, L. A., 1991 *a*, *Synth. Met.*, **41–43,** 3309.

SPRINGBORG, M., CALAIS, J.-L., GOSCINSKI, O., and ERIKSSON, L. A., 1991 *b*, *Phys. Rev.* B, **44,** 12713.

SPRINGBORG, M., DRECHSLER, S.-L., and MÁLEK, J., 1990 *a*, *Phys. Rev.* B, **41,** 11954.

SPRINGBORG, M., DRECHSLER, S.-L., and MÁLEK, J., 1991 *c*, *Synth. Met.*, **41–43,** 3535.

SPRINGBORG, M., and JONES, R. O., 1986, *Phys. Rev. Lett.*, **57,** 1145.

SPRINGBORG, M., and JONES, R. O., 1988, *J. chem. Phys.*, **88,** 2652.

SPRINGBORG, M., JONES, R. O., and HOHL, D., 1992 (in preparation).

SPRINGBORG, M., and KAVAN, L., 1992, *Chem. Phys.* (accepted).

SPRINGBORG, M., KIESS, H., and HEDEGÅRD, P., 1989, *Synth. Met.*, **31,** 281.

SPRINGBORG, M., and LEV, M., 1989, *Phys. Rev.* B, **40,** 3333.

SU, W. P., SCHRIEFFER, J. R., and HEEGER, A. J., 1979, *Phys. Rev. Lett.*, **42,** 1698.

SU, W. P., SCHRIEFFER, J. R., and HEEGER, A. J., 1980, *Phys. Rev.* B, **22,** 2099.

SUZUKI, I., PARISEAU, M. A., and OVEREND, J., 1966, *J. chem. Phys.*, **44,** 3561.

TAKEDA, K., and SHIRAISHI, K., 1989, *Phys. Rev.* B, **39,** 11028.

TANAKA, M., WATANABE, A., and TANAKA, J., 1980 *a*, *Bull. chem. Soc. Japan*, **53,** 645.

TANAKA, M., WATANABE, A., and TANAKA, J., 1980 *b*, *Bull. chem. Soc. Japan*, **53,** 3430.

UENO, N., FUJIMOTO, H., SATO, N., SEKI, K., and INOKUCHI, H., 1990, *Phys. scripta*, **41,** 181.

VARDENY, Z., ORENSTEIN, J., and BAKER, G. L., 1983 *a*, *Phys. Rev. Lett.*, **50,** 2032.

VARDENY, Z., ORENSTEIN, J., and BAKER, G. L., 1983 *b*, *J. Phys.*, Paris, **44,** C3 325.

VOGL, P., and CAMPBELL, D. K., 1989, *Phys. Rev. Lett.*, **62,** 2012.

VOGL, P., and CAMPBELL, D. K., 1990, *Phys. Rev.* B, **41,** 12797.

WALATAKA, Jr., V. V., LABES, M. M., and PERLSTEIN, J. H., 1973, *Phys. Rev. Lett.*, **31,** 1139.

WALTMAN, R. J., BARGON, J., and DIAZ, A. F., 1983, *J. phys. Chem.*, **87,** 1459.

WENDEL, H., MARTIN, R. M., and CHADI, D. J., 1977, *Phys. Rev. Lett.*, **38,** 656.

WINNEWISSER, G., MAKI, A. G., and JOHNSON, D. R., 1971, *J. molec. Spectrosc.*, **39,** 149.

WÖHRLE, D., 1971, *Tetrahedron Lett.*, **22,** 1969.

WU, C. R., NILSSON, J. O., INAGANÄS, O., SALANECK, W. R., ÖSTERHOLM, J.-E., and BRÉDAS, J. L., 1987, *Synth. Met.*, **21,** 197.

YANNONI, C. S., and CLARKE, T. C., 1983, *Phys. Rev. Lett.*, **51,** 1191.

YARKONY, D. R., O'NEIL, S. V., SCHAEFER, III, H. F., BASKIN, C. P., and BENDER, C. F., 1974, *J. chem. Phys.*, **60,** 855.

YE, L., FREEMAN, A. J., ELLIS, D. E., and DELLEY, B., 1989 *a*, *Phys. Rev.* B, **40,** 6277.

YE, L., FREEMAN, A. J., ELLIS, D. E., and DELLEY, B., 1989 *b*, *Phys. Rev.* B, **40,** 6285.

YUMOTO, Y., and YOSHIMURA, S., 1986, *Synth. Met.*, **13,** 185.

ZEMACH, R., ASHKENAZI, J., and EHRENFREUND, E., 1989 *a*, *Phys. Rev.* B, **39,** 1884.

ZEMACH, R., ASHKENAZI, J., and EHRENFREUND, E., 1989 *b*, *Phys. Rev.* B, **39,** 1891.